Spring 1-1-2011

Thiol-vinyl systems as shape memory polymers and novel two-stage reactive systems

Devatha P. Nair
University of Colorado at Boulder, devatha.nair@colorado.edu

THIOL-VINYL SYSTEMS AS SHAPE MEMORY POLYMERS AND NOVEL TWO-STAGE REACTIVE POLYMER SYSTEMS

A Thesis Submitted to the Faculty of the Graduate School of
the University of Colorado at Boulder
by

Devatha P. Nair

B.Tech. University of Kerala, 1998

M.S. University of Colorado, 2008

in partial fulfillment of the requirement for
the degree of Doctor of Philosophy
Department of Mechanical Engineering
2011

This thesis entitled:

Thiol-vinyl systems as shape memory polymers and novel two-stage reactive systems
written by Devatha Premchandran Nair
has been approved for the Department of Mechanical Engineering

_____
Robin Shandas, PhD (Committee Chair)

_____
Christopher Bowman, PhD (Committee Chair)

_____
Jeff Stansbury; Jerry Qi; and Yifu Ding (Committee Members)

Date_____

The final copy of this thesis has been examined by the signatories, and we find that both the content and the form meet acceptable presentation standards of scholarly work in the above mentioned discipline.

Nair, Devatha Premchandran (PhD, Mechanical Engineering)

THIOL-VINYL SYSTEMS AS SHAPE MEMORY POLYMERS AND NOVEL TWO-STAGE REACTIVE SYSTEMS

Thesis directed by Professors Christopher N. Bowman and Robin Shandas

Abstract

The focus of this research was to formulate, characterize and tailor the reaction methodologies and material properties of thiol-vinyl systems to develop novel polymer platforms for a range of engineering applications. Thiol-ene photopolymers were demonstrated to exhibit several advantageous characteristics for shape memory polymer systems for a range of biomedical applications. The thiol-ene shape memory polymer systems were tough and flexible as compared to the acrylic control systems with glass transition temperatures between 30 and 40 °C; ideal for actuation at body temperature. The thiol-ene polymers also exhibited excellent shape fixity and a rapid and distinct shape memory actuation response along with free strain recoveries of greater than 96% and constrained stress recoveries of 100%.

Additionally, two-stage reactive thiol-acrylate systems were engineered as a polymer platform technology enabling two independent sets of polymer processing and material properties. There are distinct advantages to designing polymer systems that afford two distinct sets of material properties – an intermediate polymer that would enable optimum handling and processing of the material (stage 1), while maintaining the ability to tune in different, final properties that enable the optimal functioning of the polymeric material (stage 2). To demonstrate the range of applicability of the two-stage reactive systems, three specific applications were

demonstrated; shape memory polymers, lithographic impression materials, and optical materials. The thiol-acrylate reactions exhibit a wide range of application versatility due to the range of available thiol and acrylate monomers as well as reaction mechanisms such as Michael Addition reactions and free radical polymerizations. By designing a series of non-stoichiometeric thiol-acrylate systems, a polymer network is initially formed via a base catalyzed 'click' Michael addition reaction. This self-limiting reaction results in a Stage 1 polymer with excess acrylic functional groups within the network. At a later point in time, the photoinitiated, free radical polymerization of the excess acrylic functional groups results in a highly crosslinked, robust material system. By varying the monomers within the system as well as the stoichiometery of thiol to acrylate functional groups, the ability of the two-stage reactive systems to encompass a wide range of properties at the end of both the stage 1 and stage 2 polymerizations was demonstrated. The thiol-acrylate networks exhibited intermediate Stage 1 rubbery moduli and glass transition temperatures that range from 0.5 MPa and -10 ºC to 22 MPa and 22 ºC respectively. The same polymer networks can then attain glass transition temperatures that range from 5 ºC to 195 ºC and rubbery moduli of up to 200 MPa after the subsequent photocure stage.

Two-stage reactive polymer composite systems were also formulated and characterized for thermomechanical and mechanical properties. Thermomechanical analysis showed that the fillers resulted in a significant increase in the modulus at both stage 1 and stage 2 polymerizations without a significant change in the glass transition temperatures (T_g). The two-stage reactive matrix composite formed with a

hexafunctional acrylate matrix and 20 volume % silica particles showed a 125% increase in stage 1 modulus and 101% increase in stage 2 modulus, when compared with the modulus of the neat matrix.

Finally, the two-stage reactive polymeric devices were formulated and designed as orthopedic suture anchors for arthroscopic surgeries and mechanically characterized. The Stage 1 device was designed to exhibit properties ideal for arthroscopic delivery and device placement with glass transition temperatures 25 – 30 °C and rubbery moduli ~ 95 MPa. The subsequent photopolymerization generated Stage 2 polymers designed to match the local bone environment with moduli ranging up to 2 GPa. Additionally, pull-out strengths of 140 N were demonstrated and are equivalent to the pull-strengths achieved by other commercially available suture anchors.

This thesis is dedicated to my husband, Zurwan Amaria; my parents in India, Prem and Shary Nair; and my parents in Colorado, Navroze and Bucky Amaria, for their love and support over the years.

Acknowledgements

I would like to thank my advisor Prof. Christopher Bowman for his guidance, research insights, his mentorship and financial support. It has truly been an honor to be a part of your group. Thank you for constantly encouraging me to do my very best and above all, thank you for believing in me.

I would like to thank my advisor Prof. Robin Shandas for the opportunity to work in his group, the financial support and technical guidance he has given me over the years.

I would like to acknowledge my committee members Profs. Jeff Stansbury, Yifu Ding and Jerry Qi. I would like to specifically thank Prof. Yifu Ding for his helpful insights into my research.

I would like thank Dr. Neil Cramer for his support and guidance. Thank you for having the patience to deal with the infinite impromptu meetings, the endless editing of my documents and for the advice you have given me over the years. You have always encouraged me to develop my ideas and I have benefited immensely from our discussions. You have been a mentor and an inspiration to me and I have learned so much from working with you. Thank you.

I would like to thank the Bowman and Stansbury Group members for their support. I have benefitted from the technical cooperation which is fostered within the groups. I would like to thank Dr. Diana Leung, Dr. Tao Gong, Dr. Sheng Ye, Dr. Heeyoung Park, Parag Shah, Chipper Couch, Raveesh Shenoy, Alan Aguirre, Abeer Alrzazani and JianCheng Leu for their insights, discussions and for making working with the group a pleasant experience. From the Mechanical Engineering department, I would like to thank Dr. Francisco Castro, Bryan Rech, Mike Lyons, Dr. Alicia Ortega, Dr. Christopher Yakacki, Dr. Krishna Madhavan, Jeanie Mar, Dr. Devon Scott, Logan Williams, Kevin Ge.

I would like to thank the undergraduate students who have worked with me over the years: John C. Gaipa, Mathew K. McBride, Emily M. Matherly, Nathan Lee and Aimee Anderson. Particularly I would like to thank John C. Gaipa and Mathew K. McBride, both of whom worked very hard in the lab.

I would like to thank CIRES glass shop and the machine shop for their cooperation. I would like to acknowledge Dennis Steffey of the CIRES glass shop for taking the time to understand the myriad and uncommon glass design requirements that came from this research and his expertise that never let us down. I would like to thank Craig Joy, Jim Kastengren and Ken Smith of the CIRES machine shop for their help.
I would also thank like to thank Dragan Mejic of the Chemical and Biological Engineering machine shop.

There have been mostly ups and a few downs in my PhD journey. I would like to particularly thank the people who encouraged me and supported me during the ‘downs’. I want to thank Sharon Anderson, the graduate advisor from the Mechanical Engineering Department for her support and friendship over the years. Her understanding of the graduate school maze, along with

her patience and tenacity has helped many a graduate student successfully navigate the path. I would like to thank Prof. Victor Bright, Prof. Ginger Ferguson and Prof. Jean Hertzberg for their support. I would also like to thank Dr. Peter Freitag for his encouragement and support over the years.

I am grateful for the support and encouragement that was given to me at key points in my life by Prem Kumar,G. Vijayaraghavan, Prem Menon and Thomas George, who played a crucial role in getting me started down this path.

I would like to thank my high school Physics teacher, K. Madhavan Nair for believing in me from the very beginning. You have been a great teacher and an inspiration to me.

My family has always been a constant, unconditional source of love and support. I am grateful for how they have stood by me over the years. Specifically, I would like to thank my late grandfathers, G.P. Nair and K. Sreekumaran Nair; my late uncle, Dr. Sarathchandran Nair; Dr. P.J. Nair; Rati Nair; Padmaja Venugopal; Dr. M. Venugopal; Vijayalakshmi Nair; Kala Madhavan; S. Kuldeep Kumar; Meherab Amaria; Gina Amaria; Veena and Mohan Janardhanan, who have been an unwavering source of love and support from half-way across the world; Harsha Pramod, whose presence in my life has been infinitely comforting and enriching; Oskar Back and Sue Capraro, whose friendship has been a source of great comfort and solace to me. My brother Rony Nair who has always been a source of unconditional love and support to me along with my sisters Dr. Aiswarya Venugopal, Dr. Rodabe Amaria and Swetha Vinod. My husband Zurwan, whose persistent support and constant encouragement combined with his gentle nature and pleasant companionship made this journey infinitely more enriching. My parents Prem and Shary Nair, who instilled in me a love of learning from a very young age and whose unpretentious, unwavering support has got me through the many ups and downs of life. I am also grateful to Navroze and Bucky Amaria for their presence in my life and the love and support they have given me to pursue my research.

Lastly, I am thankful for the love, levity and perspective that my nephew Advaith R Nair and nieces Gitanjali R Nair and Ilana M. Amaria has brought into our lives.

Table of Contents

List of Tables

Tables

List of Figures

Figures

List of Schemes

Chapter 1

Introduction and Background

Polymer networks afford the versatility and function of being able to perform as materials in applications ranging from soft lithographic substrates to high performance parts on aircrafts. [1-3]The advent of various photopolymerization mechanisms in particular, used in tandem with traditional polymerization mechanisms such as thermal initiation has enabled the optimization of polymer networks such as interpenetrating networks (IPN) which allow for their properties to be tailored for specific applications. [4] Thus, it has opened up avenues for polymers in new domains which were previously largely dominated by metals and ceramics such as biomedical implants and in aerospace applications that may require a combination of properties. [5-6] Photopolymerizations in particular are becoming a preferred mechanism to convert monomers to polymers largely due to the advantages of solventless processing, ambient curing, and both spatial and temporal control of the polymerization.

Thiol-enes and thiol-acrylates are unique photopolymer systems that, relative to acrylics, exhibit several advantageous characteristics for both curing and polymer properties such as rapid reactions to high conversion with low shrinkage and shrinkage stress, along with minimal oxygen inhibition. Woods and coworkers in the 1990s [7] and in recent years the works of Hoyle and Bowman [8-9] have renewed an interest in thiol-ene polymerizations that have opened up avenues for new industrial products and applications.

The thiol-acrylate Michael addition reaction also exhibits a wide range of application versatility. A Michael addition reaction between a thiol and an acrylate enables thiol and acrylic monomers to react stoichiometrically under relatively mild reaction conditions to yield crosslinked polymer systems. [8-10] The Michael addition reaction has been shown to progress in

a wide range of conditions that allow numerous options with respect to monomer selection, reaction temperature and the presence or absence of solvents, all resulting in sophisticated, uniform polymer networks in conditions where other reactions would not be able to proceed. Additionally, the ability of Michael addition reactions to favor high conversions and rapid cure rates at ambient temperature have made these polymer systems an ideal choice for applications that vary from industrial coatings to drug delivery [11] as well as cell scaffolds and crosslinked hydrogels. [12-13]

The primary focus of this research is the development of thiol-ene and thiol-acrylate polymer networks for biomedical shape memory polymers and novel two-stage reactive polymer applications. We demonstrate that the formulation and design of stoichiometeric and non-stoichiometeric systems and prudent choice of reaction mechanisms enables a wide range of achievable polymer network properties and opening up new solutions for polymer applications.

1.1 Thiol-Ene Reaction Mechanism

The mechanism of polymerization observed in a thiol-ene system is a step growth radical addition reaction where step growth reactions are characterized by slow and uniform molecular weight development. The thiol–ene polymerization consists of initiation, propagation and termination reactions.[13-15] The initiation step can be broken down to include the excitation of a photoinitiator by photon absorption from an irradiation source, which in turn it cleaves to form radicals that can abstract hydrogen from a thiol monomer, ultimately generating a thiyl radical.

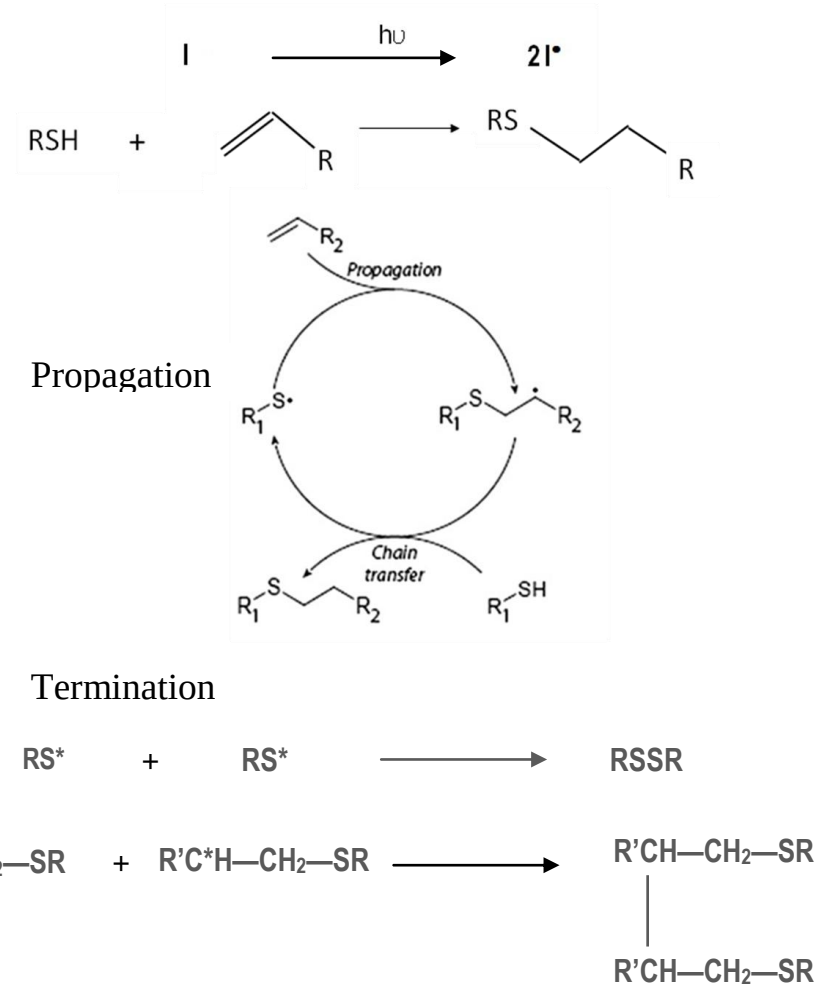

Scheme 1.1. In the thiol-ene step growth radical polymerization, after a thiyl radical is formed by the abstraction of hydrogen by the initiator; it reacts with an ene functional group to generate a carbon radical. The carbon-centered radical undergoes subsequent chain transfer to a thiol group, regenerating the thiyl radical. In this manner, by alternating propagation and chain transfer the network is formed. Termination is understood to occur via radical-radical recombination.

There are two points to be noted about the thiol-ene polymerization initiation and propagation mechanisms. First, is that oxygen does not strongly inhibit the reaction, as it does in pure acrylate systems [13-18]. If oxygen is present, it adds an additional propagation step (Figure 1.2)

that consists of an addition reaction that incorporates oxygen into the growing polymer chain as a peroxy radical. The peroxy radical then undergoes abstracts a hydrogen from a thiol to regenerate the thiyl radical. In the presence of oxygen, the photoinitiator efficiency may be reduced, but the overall polymerization proceeds with little change in the polymerization rate.

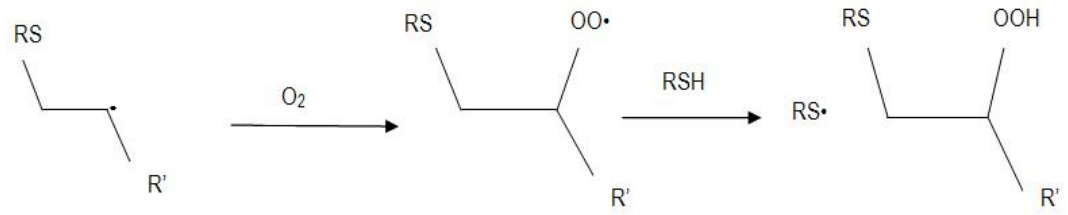

Scheme 1.2. A carbon centered radical reacts with oxygen to form a peroxy radical. Although the peroxy radical is not reactive towards addition reactions, they are reactive towards hydrogen abstraction, and hence the chain transfer results in regenerating the thiol radical.

For traditional ene monomers, such as vinyl ethers and allyl ethers, the thiol and ene monomers are consumed stoichiometrically at an identical rate. When a thiol-acrylate system is polymerized, the acrylate functional group is capable of undergoing step growth polymerization with the thiol as well as chain growth homopolymerization. The combination of both of these polymerization mechanisms in a polymerization has a significant impact on the polymer network structure and the resulting material properties. [19]

1.2. Shape Memory Polymers

Shape memory materials (SMM) have recently received significant attention as biomedical devices that enable minimally invasive surgical (MIS) procedures. [20] A shape memory material system is characterized by its ability to store a temporary shape and subsequently recover its original shape once exposed to an appropriate stimulus. The stimulus can be temperature, magnetic field, water or light, depending on the initial monomer systems. The relatively high cost of metals and ceramics and the processing and manufacturing requirements make it difficult and expensive to implement them from design to application. Shape Memory Alloys (SMA), such as Nitinol, have been developed for use in minimally invasive surgeries (MIS) for treating certain types of aneurysms such as a berry aneurysm or a saccular aneurysm. [20] While representing a significant advancement in MIS, SMAs have several drawbacks that include low recoverable strains (8%) and high modulus (83 GPa). These drawbacks limit the range of potential applications by imposing significant device design constraints and limitations associated with material properties and design. [21-22]

Shape memory polymers (SMP) are a class of SMM that are readily designed to exhibit high strain capacities (up to 800%) and can be actuated at body temperature. [20,23-26] The shape memory effect is a result of the combination of monomers that go into making the polymer and the specific processing to which the polymer is subjected. Together, the processes have been termed polymer functionalization. [24] Once the SMP is formed, the polymer is deformed and set into its temporary shape, a process that is termed programming.

For a thermoset polymer system that exhibits a shape memory response as a result of a change in temperature, the glass transition temperature, T_g, of the polymer is of paramount importance. The glass transition temperature and the glass transition temperature width (T_g

width) dictates the temperature and temperature range within which the system undergoes a transition from its temporary shape to its permanent shape. By subjecting the formulation of the shape memory polymer to minor changes in composition, a wide variety of properties can be controlled without compromising the shape memory behavior of the system [23-26]. When compared to polymers that exhibit shape memory behavior, shape memory metals and ceramics have high tensile strengths; however, in general the thermomechanical properties of a metal or ceramic system can be varied only within a limited range. [25] A comparison of properties between shape memory polymers and alloys is given in Table 1.1. Though the shape memory alloy based devices have higher moduli, they are limited in the extent of deformation that they can undergo in their temporary shape. Also, unlike shape memory polymers which can be formulated to be biodegradable, shape memory alloys cannot be made biodegradable.

Table 1.1. Comparison of different properties of shape-memory polymers and shape-memory alloys. The table is adapted from the journal article 'Review of progress in shape-memory polymers' P.T. Mather, X Luo, I.A. Rousseau, *Ann. Rev. Mater. Research*. 2009, **39**, 445

Property	**Shape Memory Polymers**	**Shape Memory Alloys**
Density/g cm^{-3}	0.9 - 1.1	6 – 8
Extent of deformation (%)	Up to 800%	< 8%
Young's modulus at $T < T_{tran}$/GPa	0.01–3	83 (Nitinol)
Stress required for deformation/MPa	1 – 3	50 – 200
Recovery speeds	<1 s–several min	< 1s
Biocompatibility and biodegradability	Can be biocompatible and/or biodegradable	biocompatible not biodegradable
Processing conditions	< 200 °C, low pressure	High temperature (> 1000 °C) and high pressure required
Cost	<$10 per lb	~$250 per lb

Thiol-enes and thiol-acrylates offer a unique combination of properties that are advantageous for shape memory polymer systems, including rapid polymerization, low volume shrinkage and shrinkage stress, the formation of homogeneous networks, and insensitivity to oxygen inhibition. [9,16] Although there have been a few notable studies on thiol-ene and thiol-ene acrylate systems in the last few years, there have been no studies that have specifically examined thiol-ene polymers for shape memory based-biomedical device. In this work, we have developed a series of thiol-ene and thiol-acrylate systems exhibiting highly desirable polymerization characteristics and material properties.

1.3 Two-stage reactive Polymer Systems

It is known that the stoichiometery of thiol-acrylate Michael addition networks must be 1:1 to form optimized networks. In this work we exploit the ability to vary the stoichiometery of thiol and acrylate functional groups to enable greater versatility of these systems, particularly a desirable two stage curing reaction. A thiol-acrylate network formed by a Michael addition reaction from an initial monomer mixture with a stoichiometeric excess of acrylate groups leads to an initial polymer network with residual acrylate functional groups. The residual acrylate functional groups can subsequently be photopolymerized in a second polymerization reaction. The ensuing dual network forming system exhibits a first polymerization reaction that is a base catalyzed, self-limiting reaction to form an initial polymer network and a second polymerization reaction, orthogonal to the first reaction that is photoinitiated to form the final polymer network. The acrylates homopolymerize via a free radically initiated chain growth polymerization mechanism (Figure 1.3) with initiation and termination steps similar to the thiol-ene mechanism.

In the initiation step a photoinitiator absorbs light and cleaves into radicals that subsequently react with the carbon-carbon double bond of the acrylate functional group generating a carbon based radical. The carbon-based radical propagates across other carbon-carbon double bonds to form a long chain. The reaction is terminated by radical-radical recombination.

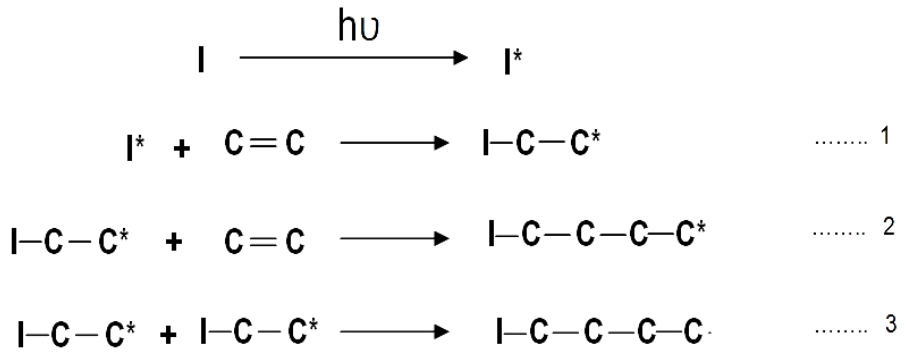

Scheme 1.3. In the first step (1), the chain growth polymerization process is initiated by generating a radical which in turns creates an active site on a monomer which will enable another molecule to attach onto the monomer. The propagation step (2) consists of the monomers adding themselves onto the active site and simultaneously generating a new active site on the newly added monomer. Polymerization is completed when all active sites are terminated (3) and this occurs either when there are no active sites remaining or when recombination of the radicals takes place.

In this study we demonstrate that by varying monomer type and stoichiometery within the initial monomers we choose, two-stage reactive polymeric systems with a wide range of moduli and glass transition temperatures at the end of both the first and second stages of cure were achieved. Further, we can optimize the polymer formulation for three different applications - shape

memory polymers, impression materials and optical materials. Scheme 1 details the mechanism of the two-stage reactive network forming systems.

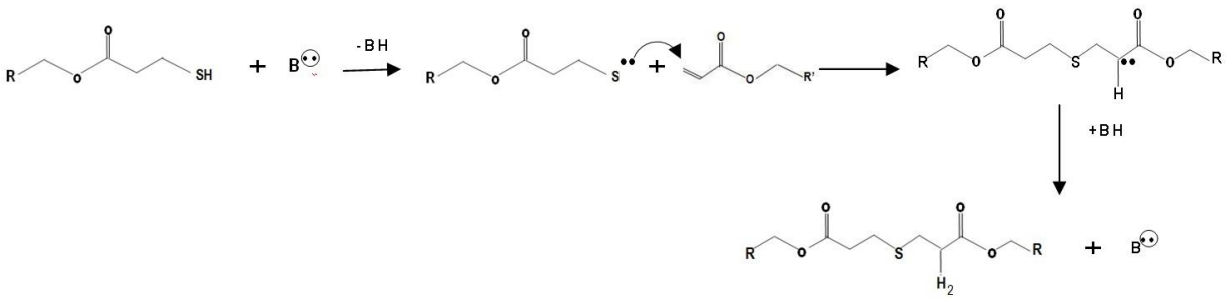

Stage 1 Reaction

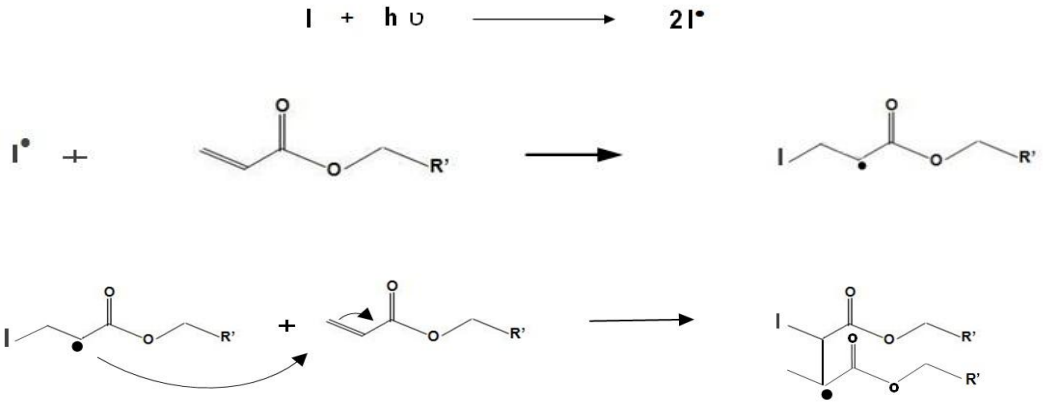

Stage 2 Reaction

Scheme 1.4: The Stage 1 reaction is a Michael addition reaction for base-catalyzed thiol-acrylate system. B(•) is the deprotonated base triethylamine and the arrows indicate the movement of electrons during the reaction from the thiolate ion (Michael-donor) to the C-C double bond of the acrylate (Michael-acceptor) and back to the base catalyst to form the Michael adduct. The Stage 2 reaction is a free radical acrylic photopolymerization mechanism that is initiated via UV irradiation.

1.3.1 Two-Stage Reactive Shape Memory Polymer Systems

The primary drawback of shape memory polymer systems, especially for thermally triggered SMPs used in biomedical applications is their low modulus in the deployed state. [23, 27-28] Fundamental to the shape changing transition of the polymer is a characteristic drop in the modulus of the material associated with undergoing the glassy to rubbery transition. The SMP modulus in its rubbery state is orders of magnitude less than the modulus in the glassy state. Approaches to increase the rubbery modulus include increasing the crosslink density [23] and incorporating fillers such as fibers and particles into the neat polymer matrix. While these methods have been seen to increase the overall mechanical strength and modulus of the polymer, generally the outcomes are either modest or attained at the expense of desirable shape memory characteristics. [23,28]

In this novel two-stage reactive shape memory polymer system, the motivation was to engineer a shape memory polymer system that has a distinct first set of mechanical properties that enables optimum shape memory –based deployment of a device and a second set of properties that can be achieved *in situ*, once the deployed device is in place. To achieve these two distinct stages within the device, the initial Michael addition reaction with an excess of acrylate functional groups forms a shape memory polymer network with initial properties that are desirable for the SMP deployment. Once the shape memory device has been deployed and is in place, in the second reaction, the remaining acrylate functional groups are photopolymerized to increase the crosslink density. The ensuing polymer exhibits a second set of material properties consisting of a second glass transition temperature (T_{g2}), where $T_{g2} > T_{g1}$ and consequently a polymer with a higher modulus is obtained.

1.3.2 Two-Stage Reactive Impression materials

There is an ever-present need to manufacture smaller devices at lower cost. As an alternative to Imprint Lithography which requires high temperatures for imprinting a pattern with nano-scale resolution, Step and Flash Imprint Lithography (SFIL) has also been a successful technique for replicating intricate patterns at both the nano- and micro- scale in ambient conditions by utilizing UV light to cure the polymer resin while being pressed against a pattern with submicrometer resolution. [29-31] The challenges in the area of both nano- and micro- size patterning is finding an appropriate photopolymerizable material with low viscosity, low shrinkage and the ability to form stable polymer networks that enable mold removal without loss of detail. During the past few years, thiol-ene reactions have been shown to perform as an excellent substrate for SFIL. [29] This soft lithography technique normally consists of pouring a liquid resin onto the pattern that is to be replicated and photocuring the resin on the patterned master. Once the polymer is cured, the thin film is peeled off the master in a repeatable manner in which multiple micron-scale imprints can be made from the same master pattern.

The same thiol-acrylate monomers in differing stoichiometeric ratios of thiol to acrylate were used to formulate a system that could be utilized for a lithography/impression gel. A thiol-acrylate network that is formed at the end of the Michael addition reaction can be used as the imprint material, which, as opposed to a liquid resin mix, would make this polymer impression material easier to handle and process. The gel that was formed at the end of Stage 1 was used to take the imprint of a micron-sized pattern mold. Once the gel pad was in place and pressed against the imprint, it was photocured and then removed from the mold.

1.3.3 Two-Stage Reactive Polymer Networks for Optical Materials

It is a challenge to obtain optical devices formed by patterned refractive index variations via traditional photoresist methodologies, especially in films that are thicker than 1 mm. [32-35] Although silver halide photographic emulsions can record holograms with sub 200 nm resolution, they involve processing steps that are solvent-based and often swell as a result, thereby degrading the quality of the recording. Photopolymeric recording materials also have the added advantage of requiring no additional wet processing to form the hologram, and these materials have been exploited for holographic data storage optical filters, gradient index lenses, and waveguides.[33-36]. The radical polymerization of the photopolymeric recording materials, which is induced via an interference beam, results in patterned local polymerization that sets up a concentration gradient of monomer within the material leading to diffusion of monomer into the irradiated areas thereby causing local changes of refractive index. One of the fundamental drawbacks is that the polymeric materials used for these applications must be rubbery for efficient diffusion, and remain rubbery during operation. This rubbery matrix requires a sealed, solid enclosure to make it physically rigid and to suppress in-diffusion of environmental contaminants.

With the two-stage reactive approach, this fundamental drawback of photopolymeric recording materials is overcome. The same thiol-acrylate monomers in differing stoichiometric ratios with an added high refractive index monomer were used to formulate an optical system for holographic materials. The dual network forming system can be optimized to form a matrix-hardening optical system, where at the end of Stage 1, a holographic recording material is obtained. Once refractive index gradients have been recorded into the material via light-induced

photopolymerization, the material is flood cured, forming a highly crosslinked matrix with embedded refractive index gradients.

1.4 Enhanced Two-Stage Reactive Polymer Systems

Two-stage reactive polymeric systems demonstrate the enhanced control and capabilities of functional polymeric networks. However, there are limitations with regard to the properties that can be achieved at the end of each stage of the two-stage reactive process. For example, at the end of Stage 1, the maximum modulus and glass transition temperature (T_g) that can be attained for a two-stage reactive system are limited by the chemical structure and functionality of the monomers used in the formulation. To demonstrate the range of moduli and glass transition temperatures that can be attained at the end of each stage, we formulated a series of polymers in which, by varying one monomer and the stoichiometery within the initial monomers we chose, two-stage reactive polymeric networks with a wide range of moduli and glass transition temperatures at the end of the each stage of cure have been achieved. Subsequently, the excess acrylates within the network are photopolymerized in a reaction that is orthogonal to the initial thiol-acrylate Michael addition, and this approach results in a highly crosslinked polymeric network.

1.5 Two-Stage Reactive Composite systems

Polymer composites have shown the ability to improve dramatically the overall material properties of polymers, such as modulus and strength, and can also be designed to yield novel functions such as biofunctionality. [37] The enhancement of material properties offers the ability to promote their use in novel functions such as automotive, aerospace, building, electrical,

optoelectronic, and biomedical applications. In particular, fiber reinforced polymer composites (FRP) and particle composites (PC) have been extensively used to tailor the desired properties into a polymer matrix system. A fiber reinforced polymer (FRP) composite is one in which the dispersed phase is a fiber and the matrix phase a polymer. There are numerous matrix materials and as many reinforcement types that can be combined in countless ways to produce just the desired properties. FRP and PC have widened the scope of polymers and their potential applications. [38,39] Both matrix and fiber properties contribute to improving the overall mechanical properties of the system; although it is to be expected that the final properties of the composite depend considerably on the nature of the polymer formulation. Fiber-matrix adhesion directly impacts the tensile strength, the modulus and the elongation at break of the composite system. [38] To improve the tensile strength of the composite system at the end of Stage 1, a strong interface between the matrix and the fiber, the presence of low stress concentration points and fiber orientation play a key role.

Particulate composite (PC) reinforcement in a polymer matrix consists of particles that are typically randomly distributed resulting in isotropic composites. Both FRPs and PC have been traditionally used to significantly enhance the material characteristics of the polymer matrix.

In this study, we consider PET and Kevlar mesh fibers embedded within a two-stage reactive polymer system, along with a micron size silica particle composite system. Initial results have shown that by reinforcing the polymer with medical grade gauze, a significant increase in the Stage 1 modulus is seen. Additionally, an increase in the Stage 2 modulus of the system has also been observed. In total, the mechanical properties of Fiber Reinforced Polymers (FRP) and Particle Composite depend on the individual material properties and on the degree of

division of the applied load between the two materials. Here, we formulate and characterize a series of two-stage reactive polymer composite systems.

1.6 Two-Stage Reactive Thiol-acrylate Systems as SMPs for Orthopedic Biomedical Applications.

The orthopedic suture anchor works as a staple or straight pin by holding the healing tissues together or the soft tissue and bone together to enable reattachment.[41] The anchor consists of placing an implant into the surrounding bone or soft tissue into which the suture is connected. There are currently more than 30 different types of suture anchors though there are a number of disadvantages for each one of the currently available suture anchors. [39-41] Metal suture anchor devices have a lack of flexibility in terms of repositioning or realigning the device once it has been inserted, can create large defects while removing metal anchors from the bone, and their inability to be constrained into temporary shapes dramatically limits their design options. Alternatively, plastic suture anchors are subject to brittle fracture, and the contact point between the suture and the anchor is much weaker compared to metals. The range of bioabsorbable suture anchors performs as well as plastics in terms of pull-out strength, but it is disputed as to whether the anchors remain in place and retain holding strength enough to facilitate full healing. The ideal suture anchor device should therefore have a distinct set of stage 1 properties which would include a high strain capacity and low modulus which would enable optimum delivery and a second set of stage 2 properties that can be tuned *in-situ* once the device has been placed in its target location. To achieve two distinct polymer stages within the device, a two-stage reactive orthopedic suture anchor system was formulated and evaluated in a test model.

1.7 References

[1] . A. R. Kannurpatti, K. J. Anderson, J. W. Anseth, C. N. Bowman, *J. Polym. Sci. Part B*, 1997, **35**, 2297

[2] . P.T. Mather, X Luo, I.A. Rousseau, *Ann. Rev. Mater. Research*. 2009, **39**, 445

[3] . C. Liu, H. Qin, P.T Mather, *J. Mater. Chem.* 2007**, 17**, 1543

[4] . F. Chen, W. D. Cook, *Euro. Poly. J*, 2008, **44**, 1796

[5] . J. J. Singh , R. H. Pater, A. Eftekhari, 1998 ,**134**, 113

[6] . G. David, M. Pinteala, B. C. Simionescu, *Dig. J. Nano. Bio.*,2006, **1**, 129

[7] . J.G. Woods, **I***n Radiation Curable Adhesives in Radiation Curing: Science and Technology;* Pappas, S. P., *Ed.; Plenum:* New York, 1992*; pp* 333–398.

[8] . C.E. Hoyle, C.N. Bowman, *Angew. Chem. Int. Ed.* 2010, **49**, 1540

[9] . C. E. Hoyle, T. Y. Lee, T. Roper, *J. Polym. Sci. Part A* 2004, **42**, 5301.

[10] . B.D. Mather, K. Viswanathan, K.M. Miller, T.E. Long, *Prog. Poly.Sci.* 2006, **31**, 487

[11] . D.L Elbert, A.B. Pratt , M.P. Lutolf, S. Halstenberg J.A. Hubbell, *J. Control. Rel.* 2004, **76**,11.

[12] . A. M. Kloxin, M. Tibbitt, A.M. Kasko, J.A. Fairbairn, K.S. Anseth, *Adv. Mater.* 2010, **22**, 61.

[13] . A. E. Rydholm, C. N. Bowman, K. S. Anseth, *Biomaterials*, 2005, **26**, 4495

[14] . A. F. Jacobine, *In Radiation Curing in Polymer Science and Technology III: Polymerization Mechanisms;* J. D. Fouassier, J. F. Rabek, *Elsevier:* London, 1993

[15] . N. B. Cramer, C. N. Bowman, *J. Poly. Sci. Part A* 2001, **39,** *3311.*

[16] . J. W. Chan, H Wei, H. Zhou, C.E. Hoyle, *Euro. Poly. J.* 2009, **45**, 2717

[17] . N.B. Cramer, J.P. Scott, C.N. Bowman, *Macromolecules*, 2002, **35**, 5361

[18] . M. Cole, M. Bachemin, C.K. Nguyen, Viswanathan, C.E Hoyle, *RadTech Japan*, 2000, 211

[19] . S.K. Reddy, N.B. Cramer, A.K. O'Brien, T. Cross, R. Raj ,C.N. Bowman. *Macromolecular Symposia*, 2004, **206**, 361

[20] . C.M. Yakacki, R. Shandas, C. Lanning, B. Rech, A. Eckstein, K. Gall, *Biomaterials*, 2007, **28**, 2255

[21] . K. Otsuka, C.M. Wayman in *Shape Memory Materials* . (Eds: University Press, Cambridge, UK , 1998)

[22] . T.W. Duerig, D. Stoeckel, A. Pelton, *Mater. Sci. Eng.* 1999, **273**, 149

[23] . M. Behl, A. Lendlein, *Mat.Today*,2007,**10**,20

[24] . A. Lendlein, S. Kelch , *Angew. Chem.* Int. Ed. 2002, **114**, 2138

[25] . C. Liu, H. Qin, P.T Mather, *J. Mater. Chem.* 2007**, 17**, 1543

[26] . D.P.Nair, N.B. Cramer, T.F. Scott, C.N. Bowman,R. Shandas, *Polymer*, 2010 ,**51**,4383

[27] . I.A. Rousseau, *Poly. Eng. Sci.* 2008,**48**, 2075

[28] . D. Ratna, J. Karger-kocsis. *J. Mater. Sci.* 2008, **8**, 254

[29] . V.S. Khire, Y. Youngwoo, N.A. Clark , *Adv. Mater.* 2007, **20**, 3308

[30] . H.D. Rowland, W.P. King, *Appl. Phys.A: Mater. Sci. Process.* 2005 **, 81**,1331

[31] . T.C Bailey, S.C. Johnson, S.V. Sreenivasan, J.G. Ekerdt, C.G. Willson, D.J. Resnick, . J. *Photopolymer Sci. Technol*. **15**, 481

[32] . J. P. Rolland, E. C. Hagberg, G. M. Denison, K. R. Carter, J. M. DeSimone, *Angew. Chem. Int. Ed*. 2004, **43**, 5796.

[33] . R. R. A. Syms in *Practical Volume Holography* (Oxford University Press, Oxford, 1990).

[34] . V. W. Krongauz, A. D. Trifunac in *Processes In Photoreactive Photopolymers* (Chapman & Hall, New York, 1994).

[35] . B. J. Chang, C. D. Leonard, Appl. Opt. 1979, **48**, 2407

[36] . D. H. Close, A. D. Jacobson, R. C. Magerum, R. G. Brault, F. J. McClung, Appl. Phys. Lett. 1969, **14**, 159-160 (1969).

[37] . S.A . Madbouly , A. Lendlein, *Adv Polym Sci* ,2010, **226,** 41

[38] . W. D. Callister. Composites, chapter 16, page 527. Material Science and Engineering an Introduction. John Wiley and Sons, Inc., sixth edition, 2003.

[39] . S. Ramakrishna, J. Mayer, E. Wintermantel, K. M. Leong. *Comp. Sci. Tech*, 2001, **61**,1189

[40] . J Parisien "Current Techniques in Arthroscopy" 1998, Thieme Medical Publishers NY, USA.

[41] . P.W. Grutter, E.G. McFarland, B.A. Zikria, Z. Dai, S.A Petersen , *Amer. J. Sports Med.* 2010,**38**,1706

Chapter 2

Objectives

In the last decade, the remarkable sensory capability of SMPs has lead to their use as 'intelligent' materials, and they are already considered a critical component of materials in engineering applications. [1-3]Currently, minimally invasive surgeries (MIS) use shape memory alloy (SMA) based devices for interventional treatments. Minimally invasively delivered SMA devices have a proven history of improved outcomes when potentially fatal conditions such as cranial aneurysms, aortic aneurysms and other vascular abnormalities such as arteriovenous malformations (AVM) are treated.[4] SMAs such as Nitinol have several drawbacks that include low recoverable strains (8%) and high modulus (83 GPa). These drawbacks limit the range of potential applications by imposing significant device design constraints and limitations associated with material properties and design. Biocompatible and biodegradable SMP systems will considerably enhance the device options available for a range of potential biomedical applications while enabling a plethora of new minimally invasive surgery (MIS) options where, in the past, open surgery was the only option. [4-6]

Also, over the last decade, there has been a renewed interest in the study of crosslinked thiol-ene and thiol-acrylate click reaction polymer systems. [7-9]These click-reaction polymer systems have been shown to perform as an excellent substrate for potential applications in fields that vary from surface coatings to tissue engineering. The thiol-ene and thiol-acrylate click chemistries are unique and offer advantages that include rapid polymerization, low volume shrinkage and shrinkage stress and the formation of homogeneous networks. [10] The overarching goal of this research was to formulate and evaluate polymer systems with properties that can be designed by

varying the thiol, ene and acrylate monomers used and by controlling the stoichiometery of the monomer mix. In doing so, we have developed and characterized a novel two-stage reactive polymer network platform that can be tailored to have optimum thermomechanical properties to suit a range of potential applications that vary from potential biomedical devices to optical storage systems . The specific aims of this research are:

Specific Aim #1: Develop and characterize thiol-ene reaction systems as SMPs for biomedical applications.

Thiol-ene systems were formulated and evaluated for shape memory, shape fixity, free strain recovery, thermomechanical and mechanical properties to demonstrate their suitability as SMPs.

Specific Aim #2: Develop and characterize a novel two-stage reactive thiol-acrylate platform for controlling polymer properties and behavior.

A novel dual –network forming materials platform is developed whereby a network is formed in stages from two distinct and orthogonal reaction mechanisms. The first stage polymerization reaction is a Michael addition reaction that forms a polymer network with controllable material properties. Subsequently, a second stage photopolymerization reaction is initiated, and this reaction results in a final polymer that achieves a second, independent set of physicochemical

properties. Three specific applications were evaluated to demonstrate the broad applicability of the dual network forming platform:

2.1 Shape Memory Polymers

2.2 Impression Materials

2.3 Optical systems

Specific Aim #3: Formulate and characterize two-stage reactive composite systems

Composite two-stage reactive systems reinforced with different continuous fiber reinforcements and micron size particle reinforcements were developed and they were seen to exhibit increased modulus at the end of the stage 1 and stage 2 cures without significantly increasing the glass transition temperature.

Specific Aim #4: Formulate and characterize two-stage reactive thiol-acrylate systems as SMPs for orthopedic biomedical applications.

Two-stage reactive thiol-acrylate systems were developed and characterized for use in orthopedic biomedical applications. The dual network forming shape memory polymer system had a first set of distinct mechanical properties enabling optimum deployment of a minimally invasively delivered orthopedic device and a second set of properties, that can be achieved *in situ*, enabling its use as an orthopedic device.

In Specific Aim 1, thiol-ene polymer networks were compared to a commonly utilized acrylic shape memory polymer. Thermomechanical and mechanical analysis were used to characterize and demonstrate that thiol-ene based shape memory polymer systems have comparable thermomechanical properties while also exhibiting a number of advantageous properties due to the thiol-ene polymerization mechanism. The resulting thiol-ene shape memory polymer systems are tough and flexible as compared to the acrylic counterparts.

In Specific Aim 2, we sought to address the primary drawback of shape memory polymer systems, especially for thermally triggered SMPs used in biomedical applications which are their lack of modulus in their deployed state. [11] Fundamental to the shape changing transition is a characteristic drop in the modulus of the material associated with undergoing the glassy to rubbery transition. The SMP modulus in its rubbery state is orders of magnitude less than the modulus in the glassy state. Approaches to increase the rubbery modulus often result in compromised shape memory properties, which severely restrict their potential as a device that can be minimally invasively delivered. To address this limitation, thiol-acrylate dual network forming systems were formulated and characterized, whereby the increase in modulus in the polymer system was attained without compromising shape memory behavior. In addition, we demonstrated that the dual network forming polymer systems represent a new technology platform can be used for a wide range of applications. Two other applications were demonstrated; dual- network forming impression materials and optical storage devices.

The studies in Specific Aim 3 were focused on formulating and characterizing two-stage reactive composite materials. Composites have long been used in polymer systems to enhance mechanical properties when compared to the neat polymer. [12] In the two-stage reactive systems formulated here, different acrylates were used to enhance the mechanical properties of the stage 1 polymer without significantly impacting the glass transition temperature and other properties of the polymer.

Finally, in Specific Aim 4, a dual network forming polymer network was designed and tested as a suture anchor system.[13]

2.2 Reference

[1] . P.T. Mather, X Luo, I.A. Rousseau, *Ann. Rev. Mater. Research*. 2009, **39**, 445

[2] . C. Liu, H. Qin, P.T Mather, *J. Mater. Chem.* 2007**, 17**, 1543

[3] . C.M. Yakacki, R. Shandas, D. Safranski, A.M. Ortega, K .Sassaman, K. Gall, *Adv. Funct. Mater.* 2008 , **v**,2428

[4] . W.J. van Rooija , M. Sluzewskia, Am. J. Neuro. Radio.2007, **28**,368

[5] . A. Lendlein, R. Langer, *Science*, 2002, **296**,1673

[6] . C.M. Yakacki, R.Shandas,C. Lanning, B. Rech, A. Eckstein, K.Gall, *Biomaterials*, 2007,**28**,2255

[7] . C.E. Hoyle, C.N. Bowman, *Angew. Chem. Int. Ed.* 2010, **49**, 1540

[8] . N. B. Cramer, C. N. Bowman, *J. Polym. Sci. Part A* 2001, **39,** *3311.*

[9] . N.B.Cramer, J.P. Scott, *C.N.* Bowman, *Macromolecules*, 2002, **35**, 5361

[10] . N. B. Cramer, C. L. Couch, K. M. Schreck, J. A. Carioscia, J. E. Boulden, J. W. Stansbury, C. N. Bowman, *Dent. Matr*, 2010, **26**,21

[11] . P.T. Mather, X. Luo, I.A. Rousseau, *Ann. Rev. Mater. Research*. 2009, **39**, 445

[12] . S. Ramakrishna, J. Mayer, E. Wintermantel, K. M. Leong. *Comp. Sci. Tech*, 2001, **61**,1189

[13] . P.W. Grutter, E.G. McFarland, B.A. Zikria, Z. Dai, S.A Petersen , *Amer. J. Sports Med.* 2010,**38**,1706

Chapter 3

Photopolymerized Thiol-Ene Systems as Shape Memory Polymers

In this study we introduce the use of thiol-ene photopolymers as shape memory polymer systems. The thiol-ene polymer networks are compared to a commonly utilized acrylic shape memory polymer and shown to have significantly improved properties for two different thiol-ene based polymer formulations. Using thermomechanical and mechanical analysis, we demonstrate that thiol-ene based shape memory polymer systems have comparable thermomechanical properties while also exhibiting a number of advantageous properties due to the thiol-ene polymerization mechanism which results in the formation of a homogeneous polymer network with low shrinkage stress and negligible oxygen inhibition. The resulting thiol-ene shape memory polymer systems are tough and flexible as compared to the acrylic counterparts. The polymers evaluated in this study were engineered to have a glass transition temperature between 30 and 40 ºC, exhibited free strain recovery of greater than 96% and constrained stress recovery of 100%. The thiol-ene polymers exhibited excellent shape fixity and a rapid and distinct shape memory actuation response.

3.1 Introduction

Shape memory materials are materials that, after deformation, are able to recover their initial shape upon exposure to a designated stimulus, such as temperature change. The reversion of a deformed shape memory material to its original shape upon heating has a vast range of potential applications in biomedical devices. For example, the shape memory alloy (SMA) Nitinol has been used extensively in implantable biomedical devices, particularly in stents, as the capacity for collapsing an otherwise unwieldy device and returning it to its original shape *in situ* enables

minimally-invasive delivery approaches for device implantation. [1] SMA-based devices have several drawbacks associated with high materials cost, limited thermomechanical property control and limited fatigue resistance. Additionally, the maximum strain that can be stored and recovered by SMAs is limited to approximately 8%, which limits the ability of SMAs to be used in certain applications. [2, 3]

The shape memory capabilities that have been demonstrated in polymeric materials, on the other hand, are extremely versatile. Given the design flexibility that is possible through appropriate formulation of polymer networks and composites, shape memory polymers (SMPs) are designed to meet a wide range of thermomechanical property specifications, including strain deformations of up to 800%. [2] SMPs possess several additional advantages in comparison to SMAs including excellent processability, low relative density, and exceptional flexibility in material property tunability. [2-5] These inherent polymeric material advantages have been exploited in several SMP-based biomedical applications, including the use of degradable SMPs to eliminate the need for any implant removal procedures. [5] Additionally, since the crosslinked polymers modulus in its rubbery state is primarily dictated by the crosslink density, this modulus is readily tuned to match the tissue modulus at the implant site or another desired specification. [5, 6] Further, implanted polymeric devices may also act as convenient drug-delivery vehicles where therapeutic agents are readily incorporated in polymeric matrices that enable subsequent and targeted drug delivery. [6]One significant drawback of a polymer based SMM is the low modulus it achieves following shape change. The poor mechanical strength of the current shape memory polymer systems in its rubbery state prevents implementation in a number of potential biomedical applications where high modulus post-deployment is required.

Processing polymers to transform them from their temporary shape to their 'permanent' shape is also relatively simple when compared to metal alloys. Casting a SMP in its transient, typically condensed shape is achieved simply by heating the polymer above its glass transition temperature (T_g), deforming it into its desired transient form, and then quenching the polymer in this transient shape to a temperature below its T_g. Once the polymeric material is again heated to a temperature near or exceeding its T_g, the deformed polymer reverts to its original, desired final shape. SMPs are readily designed to have a varying range of transition temperatures over which the shape change response occurs. By contrast, in alloys, programming the material into its temporary shape involves processing at much higher temperatures and high pressure. [2,3]

Photopolymerized (meth)acrylates represent an exciting class of SMP systems. [7-10]The ability to control the polymerization and initial polymer shape readily through photoinitiated polymerization is attractive from both the design and manufacturing perspectives. One particularly attractive option is that photopolymerization, because of the spatial control of initiation and polymerization, facilitates rapid prototyping of patient-specific devices *via* stereolithography. These systems include the use of *tert*-butyl acrylate/diethyleneglycol diacrylate/poly(ethylene glycol) dimethacrylates [7-10] oligo(ε-caprolactone) dimethacrylate/*n*-butyl acrylate [10] and polyurethane-based acrylic systems. [11,12] Shape memory hydrogels have also been developed from acrylic based monomer systems. [13] Significant limitations of the (meth)acrylate-based systems include the formation of a heterogeneous polymer network with a broader than desired temperature range for the glassy to rubbery transition as well as inhibition of the polymerization by oxygen which restricts design and manufacturing options.

Thiol-ene systems on the other hand offer a unique combination of properties that are advantageous for shape memory polymer systems, including rapid polymerization, low volume

shrinkage and shrinkage stress, the formation of homogeneous networks, and insensitivity to oxygen inhibition. [14-23] Thiol-ene systems polymerize uniquely *via* a radical–mediated, step-growth mechanism whereby a thiyl radical adds across a vinyl functional group to generate a carbon-centered radical. The carbon-centered radical undergoes subsequent chain transfer to a thiol group, regenerating the thiyl radical. [15,17] This successive addition/chain transfer mechanism is presented in Scheme 1. The geometric molecular weight evolution resulting from a step-growth polymerization mechanism leads to the formation of a more homogeneous polymer network that result in a relatively narrow glass transition temperature range. [17] The application of thiol-ene systems as shape memory materials for medical devices has not been previously described and is the motivation of this study.

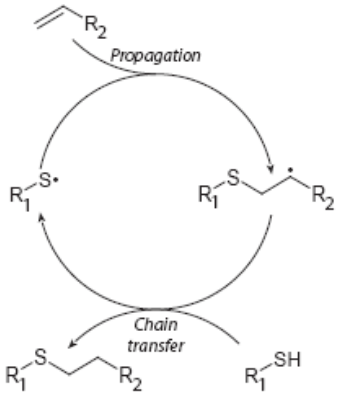

Figure 3.1. Radical step-growth polymerization mechanism of thiol-ene photopolymerization reactions.

For biomedical devices, it is desirable to actuate the SMP thermally using physiological temperatures. In such applications, the deployment of the device occurs typically from a compressed state packaged at ambient temperature. Following deployment into the desired

location, the device is exposed to higher physiological temperatures and reverts to its initial, desired shape.

There are a variety of necessary device design criteria for successful implementation of a shape memory polymer within a biomedical device. The thiol-ene shape memory polymer systems examined here were designed to respond to temperature changes as the stimulus for their shape change. In this work we have characterized shape memory polymer properties and shape memory response by evaluating tensile strength, the glass transition region, free strain recovery, shape fixity, shape recovery sharpness, constrained-stress recovery, and shape recovery. The glass transition region defines the temperature and range over which the polymer actuates. Free strain recovery, shape fixity, shape recovery sharpness, constrained stress recovery, and shape recovery are all measures of the polymer's ability to recover its original shape from a temporary shape.

3.2 Experimental

Materials

Diethylene glycol dimethacrylate (DEGDMA), poly(ethylene glycol 575) dimethacrylate (PEGDMA), and *tert*-butyl acrylate (tBA) were obtained from Sigma Aldrich. Allyl pentaerythritol (APE) was donated by Perstorp, pentaerythritol tetra(3-mercaptopropionate) (PETMP) was donated by Evans Chemetics, isophorone diisocyanate (IPDI) was donated by Bayer, the photoinitiator Irgacure 651 (2,2-dimethoxy-2-phenylacetophenone) was donated by Ciba Specialty Chemicals, and the inhibitor aluminum N-nitrosophenylhydroxylamine (N-PAL) was donated by Albemarle.

Isophorone diurethane thiol (IPDUTh) and Isophorone diurethane 6-allyl ether (IPDU6AE) were synthesized by a procedure adapted from Hoyle and co-workers. [18,19]

IPDUTh was synthesized by mixing one equivalent of isophorone diisocyante with two equivalents of pentaerythritol tetra(3-mercaptopropionate) and 0.05 wt% triethyl amine as a catalyst. The mixture was held at 60 °C until the isocyanate group was reacted to greater than 99% as determined by monitoring the infrared isocyanate peak at 2260 cm^{-1}. The reaction forms a series of oligomers with the idealized, average product shown in Figure 1. IPDU6AE was synthesized from a reaction of one equivalent of isophorone diisocyanate with two equivalents of allyl pentaerythritol (APE) with 0.05 wt% dibutyl tin dilaurate as the catalyst. The mixture was held at 60 °C until the isocyanate group was reacted to greater than 99% as determined by monitoring the infrared isocyanate peak at 2260 cm^{-1}. Structures for all monomers utilized in this study are shown in Figure 1.

The thiol-ene systems were all mixed as 1:1 stoichiometric mixtures of thiol to ene functional groups. Samples contained 1 wt% Irgacure 651, 0.1 wt% N-PAL and were cured at 8 mW/cm^2 using a UV lamp (Black-Ray Model B100AP).

Polymer Coil Fabrication

A mold for the fabrication of polymer coils consisted of a threaded Teflon cylinder inserted in a tight-fitting glass tube. The formulated resin mixture was introduced into the mold and was photopolymerized *in situ* using a UV lamp (Black-Ray Model B100AP). After curing, the glass tube was broken and the polymer was carefully removed from the mold.

Shape Memory Programming and Recovery

The coils were heated to 10 °C above their T_g and programmed into their temporary, extended tube-like shape by constraining them inside a straight catheter tube. The polymer was cooled to -5 °C in a freezer and was held within the tube for one week in this extended geometry. The polymer was then removed from the tube, observed at room temperature and then placed in

an oven maintained 10 °C above the T_g of the polymer. The time taken for the polymer to revert back into its original shape was recorded by visual observation.

Dynamic Mechanical Analysis (DMA)
DMA experiments were performed using a TA Instruments Q800 DMA.

Glass transition temperature (T_g) was determined from polymer samples with dimensions 7 × 3.5 × 1 mm. Sample temperature was ramped at 3 °C/min from -15 to 75 °C with a frequency of 1 Hz and a strain of 0.1% in tension. The T_g was assigned as the temperature at the tan δ curve maximum. The rubbery modulus values were determined at a temperature 25 °C above the T_g and the T_g width was measured as the full width at half height (FWHH) of the tan δ peak.

Free Strain Recovery, shape fixity and shape recovery sharpness were determined from fully cured samples with dimensions of 10 x 5 x 1 mm. For the free strain recovery tests, the polymers were held at a temperature 5 °C above the T_g of the system and strained in tension between 10 and 20 percent (always making sure to stay within the linear regime). The maximum strain was noted as ϵ_m. While maintaining the strain, the polymers were cooled to -10 °C at 20°C per minute. The force was then maintained at zero and the strain on unloading the polymer was recorded (ϵ_u). The strain recovery was observed as the temperature was increased to 25 °C above the T_g at the rate of 3 °C/min. The final strain of the system post recovery was recorded as ϵ_p. Free Strain recovery was defined as $R_r(\%) = (\epsilon_u - \epsilon_p)/(\epsilon_m - \epsilon_p) * 100$. Shape fixity is given by $R_f(\%) = (\epsilon_u/\epsilon_m)*100$ and shape recovery sharpness defined by $v_r = R_r/\Delta T$, where ΔT is a measure of the width of the transition and is the temperature range from the onset of the recovery to its to completion.

Constrained Stress Recovery was determined from cylindrical samples measuring 9 mm in diameter and 9 mm in length. Samples were strained in compression at 10 % at a rate of 1×10^{-3} s^{-1} at T_g. Samples were subsequently cooled to -10 °C and held for 30 minutes. At the end of

this period, the force applied on the sample was removed. The sample was then heated at the rate of 2 °C/min back to its T_g and maintained at this temperature for 30 minutes. The stress exerted by the polymer at its T_g was measured.

Materials Testing System (MTS)
Tensile strength measurements were conducted on an Instron Universal Testing Machine (Insight 2.0). Dog bone shaped samples of dimensions 40 × 6.5 × 1 mm were used. The initial separation of the system was set at 30 mm and a crosshead speed of 3 mm/min was applied.

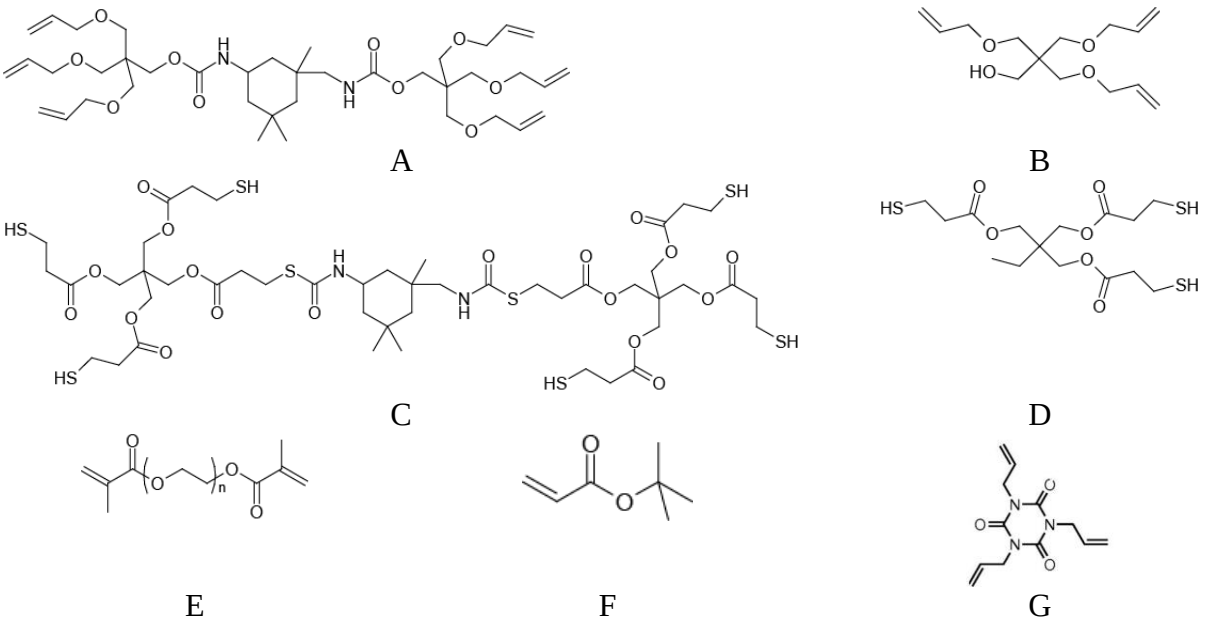

Figure 3.2. Monomers used: A) isophorone diurethane-6-allyl ether (IPDU6AE); B) allyl pentaerythritol (APE); C) isophorone diurethane thiol (IPDUT); D) trimethylolpropane tris(3-mercaptopropionate) (TMPTMP); E) diethylene glycol dimethacrylate (DEGDMA, n = 2) poly(ethylene glycol 575) dimethacrylate (PEGDMA, n_{avg} = 13); F) *tert*-butyl acrylate (tBA) and triallyl-1,3,5-triazine-2,4,6-trione (TATATO)

3.3 Results and Discussion

This work evaluates four different thiol-ene polymer systems in comparison with an acrylic polymer control system. The polymer systems chosen for this study exhibited glass transition temperatures in the range of 30 to 35°C, making them suitable for thermally induced biomedical applications. The control polymer system was a previously examined shape memory polymer comprised of 49 wt% *tert*-butyl acrylate (tBA), 0.5 wt% diethylene glycol dimethacrylate (DEGDMA), and 49.5 wt% PEGDMA (tBA/PEGDMA). [7,8] Initially, a commercially available thiol-ene system was studied. The system was comprised of a stoichiometric mixture of pentaerythritol tetra(3-mercaptopropionate) (PETMP) and allyl pentaerythritol (APE). The resulting polymer films exhibited a strong shape memory response. However, the polymer had a low glass transition temperature (7 °C) and was extremely brittle, breaking easily during handling, particularly during removal from the initial molding process. Thiol-ene systems with higher T_g's and tensile strengths such as pentaerythritol tetra(3-mercaptopropionate) (PETMP) and triallyl triazine trione (TATATO) were also considered. However, the PETMP/TATATO system exhibits a T_g much higher than physiological temperatures (55 °C). [21] To obtain tough polymeric systems with T_g closer to the physiological temperature, a thiol-ene system with a tri-thiol (trimethylolpropane tris(3-mercaptopropionate) (TMPTMP) and a tri-ene , triallyl-1,3,5-triazine-2,4,6-trione (TATATO) was formulated. The resulting polymer system had a T_g of 35 °C and excellent shape memory properties and had a tensile modulus of 63 MPa at ambient temperature. The thiol-ene system also had a very narrow T_g width, indicating a more homogenous polymer that is characteristic of thiol-ene systems. The strain at break of this system at ambient was 20 % which is typically the range within which shape memory systems are subject to strain in their temporary shape. To obtain similar thiol-ene

systems which were tough and with T_gs close to physiological temperatures and with a higher strain at break, we also synthesized urethane based thiol and ene monomers. Polyurethanes impart improved toughness to polymers and also have a history of use in shape memory polymers and a record of proven biocompatibility. [11,12] Thiourethane-based thiol-ene polymer films have been shown to possess excellent physical and mechanical properties. [18,20]

Each of the polymer systems was examined for shape memory programming and shape retention. The results are given in Table 1. A comparison of the coil diameter with the mold diameter is detailed to reflect the initial state of the polymer system. Images of polymers after removal from the mold are shown in Figure 2. Subsequently, the polymers were programmed to their temporary shape and then thermally stimulated by heating to 10 °C above their T_g to regain their original shape. The coil diameter was again observed and the percent change from the mold diameter calculated. Figure 3 depicts the procedure by which polymer coils are released from their constrained temporary shape at ambient temperature and subsequently heated to a temperature above their T_g. Ideal shape memory polymer systems will exhibit coil diameters closely resembling that of the mold both before and after programming. For biomedical applications such as cardiovascular stents, shape retention is extremely important to prevent leakage around the edges of the polymer. In comparison with the control tBA/PEGDMA system, the thiol-ene systems exhibit better mold retention both before and after programming and a more rapid and distinct shape memory response (by visual observation). Additionally, the urethane-based thiol-ene systems exhibited excellent toughness as qualitatively determined by their ability to be handled and manipulated without breaking, particularly during mold removal from tightly wound coils. Also, the smallest acrylic coil that could be made from the mold was

limited to >= 1mm and the acrylic coils of smaller diameters broke easily on attempting to remove them from the mold. On the other hand, thiol-ene coils of diameter < 0.70 mm were easily made and removed from the mold.

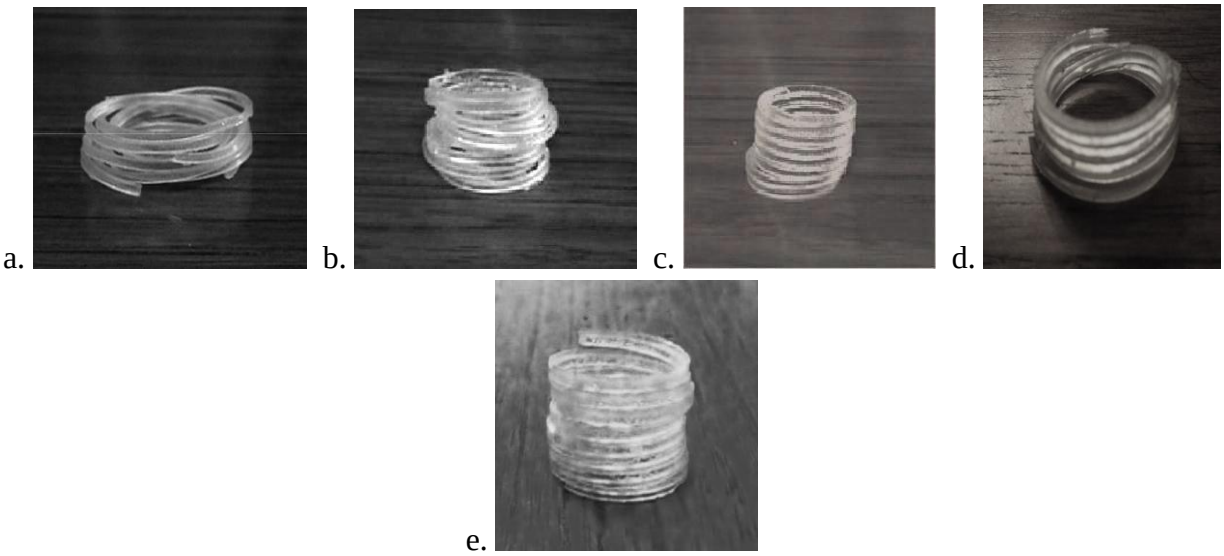

Figure 3.3. Images of polymer coils after removal from the teflon mold; (a) tBA/PEGDMA, (b) TMPTMP/IPDU6AE, (c) IPDUT/APE (d) IPDUT/IPDU6AE and (e) TMPTMP/TATATO

Table 3.1. Coil and mold diameter and percent resemblance to mold for shape memory polymers

Formulation	**Teflon Mold Diameter (mm)**	**Initial Coil Diameter (mm)**	**Coil Diameter after Programming (mm)**	**Percent Resemblance to Mold after Programming**
tBA/PEGDMA	22 ± 1	25 ± 1	26 ± 2	118%
TMPTMP/TATATO	22 ± 1	21 ± 1	21 ± 1	97%
TMPTMP/IPDU6AE	22 ± 1	22 ± 1	22 ± 1	100%
IPDUT/IPDU6AE	22 ± 1	19 ± 2	22 ± 1	101%
IPDUT/APE	22 ± 1	21 ± 1	21 ± 2	97%

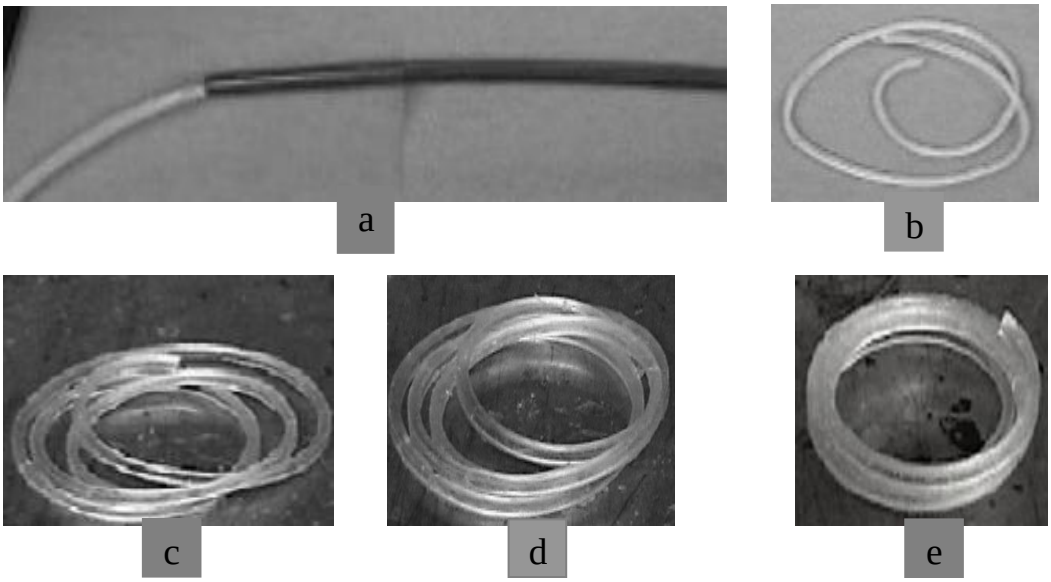

Figure 3.4. The process followed to quantify shape memory behavior is outlined in the coil images of the IPDUT/APE polymer system. (a) The polymer coils are heated to 10°C above their T_g and then constrained in tubing. The polymers are then cooled below their T_g to -5°C and stored for 1 week in the tubing. (b) The polymers are released from the tubing at ambient temperature, where upon they were observed for 4 minutes. Polymers were then placed in an oven maintained 10°C above their T_g. The time taken for the coils to form was recorded. Coil images were recorded at (c) 4 minutes, (d) 4.5 minutes, and (e) 5 minutes.

Table 3.2 details the rubbery storage moduli and glass transition temperatures of the polymer systems evaluated in this study. Shown in Figure 4 is a representative storage modulus and tan δ versus temperature curve of the control tBA/PEGDMA system and the IPDUT/APE system. As seen in Figure 4, the modulus decreases rapidly as the polymer is heated through the glass transition. It is this decrease in modulus that enables mobility within the polymer thereby inducing the shape memory actuation. The tan δ curves demonstrate that the T_g of the urethane thiol-ene polymer systems are comparable to that of the tBA/PEGDMA control. The rubbery moduli of the TMPTMP/TATATO, IPDUT/APE and the TMPTMP/IPDU6AE are both higher

than the control and exhibit better mold retention than the tBA/PEGDMA system. However, the IPDUT/IPDU6AE system exhibits the lowest rubbery modulus while still exhibiting much better mold retention than the tBA/PEGDMA system. The narrow T_g width (12°C) of the pure thiol-ene system, TMPTMP/TATATO indicates the formation a of homogenous polymer. However the thio-urethane systems show a T_g width that is comparable to the acrylic control system

Table 3.2. Rubbery moduli at T_g + 25 C along with T_g and T_g width of the shape memory polymer systems.

Formulation	**Rubbery Modulus (MPa)**	**T_g (°C)**	**T_g Width (°C)**
tBA/PEGDMA	12 ± 1	35 ± 3	24 ± 4
PETMP/APE	30 ± 3	7 ± 1	9 ± 2
PETMP/TATATO	24 ± 1	55 ± 3	14 ± 1
TMPTMP/TATATO	17 ± 1	35 ± 2	12 ± 2
IPDUT/APE	19 ± 4	33 ± 3	18 ± 3
IPDUT/IPDU6AE	7 ± 1	35 ± 3	30 ± 2
TMPTMP/IPDU6AE	17 ± 3	34 ± 4	25 ± 3

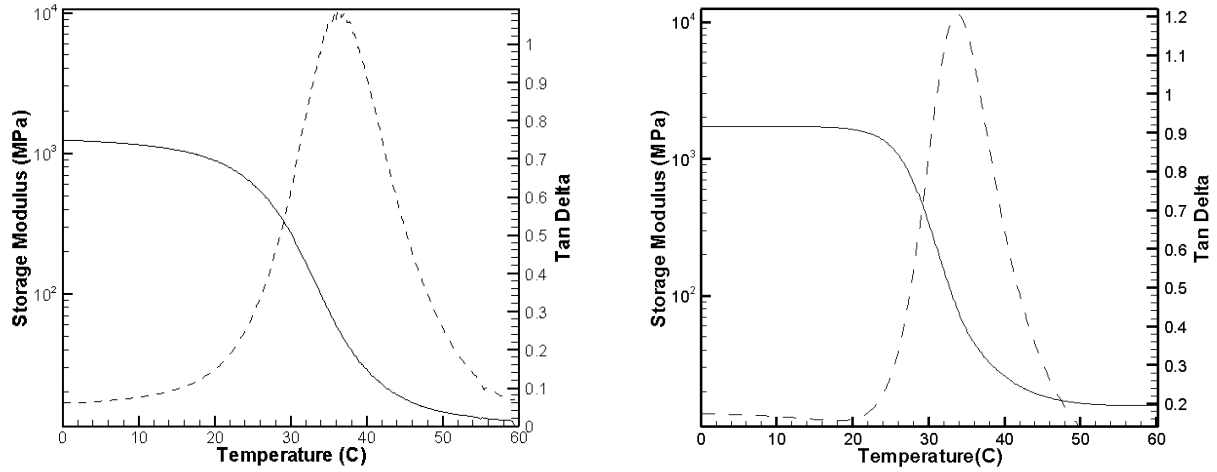

(a) (b)

Figure 3.5. The graphs above shows the storage modulus (—) and tan δ (— —) versus temperature curves for (a) the control shape memory polymer system and (b) a representative thiol-ene system (TMPTMP/TATATO).

Table 3.3 details the polymer tensile modulus and strain at break of the polymer systems. This test was performed at room temperature to determine how the systems would fare in typical ambient conditions under which the systems may be subject to processing and manufacturing events. The tensile tests showed that the TMPTMP/TATATO system was extremely tough at room temperature (63 MPa) and that although the thiol-ene systems exhibited a uniformly strong shape memory response, there were no concomitant modulus and elongation properties of the polymers correlating directly to the enhanced shape memory behavior. The range of moduli of biological tissue can vary from 20 GPa (bone) [24] to 1 kPa (eye). [25] As the modulus values of biomedical implants and devices are normally engineered to match the immediate *in vivo*

environment surrounding the material, this measure provides information on the scope of potential applications for each material.

Table 3.3 Modulus and strain at break for each of the shape memory polymer systems studied.

Formulation	Tensile Modulus (MPa)	Strain at Break (mm/mm)
PETMP/APE	11.4 ± 0.3	0.2 ± 0.1
tBA/PEGDMA	9.3 ± 0.1	1.0 ± 0.2
TMPTMP/TATATO	63 ± 10	0.2 ± 0.1
IPDUT/APE	6.9 ± 0.1	0.7 ± 0.1
IPDUT/IPDI6AE	6.7 ± 0.2	1.0 ± 0.1
TMPTMP/IPDU6AE	11.5 ± 0.1	0.6 ± 0.3

Free strain recovery was also characterized for each of the polymer systems. Free strain recovery is a measure of the ability of the polymer system to recover its permanent shape in the absence of mechanical load as a function of increasing temperature or time. The control polymer system showed a free strain recovery of 96% and the thiol-ene networks exhibited essentially identical free strain recoveries of 97 %. The shape fixity of the polymer systems is an indication of the ability of the polymer network to store a temporary shape at a temperature that is below the transition region. From an application point of view, this measure is an indication of the materials ability to store strain energy within the polymer network before the device is activated. All systems evaluated consistently showed shape fixity of ~ 97 %. The shape recovery sharpness

gives an indication of the breadth of the transition within which the polymer system would go from its temporary stored shape to its permanent shape. Smaller shape recovery sharpness indicates a rapid transition of the polymer from its stored shape to its final shape. The shape recovery sharpness of the thiol-enes systems were seen to be 3 %/°C, a value comparable to the acrylic control network and to other documented shape memory systems where other SMPs have been found to exhibit recovery sharpness values that range from 1.8 to 4.2 %/°C. [9] The temperature which marked the onset of the free strain recovery of the polymer systems indicates that the shape recovery process for all of the systems began at a temperature of ~15 °C. The onset of shape recovery at a temperature a few degrees below ambient temperature indicates that the polymer will have to be constrained at ambient temperature to maintain its ability to go from its temporary shape to its final shape. This information will impact the storage of these shape memory systems which are designed to activate at body temperature. It has been shown that the onset of strain recovery can be controlled depending on the initial temperature at which the shape memory system was set in its temporary shape. [26] The strain recovery characterization of the thiol-ene systems based on their deformation temperature and subsequent recovery temperature and behavior has not been examined in this paper. Both the thiol-ene and acrylic SMPs exhibited similar and very good strain recovery and shape recovery sharpness.

Table 3.4. Free strain recovery, shape fixity, recovery sharpness, and recovery onset temperature and transition width for each of the shape memory polymer systems

Formulation	**Free Strain Recovery (%)**	**Shape Fixity (%)**	**Shape Recovery Sharpness (%/C)**	**Strain Recovery Onset Temp (°C)**	**Strain Recovery Transition Width (°C)**
tBA/PEGDMA	96 ± 1	97 ± 2	3.0 ± 0.3	16 ± 4	37 ± 5
TMPTMP/TATATO	96 ± 3	96 ± 3	5.0 ± 0.3	17 ± 1	20 ± 2
IPDUT/APE	97 ± 2	98 ± 2	3.2 ± 1.0	19 ± 3	35 ± 1
IPDUT/IPDU6AE	97 ± 3	97 ± 2	3.0 ± 1.0	17 ± 2	47 ± 4
TMPTMP/IPDU6AE	97 ± 2	97 ± 2	3.1 ± 0.4	13 ± 3	40 ± 3

Constrained stress recovery tests measure the ability of the polymer to reachieve its final shape while being constrained. Constrained stress recovery is the stress generated by the shape memory polymer when acting against an external constraint during heating. Effectively, this value is a measure of the actuation force exerted by the shape memory polymer at a specific temperature during the shape change from its temporary shape to its permanent shape. The stress exerted by the polymer at T_g demonstrated all the thiol-ene systems generated recovery stresses that were comparable to the 50 wt% crosslinked acrylic network (Figure 5).

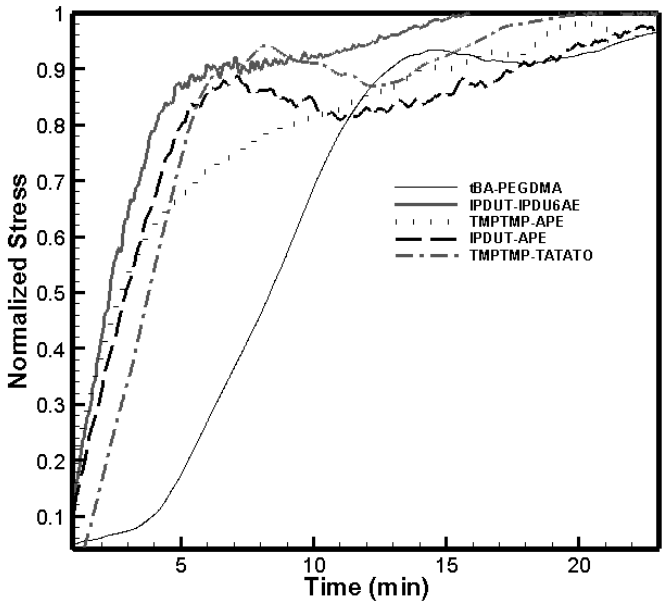

Figure 3.6. Constrained stress recovery versus time for the tBA/PEGDMA control system and the thiol-ene systems IPDUT/APE, IPDUT/IPDU6AE, TMPTMP/IPDU6AE and TMPTMP/TATATO

3.5 Conclusion

This work demonstrates novel thiol-ene based shape memory polymer systems with glass transition temperatures close to physiological temperature. We have evaluated the shape memory response, thermomechanical, and mechanical properties of the thiol-ene systems in comparison with an acrylic-based shape memory system. The thiol-ene polymer systems upon thermal stimulation exhibit a more rapid and distinct shape memory response as well as improved shape retention as compared to the control system. In comparison to the tBA/PEGDMA control system, the thiol-enes were shown to exhibit comparable tensile strength, elongation, and strain recovery. The thiol-ene systems studied in this work demonstrate new shape memory polymer systems that exhibit excellent shape memory response and characteristics and that can be tailored to exhibit a wide range of polymer mechanical properties suitable for biomedical applications.

3.5 Acknowledgments

The authors acknowledge the National Science Foundation CBET 0626023 and NIH (HL T32 HL072738, K24 HL051506).

3.6 References

[1] . T.W. Duerig, D. Stoeckel, A. Pelton, *Mat. Sci. Eng.* 1999, **A273**, 149

[2] . Y. Liu, H. Lv, X. Lan , J. Leng, *Comp. Sci. Tech.* 2009, **69**,2064

[3] . C. Liu, H. Qin, P.T. Mather, *J Mat Chem* 2007,**17**,1543

[4] . T. Xie, I.A. Rousseau, *Polymer*, 2009,**50**,1852

[5] . A. Lendlein, R. Langer, *Science* 2002, **2961**,673

[6] . S. Ghosh, *J Chem. Res*., 2004, 241

[7] . K. Gall C.M. Yakacki, L.Yiping,R. Shandas, N. Willet, K.S. Anseth, *J Biomed Mat Res.*2005,**73A**, 339

[8] . C.M. Yakacki, R. Shandas,C. Lanning, B. Rech, A. Eckstein, K. Gall., *Biomaterials* 2007,**28**,2255

[9] . P.T. Mather, X. Luo, I.A. Rousseau, *Ann. Rev. Mat Res*., 2009,**39**,445

[10] . A. Lendlein, A.M. Schmidt, R. Langer, *Nat. Acad. Sci*. 2001,**98**,842

[11] . G. Baer, T.S. Wilson, D.L. Matthews, D.J. Maitland, *J. Appl. Poly. Sci.* 2007,**103**,3882

[12] . T. Toshisada, H. Noriya, H. Shunichi, *J App. Poly. Sci.* 1996,**60**,1061

[13] . Y. Osada, A. Matsuda, *Nature*, 1995,**376**, 219

[14] . H. Lu, J.A. Carioscia, J.W. Stansbury, C.N. Bowman, *Dent. Mat.* ,2005,**21**,1129

[15] . N.B. Cramer, C.N. Bowman, *J. Poly. Sci.*, 2001,**39**,3311

[16] . C.R. Morgan, F. Magnotta, A.D. Ketley. *J Poly. Sci.*1977,**15**,627

[17] . C.E. Hoyle, T.Y. Lee, T. Roper. *J Poly. Sci.* 2004,**42**,5301

[18] . A.F. Senyurt, C.E. Hoyle, H.Wei, S.G. Piland, T.E. Gould. *Macromolecules* 2007,**40**,3174.

[19] . C.N. Bowman, C.J. Kloxin , *AIChE J.* 2008,**54**,2775-2795.

[20] . L. Qin, D.A. Wicks, C.E. Hoyle, *J. Poly. Sci.* , 2007,**45**,5103

[21] . J.A. Carioscia , L. Schneidewind, C. O'Brien, R. Ely, C. Feeser, N.B. Cramer, C.N. Bowman, *J Poly. Sci.*, 2007,**45**,5686

[22] . C.E. Hoyle, A.B. Lowe, C.N. Bowman, *Chem. Soc. Rev.* 2010, **39**,1355

[23] . C.E. Hoyle, C.N. Bowman, *Angewandte Chemie* ,2010,**49**,1543

[24] . T. Fu, J.L Zhao, K.W. Xu ,*Mat. Lett.* 2007,**61**,330.

[25] . S.A. Koopmans,T. Terwee, J. Barkhof, H.J. Haitjema, A.C. Kooijman, *Investi. Ophthal. Visual Sci.,* 2003,**44**, 250

[26] . C.M. Yakacki, S.Willis,C. Luders, K. Gall, Adv. Eng. Mat. 2008,**10**,112

Chapter 4

Two Stage Reactive Polymer Network Forming Systems

There are distinct advantages to designing polymer systems that afford two distinct sets of material properties – an intermediate polymer that would enable optimum handling and processing of the material, while maintaining the ability to tune in different, final properties that enable the optimal functioning of the polymeric material. In this study, by designing a series of non-stoichiometeric thiol-acrylate systems, a polymer network is initially formed via a base catalyzed Michael addition reaction that proceeds stoichiometrically via the thiol-acrylate 'click' reaction. This self-limiting reaction results in a polymer with excess acrylic functional groups within the network. At a later point in time, the photo-initiated, free radical polymerization of the excess acrylic functional groups results in a highly crosslinked, robust material system. We have formulated and characterized these two stage reactive thiol-acrylate networks that have intermediate stage rubbery moduli and glass transition temperatures that range from 0.5 MPa and -10 ºC to 22 MPa and 22 ºC respectively. The same polymer networks can then attain glass transition temperatures that range from 5 ºC to 195 ºC and rubbery moduli of up to 200 MPa after the subsequent photocure stage. The two stage reactive networks formed by varying the stoichiometeric ratios of the thiol and acrylate monomers have then been shown to perform as substrates for three specific applications- shape memory polymers, impression materials and as materials for writing refractive index patterns.

4.1 Introduction

Numerous polymerization reactions used to form crosslinked polymer networks are extremely complex, often having an initial resin formulation which undergoes a rapid transition

from a relatively low viscosity liquid state to a highly crosslinked, glassy solid state with corresponding changes observed in numerous material properties. The ability to react and form polymer networks with intimate control of the polymerization dynamics and the ultimate material properties has enabled their pervasive use across a broad spectrum of applications and contributed to significant technological advancements. [1-6] The wide range of fields in which polymer networks have become important vary from automobile and aircraft parts to biomedical devices to lithographic imprint materials and optical devices. [2-13] However, for many applications, it would be advantageous to have at least one stage of the polymerization occur through a self-limiting polymerization reaction that forms a stable polymer network with desirable physical attributes that simultaneously maintains the ability, upon application of a second stage curing stimulus, to react further and achieve a second and final set of material properties. Such a system enables the achievement of two distinct and largely independent sets of material properties as might be necessary for multiple stages in the processing and life-cycle of certain applications.

Here, we introduce a polymer system that is formed by two reactions capable of generating distinct first and second stage polymers. The first stage polymer takes advantage of the powerful capabilities afforded by the "click" reaction paradigm to engender a specific, self-limiting reaction that is orthogonal to the desired second stage reaction.[6] While multiple approaches are possible using a variety of reactions, here, we specifically implement the thiol-acrylate Michael addition reaction as the click reaction of choice. [4,7-10] When a mixture of a multifunctional thiol and excess multifunctional acrylate undergoes this reaction, a stoichiometric, self-limiting reaction between the thiol and acrylate functional groups occurs. This approach leaves whatever acrylates were present in excess within the initial formulation as

unreacted acrylic functional groups within an otherwise stable polymer network. In the second stage, in the presence of a photoinitiator and light, the remaining acrylic moieties polymerize to increase the crosslink density significantly wherever and whenever the light is used.

A number of other reactions could readily be used in the first stage including alcohol/isocyanate or thiol/isocyanate reactions to form urethane or thio-urethane linkages or alkyne-azide reactions to form a triazole-containing network. [2,3] For these initial reactions second stage curing is desirably initiated by light exposure to facilitate stability of the initially cured network. Hence, at the completion of stage one and with appropriate selection of monomers, the initial network contains photoreactive, polymerizable moieties such as the acrylates used here or methacrylates, epoxies, or thiols and enes that could participate in the thiol-ene reaction. Here, to avoid the necessity of producing monomers that would need to be functionalized with multiple types of chemical functionalities, we chose to use the thiol-acrylate Michael addition and photoinitiated radical-mediated acrylic polymerization so that the acrylate monomers, when used in excess, would directly participate in both reactions. This approach guarantees the simplest monomer selection and development, takes advantage of the orthogonal nature of the thiol-acrylate Michael addition, and assures to the extent possible that an overwhelming fraction of the initial monomer will be bound into the network at the end of the stage one reaction.

In particular, the thiol-acrylate reaction exhibits a wide range of application versatility due to the multitude of available thiol and acrylate monomers as well as the ability to react by Michael addition reactions or free radical polymerizations. [4,7-11] The Michael addition reaction between a thiol and an acrylate enables the thiol and acrylic monomers to react under relatively facile reaction conditions to yield crosslinked polymer networks. The Michael addition reaction

has been shown to progress robustly to completion under a wide range of conditions that facilitate numerous options with respect to monomer selection, reaction temperature and the presence or absence of solvents, all resulting in sophisticated, uniform polymer networks in conditions where other reactions would not be able to proceed. [7-11] Additionally, the ability of Michael addition reactions to favor complete conversion and rapid cure rates at ambient temperature have made these polymer systems an ideal choice for applications that vary from industrial coatings to drug delivery as well as cell scaffolds and crosslinked hydrogels. [4,13-15] It is well known that in conventional network-forming resins the stoichiometry of the monomers used to form the thiol-acrylate Michael addition networks must be 1:1 to form completely reacted networks. [4, 11,12]

The dual cure system is extremely versatile as simple and judicious variations in the choice of thiol and acrylate monomer types, functionality, and stoichiometric ratios enable a nearly limitless range of initial and final properties. The range of possibilities for this dual cure approach is illustrated herein by developing approaches suitable for three distinct applications that benefit from the formation of a transient polymer network having one set of properties and a final polymer network with distinctly different properties. Despite the range of applications, the robustness of this approach is demonstrated simply by optimizing the thiol: acrylate ratio in the initial formulation while using the same thiol and acrylic monomers in each formulation. The demonstrations of this approach will include a shape memory polymer, a lithographic impression material, and an optical material that serves as a substrate in which to write refractive index patterns. For shape memory polymers, fundamental to the change in shape is a concomitant decrease in modulus of several orders of magnitude as the polymer transitions from the glassy to the rubbery state. For impression materials, the challenge is associated with materials that are

soft and exhibit low shrinkage during the impression stage while also exhibiting high strength and durability in the final stage as these two properties are inversely related. For writing refractive index gradients in optical polymers, low modulus is required to maximize diffusion of the high refractive index material. This same low modulus state renders the material difficult to handle and vulnerable to environmental contaminants necessitating secondary containment. Here, by utilizing a dual cure system, the fundamental drawbacks of all three of these applications are uniquely addressed by maintaining the idealized properties desired for processing (stage 1) while subsequently generating an idealized and orthogonal set of polymer properties for the end application.

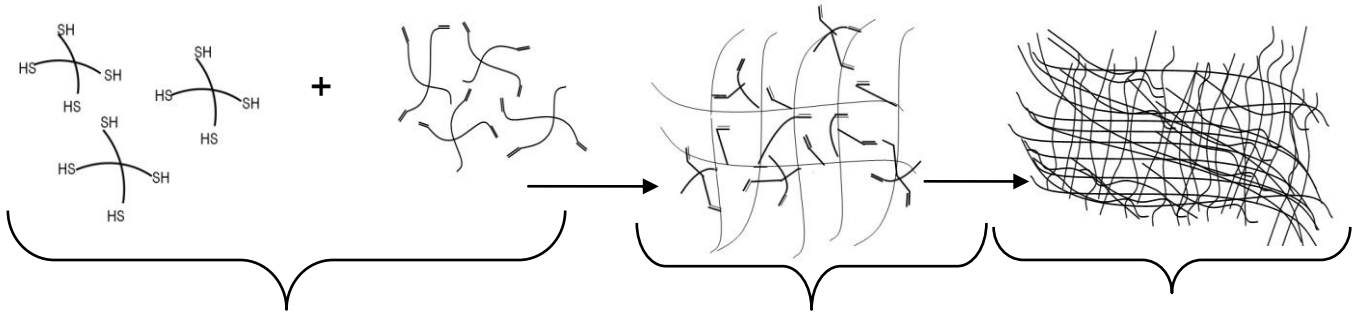

The Stage 1 reaction is a self-limiting click Michael addition reaction between multifunctional thiol and acrylate monomers with an excess of acrylate functional groups.

The resultant Stage 1 polymer is a loosely crosslinked low modulus polymers with idealized properties that are tailored for intermediate polymer processing.

The Stage 2 reaction is a photoinduced acrylate polymerization that achieves rapidly a highly crosslinked high modulus polymer with idealized properties that are tailored for the end polymer application.

Figure 4.1. Methodology for dual-network forming thiol-acrylate systems

Shape Memory Polymers

A shape memory polymer network is one with the unique ability to transition from a temporary, stored shape to a permanent shape upon the application of a stimulus such as temperature or light. [16-19] This shape change capacity is routinely exploited in minimally invasive biomedical applications in devices such as stents, endovascular coils, and orthopedic trauma fixation devices where the formation of a compressed state enables the device to be delivered through an opening that it would not otherwise fit through in its final, end application shape and state. [18] For biomedical systems, the trigger that is routinely applied to promote the final deployment is that of a temperature increase associated with the difference between ambient (or sub-ambient for refrigerated materials) and physiological temperatures. Thus, to perform as shape memory devices for biomedical applications, the glass transition temperature is typically near physiological temperature (i.e., 38 C) which, for traditional materials necessitates a softening of the material and a reduction in the modulus in its deployed state, typically in the range of 1 - 50 MPa. [16-19] This behavior implies that a limitation of biomedical shape memory polymer systems is their lack of mechanical strength and modulus after being deployed in the body due to the necessity of performing while in or near the rubbery regime. [16,19] In contrast to SMPs, the mechanical strength of shape memory NiTinol medical devices can vary from 700 - 2000 MPa. [20] NiTinol shape memory devices such as stents are currently used in minimally invasive treatment of aneurysms and in orthopedic applications such as suture anchors; devices that require a high modulus to function effectively. Generally, because of the fundamental limitations associated with the necessity of undergoing the glass transition, SMPs that are designed to have a high modulus in their rubbery regime often attain it at a cost of reduced strain capacities and compromised shape memory properties. [21-30] In particular, composite shape memory polymer

systems have been seen to increase the overall mechanical strength and modulus of the polymer, but often do so at the expense of shape memory characteristics such as Shape fixity and Shape Recovery.[16,22,28] This trade-off limits the potential biomedical applications for which SMPs can be used, where the ability of the device to be strained into its temporary geometry is an important feature.

Here, we developed dual-cure shape memory polymer system that exhibits an initial set of distinct mechanical properties suitable for deployment of a biomedical device and a second set of properties (high modulus) that are achieved *in situ* by a second stage curing that occurs after deployment and which are appropriate for the long-term success and function of the device.

Figure 4.2. Shape memory polymer coils being deployed from a catheter- the coils are at Stage 1 now and once the coils are deployed in their final shape, the second reaction (Stage 2) can be initiated to increase the polymer modulus significantly.

Lithographic Impression Materials

There is an ever-present need to manufacture smaller devices at lower cost. As an alternative to Imprint Lithography which requires high temperatures for imprinting a pattern with micron and nano-scale resolution, Step and Flash Imprint Lithography (SFIL) has also been a successful

technique for replicating intricate patterns at both the nano- and micro- scale in ambient conditions by utilizing UV light to cure the polymer resin while being pressed against a physical mask which contains submicron size features. [31-34] A challenge in this area for both nano- and micro-patterning is finding an appropriate photopolymerizable material with low viscosity, low shrinkage and the ability to form stable polymer networks that enable mold removal without loss of detail. Although soft and highly flexible molds such as those made from PDMS enable imprinting at reduced pressures, the elastomeric behavior of the polymer can result in a non-uniform negative being formed from the master pattern. Also, as PDMS will swell in most organic solvents that are used to lower its viscosity, this results in further distortion of the master pattern.[31] During the past few years, radical-mediated thiol-ene click reactions have been shown to perform as an excellent substrate for SFIL.[33,34]This Soft lithography technique normally consists of pouring a liquid resin onto the pattern that is to be replicated and UV curing the resin on the patterned master. Once the polymer is cured, the thin film is peeled off the master pattern in a repeatable manner in which a large number of nano-imprints are produced from the same master pattern.

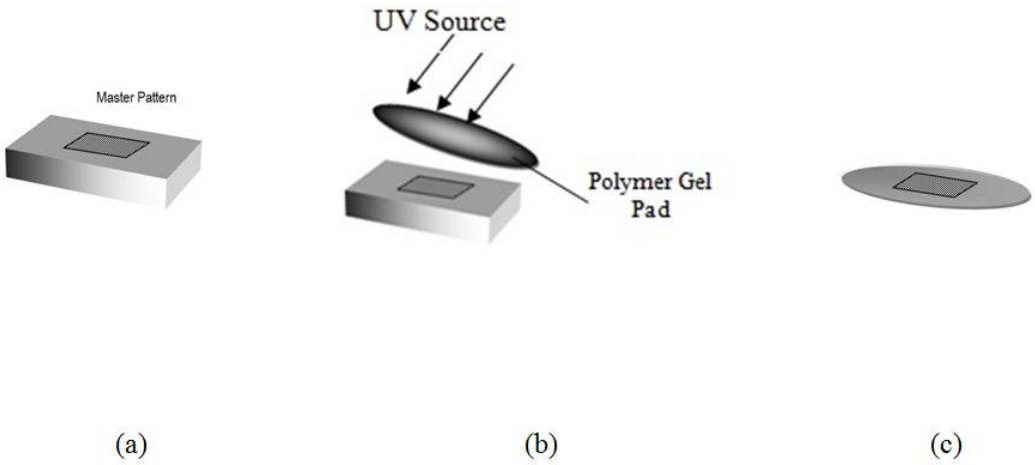

Figure 4.3. A master pattern with a micro-imprint pattern imprinted is utilized as a mold (a). Then the polymer gel pad that is formed after the Stage 1 reaction is placed on the pattern block and UV cured (b). At the end of the Stage 2 cure, the negative of the pattern is imprinted on the polymer pad (c)

This study utilized the thiol-acrylate Michael addition reaction to form a Stage 1 gel that is suitable as an imprint material. At the end of the Stage 1 cure, a thiol-acrylate network is formed that can be used as the imprint material, which, as opposed to a liquid resin, would make this polymer impression material easier to handle and process. The physical master is pressed into the Stage 1 material at ambient conditions and exposed to a UV source, where the Stage 2 reaction is initiated. Once the material is fully cured, the patterned polymer is removed from the master, whereupon an imprint of the pattern is obtained.

Optical Materials

Optical devices formed by patterned refractive index variations in thick (>> 1 mm) solids are difficult to achieve via traditional photoresist methodologies. [35-37] Silver halide photographic emulsions can record holograms with sub 200 nm resolution, but these systems suffer from a need for solvent-based processing, swelling during wet processing, and film thicknesses that are limited to approximately 10 μm. [38] Dichromated gelatin (DCG) is another important holographic material and can achieve index contrasts of approximately 0.1 or greater. However, in addition to requiring complex wet processing , these holograms are extremely sensitive to moisture and must be protected from ambient H_2O to remain stable .DCG can achieve index contrast of approximately 0.1 or greater but must be protected from ambient H_2O to remain stable Self-developing photopolymers can achieve index variations of approximately 0.01 in films of several millimeters without necessitating any solvent-based processing. [39] Structured illumination initiates polymerization, locally depleting monomer and reducing free-volume. This approach drives diffusion of replacement monomer into and/or of binder out of the illuminated region, locally changing the density and the refractive index. After mass transport is completed, a uniform optical flood cure consumes the remaining photo-initiator and monomer, leaving an index-patterned, photo-insensitive structure that is stable to most environmental conditions.

This process must take place within a solid matrix which provides a physical scaffold for the photopolymer structure, allows rapid diffusion of low molecular-weight species, and has the required passive mechanical and optical properties. In "single-component" systems, this matrix is formed by optically or thermally polymerizing a single monomer past its gel point, leaving the remaining photoinitiator and monomer for structuring. Greater control over material properties is obtained by using a separate polymer to form the matrix in a "two-component" approach.

Thin films can be solvent-cast with an inert binder while high quality volumes up to centimeter scale are possible with a thermosetting matrix formed via an orthogonal polymerization. [38, 41] These polymeric materials have been exploited for holographic data storage, optical filters, gradient index lenses, and waveguides. [42-45] However, both the single-component and two-component approaches have a fundamental problem for these applications in that the matrix, which must be above its glass-transition temperature for efficient diffusion, remains so during operation. This rubbery matrix requires a sealed, solid enclosure to make it physically rigid and to suppress in-diffusion of environmental contaminants. Many applications are not compatible with this rubbery, high-diffusion state and instead require a final polymer which is mechanically and chemically robust. The approach reported here addresses this limitation by forming a first-stage polymer matrix with low glass-transition temperature, followed by photo-patterning the desired refractive index pattern, and ultimate crosslinking of the second-stage polymer to yield a glassy polymeric material.

4.2 Experimental

Materials

Pentaerythritol tetra(3-mercaptopropionate)(PETMP) was donated by Bruno Bock, tricyclodecane dimethanol acrylate (TCDDA) was donated by Sartomer, and Ebecryl 1290 was donated by Cytec. Trimethylolpropane triacrylate (TMPTA) was purchased from Sigma-Aldrich. The photoinitiator Irgacure 651 (2,2-dimethoxy-2-phenylacetophenone) was donated by Ciba Specialty Chemicals. All samples contained 0.8 wt% triethyl amine, as a catalyst for the first stage reaction, and 1 wt% Irgacure 651 to initiate the second reaction. Although nucleophilic catalysts such as alkylarylphosphines have been shown to rapidly initiate and complete the

Michael addition reaction efficiently, triethylamine was chosen for this study for the control it afforded over the initial rate of the reaction, allowing processing time while the monomer mixture could be subject to molding. [7-9] For the photopolymerization during the second stage of the reaction, samples were cured at 8mW/cm^2 using a UV lamp (Black-Ray Model B100AP).

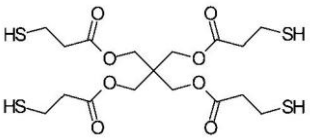

PETMP
pentaerythritol tetra(3-mercaptopropionate)

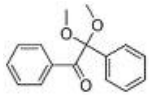

DMPA
2,2-Dimethoxy-2-phenylacetophenone

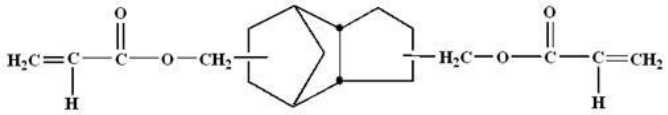

TCDDA

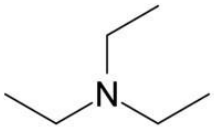

TEA
Triethylamine

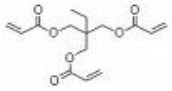

TMPTA
Trimethylolpropane triacrylate

Figure 4.4. Chemical structures of the monomers used in this study.

Dynamic Mechanical Analysis (DMA)

DMA experiments were performed using a TA Instruments Q800 DMA.

Glass transition temperature (T_g) was determined from polymer samples with dimensions of 10 x 3.5 x 1 mm. Sample temperature was ramped at 3^{o}C/min from -50 to 300^{o}C with a frequency of 1 Hz and a strain of 0.01 % in tension. The T_g was assigned as the temperature at the tan δ curve maximum. The rubbery modulus was measured at T_g + 35 at the end of stage 1 and T_g+ 65 at the end of Stage 2.

Free Strain Recovery, shape fixity and shape recovery sharpness were determined from fully cured samples with dimensions of 10 X 5 X 1 mm. For the free strain recovery tests, the polymers were held at a temperature 5^{o}C above the T_g of the system and strained in tension between 20 and 40 percent (always making sure to stay within the linear regime). The maximum strain was noted as ε_m. While maintaining the strain, the polymers were cooled to -25^{o}C at 20^{o}C per minute. The force was then maintained at zero and the strain on unloading the polymer was recorded (ε_u). The strain recovery was observed as the temperature was increased to 25^{o}C above the T_g at the rate of 3 ^{o}C/min. The final strain of the system post recovery was recorded as ε_p. Free strain recovery was defined as $R_r(\%) = (\varepsilon_u - \varepsilon_p)/(\varepsilon_m - \varepsilon_p)* 100$. Shape fixity is given by R_f $(\%) = (\varepsilon_u/ \varepsilon_m) *100$, and the shape recovery sharpness is defined by $v_r = R_r/\Delta T$, where ΔT is a measure of the width of the transition and is the temperature range from the onset of the recovery to its completion.

Polymer Coils

For the fabrication of polymer coils, a Teflon cylinder was inserted into a tight-fitting glass tube. The monomer mixture was added into the mold and the stage 1 cure was allowed to proceed for approximately 48 hours. The glass tube was broken and the Stage 1 polymer was carefully removed from the mold. For second stage curing, coils were photopolymerized using a UV lamp (Black-Ray Model B100AP) at 8 mW/cm^2 for 10 minutes.

Fourier Transform Infrared Spectroscopy (FTIR)

FTIR experiments were performed using a Nicolet Magna 760. Thiol peak absorbance was measured at 2570 cm^{-1} and acrylate peak absorbance was measured at 814 cm^{-1}. Samples

were prepared and mounted between salt crystals, and spectra were taken before the addition of initiator (TEA), and the thiol and acrylate peak areas were recorded as A_{thiol} and $A_{acrylate}$, respectively. Samples were then prepared with TEA, mounted between salt crystals, and stored for 48 hours to allow substantial time for the first stage curing. After 48 hours, spectra were taken, and the peak areas for the thiol and acrylate were recorded, both before and after exposure to UV light for 10 minutes. Thiol conversion was defined as $\alpha_{thiol}= 1- ((A_{thiol})_{t=final}/(A_{thiol})_{t=initial})$. Acrylate conversion is given by $\alpha_{acrylate}= 1- ((A_{acrylate})_{t=final}/(A_{acrylate})_{t=initial})$.

Rheology

Rheology experiments were performed using a TA Instruments ARES rheometer. Samples were prepared on 8mm parallel geometry plates for dynamic testing. A dynamic time sweep test was performed using a strain of 0.2% and a frequency of 10Hz, with data points being recorded once every second. The first stage was observed for up to 100 minutes after the monomers were mixed and then samples were concurrently exposed to UV light for 10 minutes 8 mW/cm^2 during testing. The evolution of the modulus from Stage 1 to Stage 2 was measured.

4.3 Results and Discussion

Thiol-acrylate polymer systems consisting of a tetrathiol (PETMP), a triacrylate (TMPTA), and a diacrylate (TCDDA) were designed to demonstrate the potential value of the dual cure behavior in a range of applications. Each of the application demonstrations comprises simple formulation manipulations; however, the differences in polymer properties and application potential are dramatic. To demonstrate this proof of concept, the thiol-acrylate systems were prepared with 1:1, 1:1.5 and 1:2 stoichiometric mixtures of thiol to acrylate functional groups, with the 1:1

systems serving as the control. Basic dual cure capability was demonstrated by evaluating functional group conversion, glass transition temperature, and modulus after both the first and second stages of polymerization. In the 1:1 systems, both the thiol and acrylate functional groups achieve nearly complete conversion in the first polymerization stage and no significant change in modulus or glass transition temperature was expected between the first and second stages of cure for the stoichiometeric systems. Table 1 shows conversions for each of the polymer systems after the stage 1 Michael addition reaction and the stage 2 acrylic homopolymerization. As expected, due to the click nature of the thiol-acrylate Michael addition, the thiol achieves nearly 100% conversion for all stoichiometric ratios during the stage 1 curing, and the stage 1 acrylate conversion is dictated by the stoichiometric amount of thiol initially present for this reaction stage. During the second stage of curing, the acrylate conversion increases significantly due to the radical-mediated homopolymerization.

Polymer T_g and modulus are shown in Tables 3 and 4. Both the 1:1.5 and 1:2 systems demonstrate a significant increase in both T_g and modulus during the 2^{nd} stage curing, in contrast to the minimal response in the 1:1 systems that serve essentially as controls. The control thiol-acrylate systems with 1:1 stoichiometric ratios represent the highest achievable T_g and modulus for a given set of monomers at the end of Stage 1; however, these polymers also represent a minimum for the Stage 2 modulus and glass transition temperature. Stage 1 systems exhibited a T_g of 22 °C for the PETMP/TMPTA system and 15 °C for the PETMP/TCDDA system. Increasing the amount of acrylate reduces the initial T_g to 2 °C and -6°C, respectively, for the 1:1.5 and 1:2 systems. The excess acrylate in these systems reduces the Stage 1 T_g and modulus

values, but when Stage 2 curing is enabled, this difference results in dramatic increases in T_g and modulus with the 1:2 systems showing the greatest increase in modulus due to the presence of the greatest amount of unreacted acrylate available for curing in the second stage. The response seen during second stage curing is directly related to the amount of acrylate functional groups remaining after the first reaction.

Table 4.1. Thiol and acrylate conversions after Stage 1 and Stage 2 curing. The PETMP/TMPTA samples contain varying stoichiometeric ratios of thiol to acrylate functional groups, with 0.8 wt% TEA to catalyze the Stage 1 cure and 1 wt% Irgacure 651 for the Stage 2 cure. A UV Black ray lamp with the power set to 8 mw/cm^2 was used to initiate the Stage 2 photopolymerization.

Formulation	**Thiol-Acrylate Ratio**	**Stage 1**		**Stage 2**	
		Thiol Conversion (%)	**Acrylate Conversion (%)**	**Thiol Conversion (%)**	**Acrylate Conversion (%)**
PETMP/TMPTA	1:1	97 ± 2	99 ± 1	97± 2	99 ± 1
	1:1.5	98 ± 2	61 ± 5	99 ± 1	98 ± 2
	1:2	96 ± 4	52 ± 5	95± 3	95 ± 5

Table 4.2. Thiol and acrylate conversions after Stage 1 and Stage 2 curing. The PETMP/TCDDA samples contain varying stoichiometeric ratios of thiol to acrylate functional groups, with 0.8 wt% TEA to catalyze the Stage 1 cure and 1 wt% Irgacure 651 for the Stage 2 cure. A UV Black ray lamp with the power set to 8 mw/cm^2 was used to initiate the Stage 2 photopolymerization.

Formulation	**Thiol-acrylate Ratio**	**Stage 1**		**Stage 2**	
		Thiol Conversion (%)	**Acrylate Conversion (%)**	**Thiol Conversion (%)**	**Acrylate Conversion (%)**
PETMP/TCDDA	1:1	96 ± 3	98 ± 1	96 ± 3	99 ± 1
	1:1.5	94 ± 3	65 ± 2	97 ± 1	94 ± 1
	1:2	95 ± 1	53 ± 4	97± 2	97 ± 2

Table 4.3 Dynamic Mechanical Analysis (DMA) shows the distinct rubbery modulus and glass transition temperatures attained at the end of Stage1 and Stage 2 for the PETMP/TMPTA dual-cure polymer systems. The rubbery modulus was measured at Tg + 35°C at the end of Stage 1 and Tg+ 65°C at the end of Stage 2.

Formulation	**Thiol-Acrylate Ratio**	**Stage 1**		**Stage 2**	
		T_g (°C)	**Rubbery Modulus (MPa)**	**T_g (°C)**	**Rubbery Modulus (MPa)**
PETMP/ TMPTA	1:1	22 ± 3	22 ± 5	22 ± 2	20 ± 5
	1.5:1	9 ± 3	14 ± 2	41 ± 6	45 ± 10
	2:1	2 ± 1	9 ± 1	67 ± 2	81 ± 6

Table 4.4. DMA shows the distinct rubbery modulus and glass transition temperatures attained at the end of Stage 1 and Stage 2 for the PETMP/TCDDA dual-cure polymer systems. The rubbery modulus was measured at Tg + 35°C at the end of stage 1 and Tg+ 65°C at the end of Stage 2.

Formulation	**Thiol-Acrylate Ratio**	**Stage 1**		**Stage 2**	
		T_g (°C)	**Rubbery Modulus (MPa)**	**T_g (°C)**	**Rubbery Modulus (MPa)**
PETMP/ TCDD**A**	1:1	16 ± 2	7 ± 1	15 ± 1	8 ± 1
	1.5:1	4 ± 2	5 ± 1	27 ± 3	16 ± 2
	2:1	-6 ± 2	2 ± 1	46 ± 2	23 ± 1

Polymer properties, such as glass transition temperature and modulus were characterized for the samples using DMA, as shown in Tables 4 and 5. All experimental systems showed a significant increase in both T_g and modulus during the 2nd stage curing.

Modulus versus irradiation time is shown in Figure 4 where the modulus evolution is compared for the 1:1.5 and 1:2 PETMP-TCDDA and PETMP-TMPTA systems. For the 1:2 systems, the initial modulus is lower than the 1:1.5 system due to the reduced amount of stage 1 curing; however, the subsequent increase in modulus was notably more dramatic, and ultimately, a higher final modulus is achieved (Figure 4). The results show that as the acrylate to thiol ratio increases, the modulus for the first stage polymer decreases, while the modulus for the second stage polymer increases.

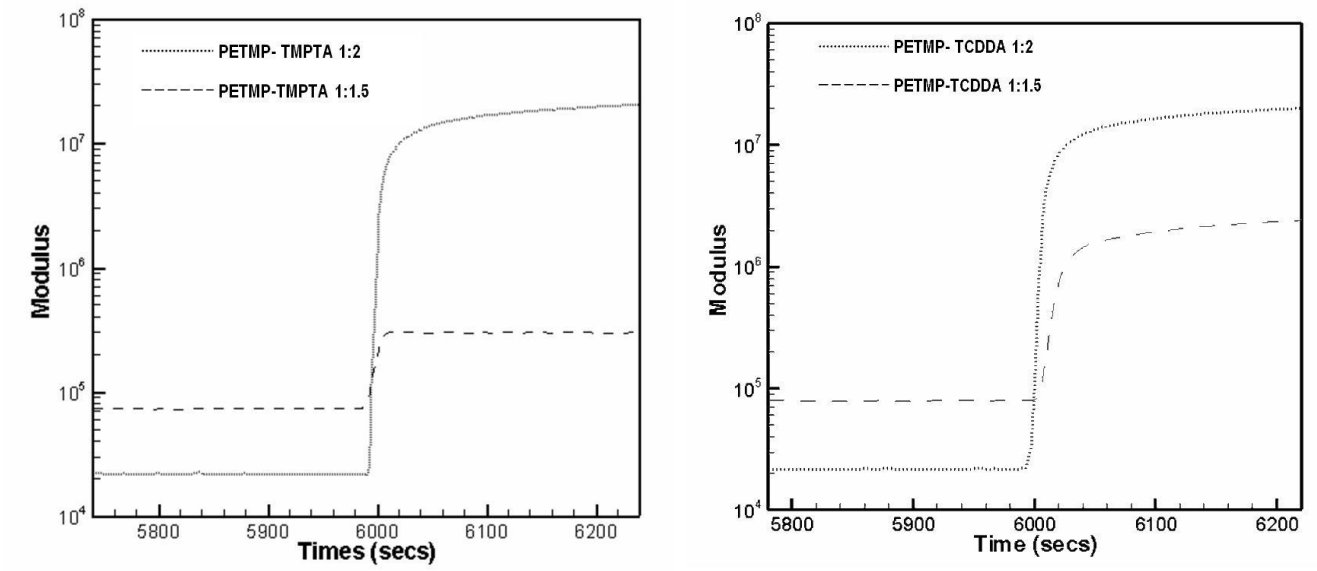

Figure 4.5. Rheology results showing the evolution of modulus from Stage 1 to Stage 2 cure for the PETMP-TMPTA system and the PETMP-TCDDA system. After the Stage 1 cure, at 6000 secs, the exposure to UV light causes radical-mediated acrylate polymerization and a corresponding increase in the modulus.

The results demonstrate that both Stage 1 and Stage 2 polymer properties can be engineered into the polymer network by incorporating simple formulation manipulations related to the monomer

type, functionality, and stoichiometric ratio with initial Stage 1 T_g and modulus values ranging from -6°C to 2 °C and 2 to 9 MPa and Stage 2 T_g and modulus values ranging from 46°C to 67 °C and 23 to 81 MPa. To demonstrate the utility of the independent Stage 1 and Stage 2 properties, three proof of concept application examples are presented with dramatically different requirements for Stage 1 properties and processing and final Stage 2 properties. As discussed previously, these target applications are shape memory polymers, impression materials, and optical materials.

Shape Memory Polymers

To formulate a SMP system, a hexafunctional urethane acrylate (Ebecryl 1290) was incorporated into the monomer resin with the PETMP and TCDDA. Urethane acrylates have been shown to impart improved toughness to polymer networks and also have a history of use in shape memory polymers and a record of proven biocompatibility [16,17]. The theoretical gel point of this off-stoichiometeric system which had a 1 to 1.5 ratio of thiol to acrylate was calculated from the Flory-Stockmayer equation to be 0.30. The Stage 1 reaction forms a shape memory polymer network with initial properties including a 33 °C T_g and an 20 MPa, modulus, that make it a potential polymer system for both biomedical and non-biomedical applications that require a low modulus, high strain shape memory material that can be easily programmed and confined to its temporary shape. Once the shape memory device has been deployed and is in its permanent configuration, the Stage 2 reaction is initiated via UV irradiation and the remaining acrylate functional groups are photopolymerized to achieve the desired Stage 2 material properties *in situ*.

The system utilized here exhibited a Stage 2 Tg of 95 °C. After the Stage 2 cure of the system, at 38 °C the system had a modulus of 1500 MPa. The high Stage 2 modulus at physiological

temperature enables the SMP to be used for potential new applications such as orthopedic devices in which the low modulus of SMPs in their deployed state has prevented them from being used in the past. To characterize this shape memory polymer system fully, free strain recovery, shape fixity, and shape recovery sharpness were evaluated and are presented in Table 5. Free strain recovery is a measure of the ability of the polymer system to recover its permanent shape in the absence of mechanical load as a function of increasing temperature or time. The SMP system showed a free strain recovery of 95%, and this response compares with other SMP system, where strain recovery typically falls between 90-100%.[14]

The shape fixity of a polymer system is an indication of the ability of the polymer network to store a temporary shape at a temperature that is below its transition region. In terms of applications, this measure is an indication of the material's ability to store strain energy within the polymer network before the device is activated. The polymer system consistently showed shape fixity of approximately 97%, which is compares favorably to other shape memory polymer systems , where shape fixity ranges between 80 to 100 % . [13,27]

The shape recovery sharpness gives an indication of the breadth of the transition within which the polymer system would go from its temporary stored shape to its permanent shape. Larger shape recovery sharpness and a narrow strain recovery transition width indicate a rapid transition of the polymer from its stored shape to its final shape. Other SMP systems have been found to exhibit recovery sharpness values that range from 1.8 to 4.2 %/^{o}C. [16] Compared to these polymers, the systems formulated here demonstrated a relatively rapid recovery level of 3%/^{o}C as shown in Table 5.

Table 4.5. Thermo-mechanical shape memory characterization data for two stage reactive SMP system.

Formulation	**Stage1 T_g (°C)**	**Stage1 RubberyModulus (MPa)**	**Stage2 T_g (°C)**	**Stage2 Rubbery Modulus (MPa)**	**Stage2 Modulus At 38 °C (MPa)**	**Free Strain Recovery (%)**	**Shape Fixity (%)**	**Shape Recovery Sharpness (%/C)**
PETMP/ TCDDA/ Ebecryl1290	30 ± 3	21 ± 1	95 ± 8	64 ±8	1520 ± 60	96 ± 1	97 ± 1	3 ± 1

.

Impression Materials

The same thiol-acrylate monomers that were utilized in the SMP system, but in differing stoichiometeric ratios, were used to formulate a polymer system for a lithographic/impression gel. In this formulation the thiol to acrylate stoichiometery was 1:7. Based off of the Flory-Stockmayer equation, the gel point conversion of this off-stoichiometeric system was calculated to be 0.76. The results for T_g and modulus at the end of the Stage 1 and Stage 2 reactions are detailed in Table 6. The polymer that was formed at the end of Stage 1 was used to take the imprint of a micron-sized pattern mold. Once the gel was formed, the physical mask was placed in contact with the polymer film and exposed to light at 8 mw/cm^2 for 5 minutes, after which the Stage 2 polymer was removed and brightfield images of the imprinted pattern were obtained. As shown in Figure 5, excellent negatives of the pattern from the mold were obtained in which the width of the structure matched that of the mold.

Table 4.6. Thermo-mechanical characterization of the two stage impression lithography polymer

Formulation	Stage 1 T_g (°C)	Stage 1 Rubbery Modulus (MPa)	Stage 2 T_g (°C)	Stage 2 Rubbery Modulus (MPa)
PETMP/TCDDA/Ebecryl1290	-10 ± 4	0.5 ± 0.2	195 ± 10	200 ± 20

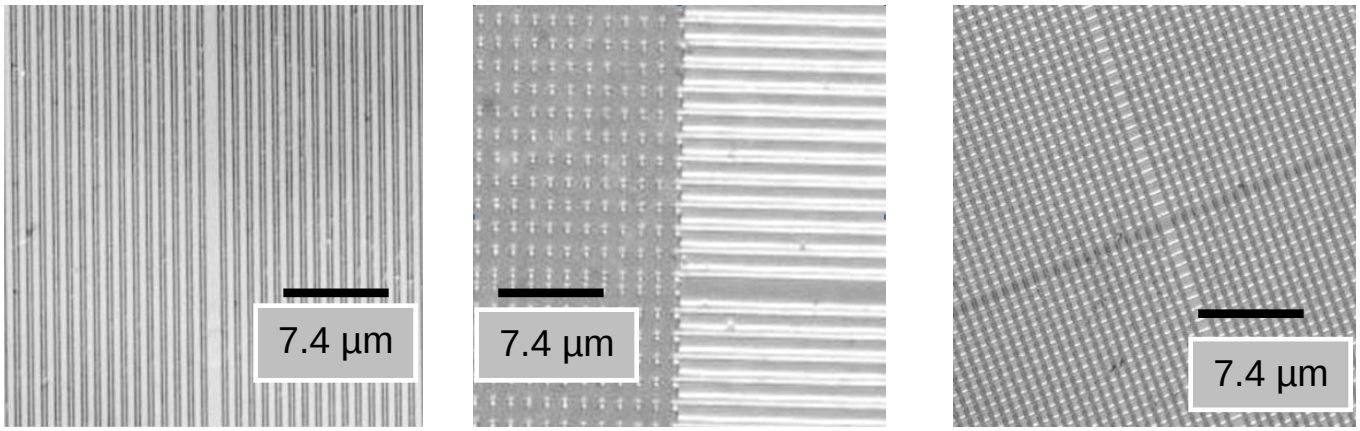

Figure 4.6. Brightfield images of the lithography pattern obtained from the two-stage polymer gel after stage 2 curing.

Optical Materials

In this third application, we have demonstrated a dual–cure system formulation for optical systems that comprises an initial 6.5:1 ratio of acrylate to thiol functional groups. The system contains PETMP, TCDDA and Ebecryl 1290 along with 5 wt% of a high refractive index monomer 2,4,6 tribromophenyl acrylate. The theoretical gel point conversion of the base system was calculated to be 0.58 from the Flory-Stockmayer equation. The high refractive index

monomer is incorporated to facilitate the formation of areas with higher refractive index than the base system, thereby generating refractive index patterns that mirror the stage 2 light exposure pattern. The dual-cure material system at the end of Stage 1 was exposed to a holographic writing set-up using a 365 nm argon laser. The collimated laser beam is split into two beams and redirected to interfere in the recording material with a spatial period of 2 μm. Following the Stage 1 curing, two sequential exposures of the material are implemented in Stage 2, the first being a patterned exposure to create the refractive index pattern and the second being a uniform (i.e., flood) curing to react the polymer fully. Here, the flood cure step was initiated by exposing the material to UV light at 8 mW/cm^2 for 5 minutes. Differential interference contrast (DIC) phase images of the recorded grating were obtained and the pitch of the grating was measured at 2 μm which matched with the holographic writing set-up.

Table 4.7. Thermomechanical characterization of the two stage holographic polymer material

Formulation	**Stage 1 T_g (°C)**	**Stage 1 Rubbery Modulus (MPa)**	**Stage 2 T_g (°C)**	**Stage 2 Rubbery Modulus (MPa)**
PETMP/TCDDA/Ebecryl1290	30 ± 4	6 ± 1	90 ± 10	45 ± 4

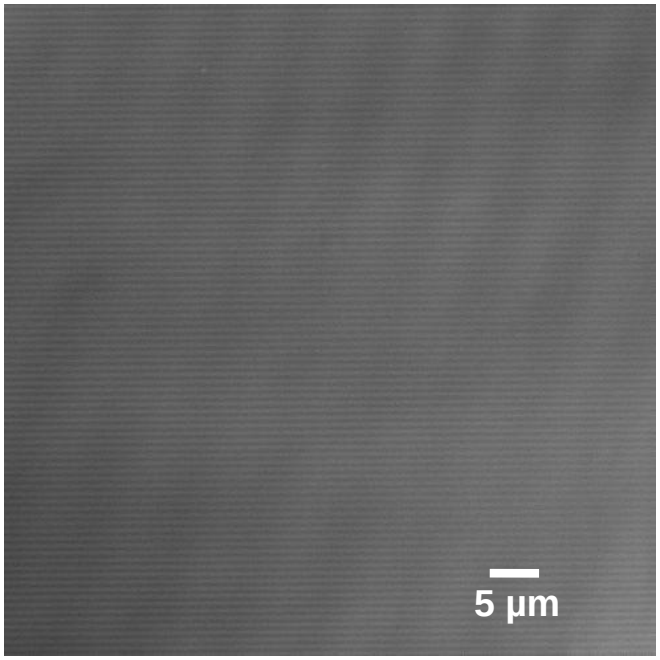

Figure 4.7. The image above is that of a hologram image recorded on the dual-cure polymer matrix. The Stage 1 polymer was used as a photoresist to capture the interference pattern that was recorded on it. The diffraction grating is seen as a result of interference, indicating a refractive index gradient which was then imaged on a brightfield microscope

4.4 Conclusions

In this work we have demonstrated a dual cure polymer system that serves as a materials platform for creating polymer systems with distinct Stage 1 and Stage 2 properties. The polymer networks for both Stage 1 and Stage 2 are achieved orthogonally to each other such that additional polymer processing can occur after Stage 1 curing to enable the attainment of two largely independent sets of material properties at different stages of the material processing and application lifetime. The ability to achieve a wide range of properties for both the Stage 1 and Stage 2 polymers enables a wide range of potential applications including the potential

demonstrated here for high modulus shape memory polymers, lithographic impression materials, and optical materials with controlled refractive index patterns.

4.5 Acknowledgements

The authors would like to acknowledge National Science Foundation CBET 0626023, National Institute of Health T32HL072738 and the University of Colorado Technology Transfer Office CU2615B-01 for providing funding for this research.

4.6 References

[1] . A. R. Kannurpatti, K. J. Anderson, J. W. Anseth, C. N. Bowman, *J. Polym. Sci. Part B*, 1997, **35**, 2297

[2] . C. N. Bowman, C. J. Kloxin, *AIChE Journal*, 2008, **54**, 2775

[3] . A. F. Jacobine, *In Radiation Curing in Polymer Science and Technology III: Polymerization Mechanisms;* J. D. Fouassier, J. F. Rabek, *Elsevier:* London, 1993*;*

[4] . B.D. Mather, K. Viswanathan, K.M. Miller, T.E. Long, *Prog. Poly.Sci.* 2006, **31**, 487

[5] . N. B. Cramer, C. N. Bowman, *J. Polym. Sci. Part A* 2001, **39,** *3311*.

[6] . C.E. Hoyle, C.N. Bowman, *Angew. Chem. Int. Ed.* 2010, **49**, 1540

[7] . L. Qin, D.A. Wicks, C.E. Hoyle, *J. Poly. Sci. A* 2007, **45**, 5103

[8] . J. W. Chan, H Wei, H. Zhou, C.E. Hoyle, *Euro. Poly. J.* 2009, **45**, 2717

[9] . J. W. Chan, C.E. Hoyle, A.B. Lowe, *J.A.C.S* 2009,**131**,16

[10] . J. W. Chan, C.E. Hoyle, A.B. Lowe, M. Bowman, *Macromolecules* 2010,**43**, 15

[11] . A.B. Lowe, *Poly.Chem.* 2010,**1**,17

[12] . C. E. Hoyle, T. Y. Lee, T. Roper, *J. Polym. Sci. Part A* 2004, **42**, 5301

[13] . D.L Elbert , A.B. Pratt , M.P. Lutolf, S. Halstenberg J.A. Hubbell, *J. Control. Rel.* 2004, **76**,11.

[14] . A. M. Kloxin, M. Tibbitt, A.M. Kasko, J.A. Fairbairn, K.S. Anseth, *Adv. Mater.* 2010, **22**, 61.

[15] . A. E. Rydholm, C. N. Bowman, K. S. Anseth, *Biomaterials,* 2005, **26**, 4495

[16] . P.T. Mather, X Luo, I.A. Rousseau, *Ann. Rev. Mater. Research*. 2009, **39**, 445

[17] . C. Liu, H. Qin, P.T Mather, *J. Mater. Chem.* 2007**, 17**, 1543

[18] . C.M. Yakacki, R. Shandas, D. Safranski, A.M. Ortega, K .Sassaman, K. Gall, *Adv. Funct. Mater.* 2008 , **v**,2428

[19] . C.M. Yakacki, R. Shandas, C. Lanning, B. Rech, A. Eckstein, K. Gall, *Biomaterials,* 2007, **28**, 2255

[20] . K. Otsuka, C.M. Wayman in *Shape Memory Materials* . (Eds: University Press, Cambridge, UK , 1998)

[21] . A. Lendlein, S. Kelch , *Angew. Chem.* Int. Ed. 2002, **114**, 2138

[22] . I.A. Rousseau, *Poly. Eng. Sci.* 2008,**48**, 2075

[23] . D. Ratna, J. Karger-kocsis. *J. Mater. Sci.* 2008, **8**, 254

[24] . T.W. Duerig, D. Stoeckel, A. Pelton, *Mater. Sci. Eng.* 1999, **273**, 149

[25] . M.Y. Razzaq , L. Frormann , *Poly.Comp.* 2007 , **28**, 287

[26] . Q.H. Meng, J.F. Hu ,*Composites,* 2008, **39**,314

[27] . J.W. Xu , W.F. Shi, W.M. Pang. *Polymer*, 2006 **47**,457

[28] . K.Gall, M.L. Dunn, Y. Liu *Microscope,* 2002, **50**,5115

[29] . T. Xie, I.A. Rousseau , *Polymers*, 2009, **50**,1852

[30] . D.P.Nair, N.B. Cramer, T.F. Scott, C.N. Bowman,R. Shandas, *Polymer*, 2010 ,**51**,4383

[31] . Y. Xia, G. M. Whitesides, *Angew. Chem. Int. Ed*. 1998, **37**, 550

[32] . H.D. Rowland, W.P. King, *Appl. Phys.A: Mater. Sci. Process.* 2005 **, 81**,1331

[33] . T.C Bailey, S.C. Johnson, S.V. Sreenivasan, J.G. Ekerdt, C.G. Willson, D.J. Resnick, . J. *Photopolymer Sci. Technol*. **15**, 481

[34] . V.S. Khire, Y. Youngwoo, N.A. Clark , *Adv. Mater.* 2007, **20**, 3308

[35] . R. R. A. Syms in *Practical Volume Holography* (Oxford University Press, Oxford, 1990).

[36] . V. W. Krongauz, A. D. Trifunac in *Processes In Photoreactive Photopolymers* (Chapman & Hall, New York, 1994).

[37] . B. J. Chang, C. D. Leonard, Appl. Opt. 1979, **48**, 2407

[38] . D. H. Close, A. D. Jacobson, R. C. Magerum, R. G. Brault, F. J. McClung, Appl. Phys. Lett. 1969, **14**, 159-160 (1969).

[39] . W. S. Colburn , K. A. Haines, , *Appl. Opt.* 1971,**10**, 1636

[40] . L. Dhar, A. Hale, H. E. Katz, M. L. Schilling, M. G. Schnoes, F. C. Schilling, *Opti. Lett*. 1999, **24**, 487

[41] . K. Curtis, L. Dhar, A. Hill, W. Wilson, M. Ayres, in *Holographic Data Storage: From Theory to Practical Systems*. (Wiley, New York, 2010).

[42] . A. Sato, M. Scepanovic, and R. K. Kostuk, Appl. Opt. 2003, **42**, 778

[43] . C. Ye, R. R. McLeod, *Opt. Lett.* 2008, **33**, 2575

[44] . A. C. Sullivan, M. W. Grabowski, R. R. McLeod, *App. Opt.* 2007**, 46,** 295

[45] . J. Parisien, Thieme Med. Publishers NY, USA 2006.

Chapter 5

Enhanced Two-stage reactive Polymer Systems

In this study, we develop thiol/acrylate two-stage network forming polymer systems that exhibit two distinct and orthogonal stages of curing. Using a thiol-acrylate system with excess acrylate functional groups, a first stage polymer network is initially formed via a 1 to 1 stoichiometric thiol-acrylate Michael addition reaction. At a later point in time, the excess acrylate functional groups are homopolymerized via a photoinitiated free radical polymerization to form the second stage polymer network. By varying the monomers within the system as well as the stoichiometery of thiol to acrylate functional groups, we demonstrate the ability of the two-stage reactive systems to encompass a wide range of properties at the end of both the stage 1 and stage 2 polymerizations. Using urethane di- and hexa-acrylates within the formulations formed two-stage reactive polymeric systems with stage 1 T_gs that ranged from -12 to 30 °C. The systems were then photocured, upon which the T_g of the systems increases up to 90 °C while also achieving up to an 18 fold increase in the modulus.

5.1 Introduction

Click chemistry is a powerful tool for polymer modification, small molecule synthesis, and polymerizations. [1-3]Recently, the thiol-acrylate "click" Michael addition reaction has been utilized as a platform for biomaterial applications ranging from tissue scaffolds to drug delivery applications. [4] In addition to being insensitive to oxygen or water, and proceeding under relatively mild and solventless reaction conditions, the thiol-acrylate Michael addition reaction is also orthogonal to other common organic reactants. [5-6]

Photopolymer networks afford the versatility and function of being able to perform as materials that vary from soft lithographic substrates to biomaterials such as dental restorative materials to high performance parts on aircrafts. [7-9] Photopolymerizations is an exciting and rapidly growing field due to the combination of rapid polymerizations, spatial and temporal control, solventless processing, and a wide range of achievable properties. [10-13]This work expands on the applicability of photopolymerizations by combining it with thiol/acrylate click chemistry to form a dual cure polymer platform capable of achieving a wide range of properties and enabling two stages at which the system can be processed to increase functionality.

In a thiol-acrylate monomer system which has excess acrylates present, the initial stable network formed by a stoichiometric 1:1 thiol-acrylate Michael addition reaction leaves unreacted acrylate moieties attached to and throughout the polymer network. After this first stage reaction, intermediate polymer processing can be performed. The acrylates can then be induced to homopolymerize at a later point via photopolymerization, forming a highly crosslinked, high modulus polymeric network at the end of the reaction.

This generalized scheme is shown in Figure 1. We previously demonstrated that these systems enable the achievement of two distinct and largely independent sets of material properties at the end of the stage 1 Michael addition and later at the end of the stage 2 photopolymerization. [14] The stage 1 and stage 2 properties are varied dramatically by simple changes in initial thiol to acrylate stoichiometery. Also, forming the intermediate polymer network in this manner ensures that the overwhelming fraction of the monomer will be bound into the network at the end of the stage 1 reaction. This covalent attachment is an advantage when the polymer is considered for applications such as biomedical devices in which the amount of extractables within the network

can be detrimental to the material being considered as a potential device. [15] The broad range of applications of the two stage reaction were demonstrated by utilizing simple changes in formulation and stoichiometry to enable applications of impression materials, optical materials, and shape memory polymers. After photocuring, these networks exhibited stage 2 properties with glass transition temperatures and moduli as high as 195 °C and 200 MPa respectively. In this work, we explore the breadth of properties that can be achieved in the two-stage reactive systems by varying the stoichiometery, monomer structure, and monomer functionality. In doing so, we have shown that a wide range of stage 1 and stage 2 properties are achievable that may be suitable for an even broader range of applications than previously demonstrated.

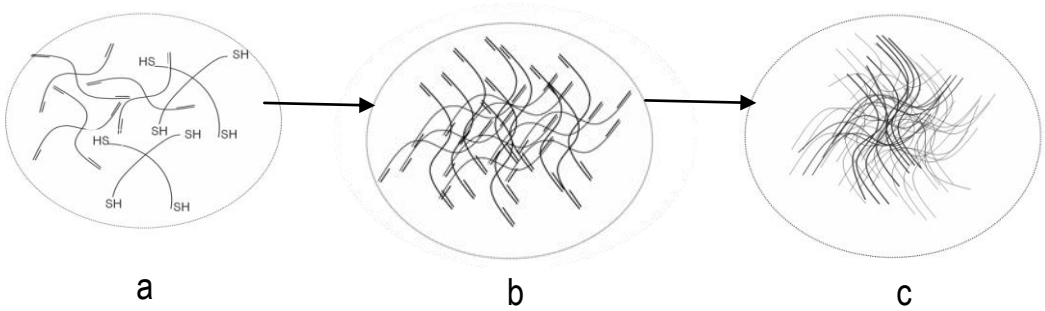

Scheme 5.1. Non-stoichiometeric molar mixtures of thiol and acrylate functional groups with excess acrylate groups present are reacted in a amine mediated Michael Addition reaction (a). At the end of this reaction a stage 1 polymer is formed, which is now capable of undergoing additional application specific processing. After processing, the excess acrylate functional groups are largely tethered within the network. At a later stage, the acrylates can be photopolymerized on command to result in the formation of a highly crosslinked, glassy network.

5.2 Experimental

Materials

Pentaerythritol tetra(3-mercaptopropionate)(PETMP) was donated by Bruno Bock, tricyclodecane dimethanol diacrylate (TCDDA) was donated by Sartomer, and Ebecryls 220, 1290, 230, and 8402 were donated by Cytec. The photoinitiator Irgacure 651 (2,2-dimethoxy-2-phenylacetophenone) was donated by Ciba Specialty Chemicals. All samples contained 0.8 wt% triethyl amine, as a catalyst for the first stage reaction, and 0.5 wt% Irgacure 651 to initiate the second reaction. For the photopolymerization during the second stage of the reaction, samples were cured at 8 mW/cm^2 using a UV lamp (Black-Ray Model B100AP).

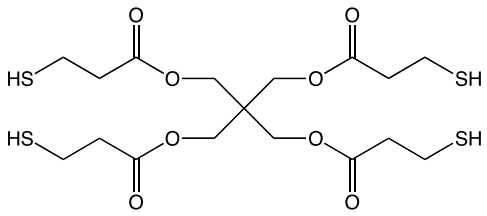

PETMP
pentaerythritol tetra(3-mercaptopropionate)

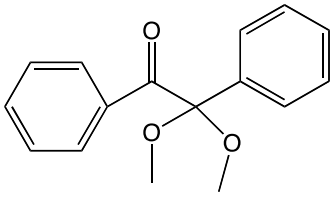

DMPA
2,2-Dimethoxy-2-phenylacetophenone

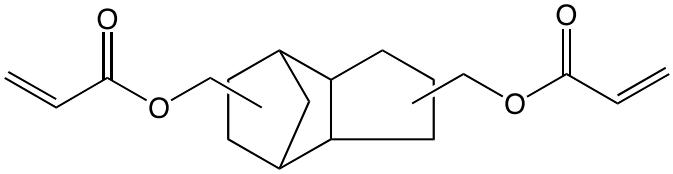

TCDDA

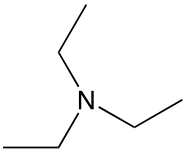

TEA
Triethylamine

Figure 5.1. Chemical structures of the monomers used in this study.

Dynamic Mechanical Analysis (DMA)

DMA experiments were performed using a TA Instruments Q800 DMA.

Glass transition temperature (T_g) was determined from polymer samples with dimensions of 10 x 3.5 x 1 mm. Sample temperature was ramped at 3 ^oC/min from -50 to 300 ^oC with a frequency of 1 Hz and a strain of 0.01 % in tension. The T_g was assigned as the temperature at the tan δ curve maximum. The rubbery modulus values were determined at a temperature 35^o C above the T_g for the stage 1 and 65 ^oC above the T_g for the stage 2 polymers.

Materials Testing System (MTS)

Compression test measurements were conducted on an Instron Universal Testing Machine (Insight 2.0) to ascertain the Peak stress, strain at break and toughness measures of the system at the end of stage 1 and stage 2. Cylindrical samples of dimensions of 5 mm (diameter) × 6.5 mm (height) were used. The initial separation of the system was set at 22 mm and a crosshead speed of 5 mm/min was applied.

Fourier Transform Infrared Spectroscopy (FTIR)

FTIR experiments were performed using a Nicolet Magna 760. The acrylate peak absorbance was measured at 814 cm^{-1} and the thiol peak at 2575 cm^{-1}. Samples were prepared with TEA, mounted between salt crystals, and stored for 48 hours to allow substantial time for the first stage curing. After the first stage cure was complete, as observed by the total disappearance of the thiol peak, series runs were taken, and the peak areas for the acrylate were recorded, both before and after exposure to UV light for 15 minutes at 20 mW/cm^2

5.3 Results And Discussion

Two-stage reactive thiol/acrylate systems were formulated and characterized with varying monomers and stoichiometeries to explore the range of properties that could be achieved.

Table 5.1. T_g and rubbery modulus for the 1:1 thiol-acrylate systems is detailed below. All formulations contained 0.8 wt% TEA and rubbery modulus was measured at T_g + 35°C

Polymer System	Thiol:Acrylate Ratio	T_g (°C)	Rubbery Modulus (MPa)
PETMP/TCDDA	1:1	16 ± 2	7 ± 1
PETMP/Ebecryl 230	1:1	-33 ± 2	0.8 ± 0.2
PETMP/ Ebecryl 8402	1:1	-8 ± 2	3 ± 2
PETMP/ Ebecryl 220	1:1	33 ± 3	18 ± 8
PETMP/ Ebecryl 1290	1:1	41 ± 2	25 ± 1

Initially, formulations with 1:1 molar ratio of thiol to acrylate functional groups were prepared. Four different urethane acrylates were evaluated along with the tetrathiol PETMP and the diacrylate TCDDA. The urethane acrylates consisted of di-acrylates with molecular weights of 5000 (Ebecryl 230) and 900 (Ebecryl 8402) that resulted in soft flexible networks. The remaining urethane acrylates in the study were a hexa-functional aromatic urethane acrylate, Ebecryl 220 and Ebecryl 1290, an aliphatic hexa-functional urethane acrylate. Ebecryl 220 and Ebecryl 1290 had a molecular weight of 1000. All of the formulations contained TCDDA as a viscosity modifier to maintain similar, low viscosities. The 1:1 stoichiometeric formulations of thiol to acrylate were characterized using dynamic mechanical analysis to record the glass transition temperature, T_g, and the rubbery modulus. The thermomechanical property results for the 1:1 thiol-acrylate systems represents the maximum achievable T_g and modulus at the end of the stage 1 Michael addition reactions for the chosen monomers. As shown in Table 1, the ideal

stoichiometeric thiol/acrylate formulations exhibited glass transition temperatures that ranged from -33 °C for the PETMP/Ebecryl230 system to 41 °C for the PETMP/Ebecryl1290 system. As all of the acrylates react in the Michael addition reaction, there are no remaining acrylate functional groups to react via the photoinitiated radical polymerization, and thus, no significant change in properties is observed upon irradiation of these samples.

Table 5.2. Thiol to diacrylate and thiol to Ebecryl urethane acrylate ratios are detailed here

Polymer System	Thiol :TCDDA Ratio	Thiol :Urethane Acrylate Ratio
F-230	1:2.4	1:0.4
F-8402	1:1.5	1:1.5
F-220	1:0.5	1:2.5
F-1290	1:0.5	1:1.5

Based on the data from Table 1, off-stoichiometeric systems were formulated to achieve a range of T_g and moduli at the end of the stage 1 and stage 2 polymerizations. Formulations which contained the thiol, PETMP, the diacrylate, TCDDA, and urethane acrylates were formulated as detailed in Table 2. These formulations are referred to as F-230, (PETMP/TCDDA/Eb230), F-8402, (PETMP/TCDDA/Eb8402), F-220 (PETMP/TCDDA/Eb220) and F-1290(PETMP/TCDDA/Eb1290). The ratios were chosen to yield a range of stage 1 and stage 2 properties for the two-stage reactive thiol/acrylate systems.

Two-stage reactive systems enable a material to have an intermediate processing step, along with the ability to 'dial in' a final set of material properties that would optimize the ability of the material to function as a device or for a specific application. Formulating materials with a range of both stage 1 material properties would considerably enhance the processing capabilities of such two-stage reactive systems. The stage 1 F-230 system is soft and flexible at ambient temperature with a modulus of 1 MPa and a T_g of -12 °C as shown in Figure 2. The observed properties are largely due to the excess unreacted acrylic groups within the network. Additionally, as the urethane acrylate Ebecryl 230 is a high molecular weight, di-functional molecule, the crosslinks formed by this polymer system in stage 2 would also enable a highly flexible polymer network. As this formulation goes from stage 1 to stage 2, the T_g increases 12 fold and the modulus goes from 1 MPa to 5 MPa. However, the material still remains soft and retains considerable flexibility at stage 2 at ambient conditions. F-230 is ideal for applications that can benefit from a polymer that is soft and flexible for the intermediate processing step, but would also require a system that has retained considerable elasticity at the end of stage 2 such as vibration dampeners and soft dental lining materials. [16-17] The F-8402 formulation, relative to the F-230 system, had slightly higher modulus at the end of stage 1 at 6 MPa. The stage 1 formulation also retained considerable flexibility at ambient, as it had a T_g of -2º C. Ebecryl 8402 is also a difunctional urethane acrylate with smaller molecular chain length than Ebecryl 230. Consequently, the crosslinks formed by this system would be shorter, thereby restricting chain mobility and increasing the modulus of this system. F-8402 system was formulated as a variation to the F-230 system in which the stage 1 modulus F-8402 was 6 times the stage 1 modulus of F-230. F-8402 has a modulus of 14 MPa in stage 2, which is more than twice the stage 2 modulus of the F-230 formulation. The T_g of this system also went from -2 to 18 °C, such that the

polymer still remained rubbery and flexible at ambient temperature. This stage 2 T_g would enable F-8402 to function in environments that require a mechanically stronger polymer than F-230. The stage 1 and stage 2 thermomechanical properties of the F-230 and F-8402 system make them ideal for applications such as dental soft lining materials and bioimplants that have to function in a mechanically dynamic environment.[18-19]

The stage characteristics of a dual- network forming system such as the F-220 with a stage 1 T_g of 18 ºC and modulus of 7 MPa, would be ideal for applications such as a holographic writing material which would have to be sufficiently rubbery at ambient conditions to allow index patterning and enable diffusion.[20] In a holographic polymeric storage device, structured illumination is used to initiate polymerization, which sets up a local diffusion that drives changes in density and refractive index. However, once diffusion is complete and the structures are stored within the material, there is no processing or functional advantage for the material to remain soft and flexible. A disadvantage is that such a material is now susceptible to environmental contaminants that can diffuse into the network.[21] A two-stage reactive system such as F-220 at stage 1 would have a polymer matrix with the excess, unreacted, acrylate functional groups within the network. The unreacted acrylate moieties would essentially act as a plasticizer within the network, enabling chain mobility and therefore diffusion. Once diffusion is complete and the holographic structure are formed, the stage 2 photopolymerization can be initiated to form a highly crosslinked and robust glassy network at ambient. This material has a stage 2 T_g of 90º C and is highly crosslinked with a rubbery modulus of 125 MPa. F-220 contains the low molecular weight, hexafunctional aromatic urethane acrylate Ebecryl 220 and crosslinking the excess acrylates in stage 2 gives rise to a highly rigid network with short crosslinks. Although both F-220 and F-8402 have stage 1 modulus that are similar, there is a 7-fold increase in the stage 2

modulus of F-220 in comparison with F-8402, thereby showing that the stage 2 properties that can be attained for the dual-networking forming polymer formulations can be largely independent of their stage 1 properties.

Similarly, for applications that call for similar stage 2 properties as the F-220, such as high modulus, glassy polymer system, but require a more mechanically robust stage 1 polymer network, the F-1290 system has a modulus of 20 MPa and T_g of 30º C. The F-1290 system contains a low-molecular weight, hexafunctional aliphatic urethane acrylate, Ebecryl 1290. The 1 to 1 stoichiometery of thiol to acrylate formulation for this system yielded a T_g of 41 º C and a modulus of 25 MPa. Along with the benefits of achieving an intermediate, stable processing step at stage 1, the ability to tune in a specific final mechanical modulus by controlling the crosslinked network formed at stage 2 is of importance as very often, in application such as biomedical implant devices, it is important that the device be able to match the modulus and mechanical properties of the surrounding environment in order to function effectively as an implant. [21]The F-1290 system has stage 2 modulus of 77 MPa and T_g of 82 ºC. A potential biomedical device made from a two-stage reactive polymer system such as F-1290 can have the advantage of keeping the stage 1 modulus of the device low. This would aid the delivery of the device to its location *in-vivo* with minimal trauma. Once in its target location, the ability to increase the modulus of the material *in-situ* so as match its local environment and function optimally as a device is an advantage for polymers that will enable their potential use in applications such as orthopedic devices, where high mechanical strength is often a prerequisite for potential orthopedic materials.

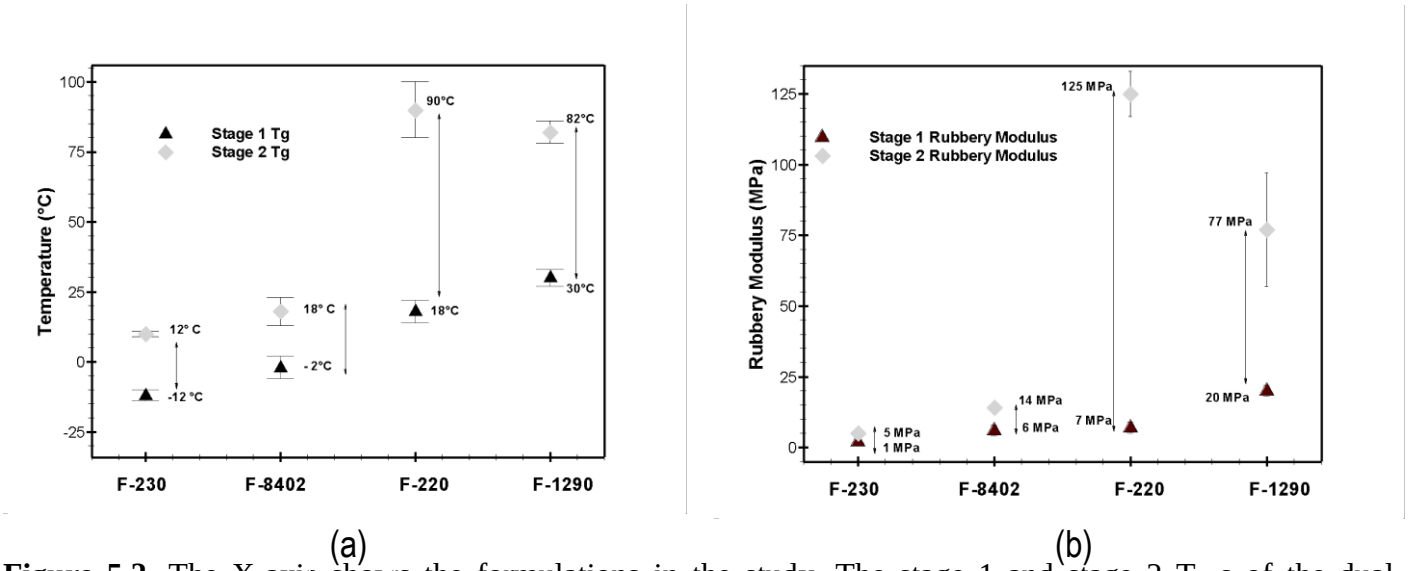

Figure 5.2. The X-axis shows the formulations in the study. The stage 1 and stage 2 T_g s of the dual-networking forming systems F-230, F-8402, F-220 and F-1290 show the distinct T_g achieved at the end of each stage (a). The rubbery modulus of the systems was measured at T_g + 35 for the stage 1 systems and at T_g + 65 for the stage 2 systems (b).

At the end of stage 1 Michael addition reaction in the two-stage reactive systems, the photo-initiated evolution of the stage 2 network via the conversion of the excess acrylate functional groups was recorded as shown in Figure 3.

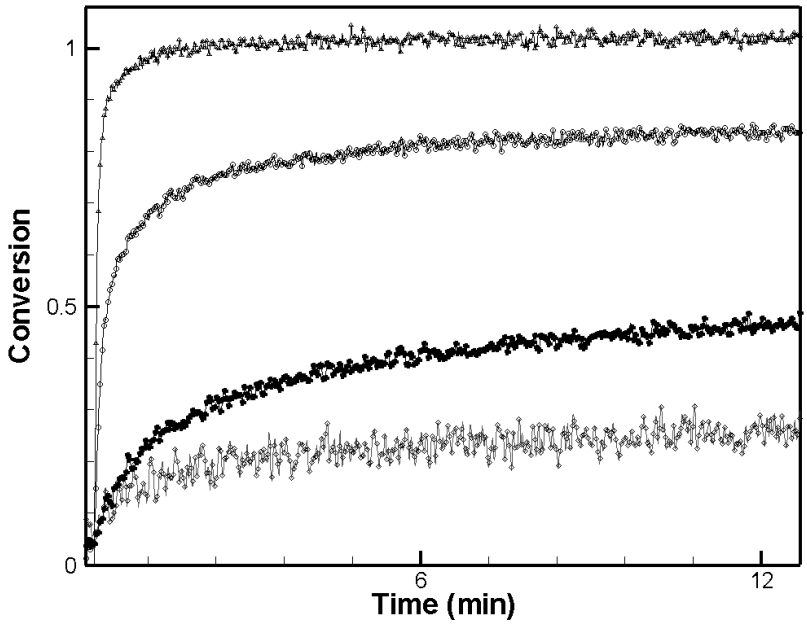

Figure 5.3. Stage 2 acrylate conversion F-Eb230 (Δ), F-Eb8402 (O), F-Eb220 (Λ), and F-Eb2190 (■). The systems contained 0.8 wt% TEA and 0.5 wt% Irgacure 651and were irradiated at 20 mW/cm^2. At the end of stage 1, 28.5% of the acrylates in the F-230 system were unreacted, whereas the F-8402, F-220, and F-1290 systems had 33% of the acrylates unreacted within the network.

The F-230 formulation system exhibited close to 100% conversion of the remaining 28.5% of the unreacted acrylate monomers during stage 2 curing within the first minute of being exposed to the UV light, whereas close to 80% of the remaining 33% of the acrylate groups were polymerized by the end of Stage 2 for the F-8402, comprising 6 minutes of irradiation. The high stage 2 T_g systems, F-220 and F-1290 had much lower stage 2 acrylate overall conversions, with 25% of the acrylate reacting for the F-220 system and 40% of the acrylates reacting for the F-1290 system. The reduced conversion in the hexafunctional system can be explained by the severe mobility restriction on the radicals due to vitrification of the polymer matrix. As the

polymerization proceeds, the decrease in free volume and the restricted mobility of radicals and their ability to reach the double bonds gives rise to the phenomenon of autodeceleration.[7] The reduced stage 2 conversion post-vitrification has also been observed in polymers in which the cure temperature of the systems is far below the T_g of the polymer network. [22]However, in spite of the relatively low stage 2 conversions, the hexafunctional urethane systems exhibits a significant increase in modulus, with the F-220 system showing an 18 fold increase in modulus and the F-1290 system showing a 4 fold increase in modulus, even with more than 50% of the remaining acrylate moieties remaining unreacted.

To characterize further the mechanical properties of the polymer networks at the end of stage 1 and stage 2, compression tests were used to measure the peak stress, the strain at break and the toughness of the two-stage reactive systems. The presence of the urethane moieties within the polymer network is known generally to enhance the toughness of materials by providing extensive hydrogen bonding in these types of acrylic networks. [23] As shown in Figure 4, there were distinct differences in the peak stresses and strain to break that were attained at the end of each stage. The F-230 polymer at stage 1 had 80% strain at break, along with toughness at 3.3 J/m^3, and peak stress at 8 MPa. The F-230 formulation showed no considerable increase in the peak stress and toughness values between stage 1 and stage 2. However, this system was able to achieve up to 70% strain at break even at stage 2. Given that Ebecryl 230 is a high molecular weight, di-acrylate, the high strain capacities at the end of each stage can be attributed to the considerably longer, flexible chains in the polymer network. The presence of the flexible chains extends mobility to the network and dominates the properties of this system, thereby offsetting

any increase in toughness from the added crosslinking in the stage 2 photopolymerization. The F-8402, however, showed a 30% reduction in strain between stage 1 and stage 2. The stage 2 crosslinking of the polymer matrix also resulted in a 60% increase in toughness and a 2-fold increase in peak stress as it went from stage 1 to stage 2. Although F-230 and F-8402 system are formulated from urethane di-acrylates and have similar stage 1 and stage 2 thermomechanical properties, it is of note that the F-8402 formulation can withstand 75% more stress in compression than the F-230 formulation. The variation in mechanical properties of the two urethane di-acrylate systems should factor in to application specific design considerations. The highly crosslinked F-220 stage 2 polymer system exhibited a dramatic a 12-fold increase in toughness from stage 1. The compression tests results for this system correlate with the thermomechanical data, which showed a highly crosslinked, high T_g stage 2 polymer network with a rubbery modulus of 125 MPa. However, the strain measures for the F-220 system did not show considerable differences between stage 1 and stage 2 and remained at 30%. A possible reason for this result could be that the significant amount of unreacted acrylate moieties within the network at stage 2 have a plasticizer effect within the highly crosslinked polymer and therefore enable sufficient chain mobility for the system to have a higher strain at break than it otherwise would in a system that had a higher stage 2 conversion than 25%. Interestingly, the hexa-functional urethane acrylate system, F-1290, had a stage 1 toughness that was 28 times that of F-220. This value is important as the mechanical measures at stage 1 can decide the type of intermediate processing that the two-stage reactive systems can be subject to. The F-1290 formulation though, showed a reduction in both strain and toughness measures as it went from stage 1 to stage 2. Although the peak stress values remained within error close to a 100 MPa at both stage 1 and stage 2, a 33% reduction in strain in addition to a 31% reduction in toughness

was observed for this system. Though a reduction in strain is expected at stage 2 due to the increased crosslinking of the hexafunctional acrylates within the polymer matrix, a reduction in toughness could be a result of the crosslinking resulting in a relatively brittle material.

Overall, all systems showed that the strain at break, peak stress and toughness measures were a function of the amount of crosslinking within the polymer network and the specific nature of the monomers used within the formulations.

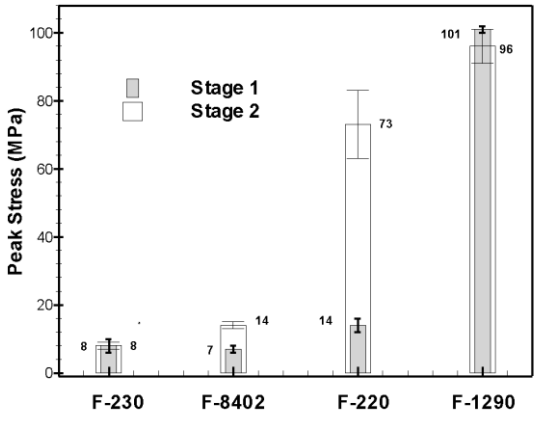

(a)

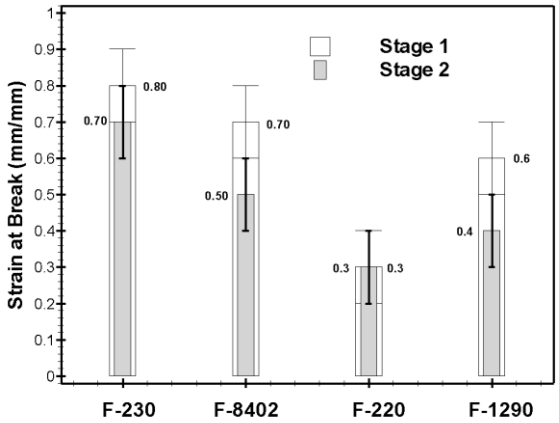

(b)

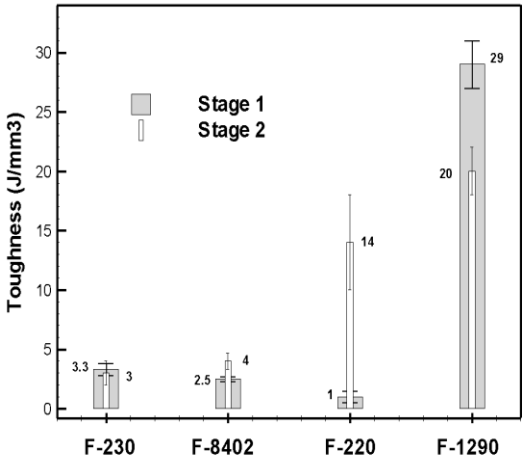

(c)

Figure 5.4. The peak stress that the polymer networks achieved at the end of each stage is contrasted in 2(a). 2(b) shows the reduction in strain as a result of the stage 2 cure and 2(c) is the calculated toughness at the end of each stage.

5.4 Conclusions

In this study, we have shown that within different monomer types with the same functionality, it possible to get a range of properties that meet a series of stage 1 material properties and stage 2 application specific material parameters. The F-8402 and F-220 systems showed it was possible to have 2 different formulations with similar stage 1 properties and vastly different stage 2 properties. F-230 formulation have very similar mechanical properties as it went from stage 1 to stage 2, retaining a highly flexible polymer in spite increased crosslinking. F-8402, with similar stage 1 properties to F-230, formed a tougher, stronger polymer at stage 2, whereas the F-220 and F-1290 formulations had varied stage 1 properties, but displayed similar behavior at stage 2. The four formulations thermomechanicaly and mechanically analyzed here show a range of largely independent properties that can be achieved at stage 1 and stage 2. However, given the range of possible stoichiometeries and monomer types that can be used to formulate dual-networking forming systems, this study is representative of the two-stage reactive systems that can be designed for a vast range of applications.

5.5 Acknowledgements

The authors would like to acknowledge National Science Foundation CBET 0626023, National Institute of Health T32HL072738 and the University of Colorado Technology Transfer Office CU2615B-01 for providing funding for this research.

5.6 References

[1] . C.E. Hoyle, C.N. Bowman, *Angew. Chem. Int. Ed.* 2010, **49**, 1540

[2] . H. Matsushima, J. Shin, C. N. Bowman, C. E. Hoyle, *J. Poly. Sci.* , 2010,**48**,3255

[3] . A.B. Lowe, C. E. Hoyle, C. N. Bowman, *J. Mater. Chem.*, 2010, **20**, 4745

[4] . A. E. Rydholm, C. N. Bowman, K. S. Anseth, *Biomaterials*, **2005**, 26, 4495-4506.

[5] . D.L Elbert , A.B. Pratt , M.P. Lutolf, S. Halstenberg J.A. Hubbell, *J. Controlled Release.* **2004**, 76,11-25

[6] . J. W. Chan, H Wei, H. Zhou, C.E. Hoyle, *Euro. Poly. J.* 2009, **45**, 2717

[7] . B.D. Mather, K. Viswanathan, K.M. Miller, T.E. Long, *Prog. Poly.Sci.* 2006, **31**, 487

[8] . A. R. Kannurpatti, K. J. Anderson, J. W. Anseth, C. N. Bowman, *J. Polym. Sci. Part B,* 1997, 35, 2297

[9] . C. N. Bowman, C. J. Kloxin, *AIChe J*, 2008, **54**, 2775

[10] . G. Andrei, D. Dima, L. Andrei, *J. Optoelectronics Adv. Mat*., 2006, **8**, 726

[11] . N. B. Cramer, C. N. Bowman, *J. Polym. Sci. Part A* 2001, 39**,** *3311*

[12] . K. P. Matabola ,A. R. De Vries , F. S. Moolman , A. S. Luyt, *J. Mater Sci.* 2009, **44**,6213

[13] . C. Decker, *Poly.Int.*,1998,**45**,133

[14] . J.G. Kloosterboer, *Adv.Poly.Sci.*,1988,**84**,1

[15] . D.P.Nair, N.B. Cramer, J.C.Gaipa, M.M.McBride, E.M. Matherly, R.M. McLeod, R. Shandas, C.N. Bowman, *Adv. Func. Mat.*, 2011

[16] . F.Chiellini, *J. Bioactive Compatible Poly.* 2006,**21**,157

[17] . H. H. Winter**,** *Korea-Australia Rheology J*,1999,**11**,275

[18] . J. Park, Q. Ye, E. M. Topp, C. H. Lee, E.L. Kostoryz, A.Misra, P. Spencer, *J Biomed Mater Res B Appl Biomater,* 2009,**91**,61

[19] . B.S. Graham,D.W. Jones, E.J. Sutow, *J. Dent Res.*,1991,**70**,870

[20] . Y. Wang, G. A. Ameer, B.J. Sheppard, R. Langer,*nature biotechnology*,2002,**20**,602

[21] . V. W. Krongauz, A. D. Trifunac in *Processes In Photoreactive Photopolymers* (Chapman & Hall, New York, 1994).

[22] . C. Ye, R. R. McLeod, *Opt. Lett.* 2008, **33**, 2575

[23] . S Ramakrishna, J Mayer , E Wintermantel, K. W Leong,*Comp.Sci. Tech***,** 2001,**61**,1189

[24] . S.Ye, N. B. Cramer, C. N. Bowman, Macromolecules, 2011,**44**,490

[25] . A..F Senyurt, H. Wei, C. E Hoyle, S. G Piland, T. E Gould, Macromolecules,2007,**40**,4901

Chapter 6

Two-Stage Reactive Composite Polymer Systems

Two-stage reactive polymer composite systems are formulated and characterized in regards to their thermomechanical properties and behavior. The composite formulations have two-stage reactive thiol-acrylate systems as the matrix in which a stage 1 polymer matrix is initially formed via an amine catalyzed 'click' Michael addition reaction. This self-limiting reaction results in a polymer with excess acrylic functional groups within the network. At a later point in time, the photoinitiated, free radical polymerization of the excess acrylic functional groups results in a highly crosslinked, stage 2 polymer. Two, dual-stage forming thiol-acrylate off stoichiometeric matrices were designed and subsequently formulated into composite systems using three different filler types. The fillers used were 0.7 μm methacrylated silica particles, translucent Kevlar veil and PET mesh. Thermomechanical analysis showed that the fillers resulted in a significant increase in the modulus at both stage 1 and stage 2 polymerizations without a significant change in the glass transition temperatures (T_g). The two-stage matrix composite formed with a hexafunctional acrylate matrix and 20 volume % silica particles showed a 125% increase in stage 1 modulus and a 100% increase in stage 2 modulus, when compared with the modulus of the neat matrix. For a composite system with superambient stage 1 and stage 2 glass transition temperatures, the tensile modulus measurements at ambient conditions showed that filler concentration and type dominated the stage 1 modulus, whereas the matrix properties dominated the stage 2 tensile properties. For a composite system with subambient stage 1 and 2 glass transition temperatures, the filler type continued to dominate the stage 2 tensile properties.

6.1 Introduction

Although polymers can be tailor-made to exhibit a wide range of properties and be fabricated into complex shapes and structures, they often require the use of fillers to achieve the mechanical demands of applications such as aerospace materials which require a high strength to weight ratio. [1-2] Polymer-based composites afford much of the same processing ease and low costs that are inherent to polymers along with the ability to achieve a range of different properties by varying the filler type, structure and quantity. As such, polymer composites can be engineered to be lightweight with properties that range from high strength and stiffness to materials with increased electrical conductivity. [3-4]

Recently, our group developed novel two-stage reactive polymer systems, to engineer polymer networks that had a first set of properties and a distinct second set of properties that were achieved on-command by photoinitiating a second polymer reaction that was orthogonal to the first reaction. [5] To achieve the two distinct stages within the polymer network, an initial amine catalyzed 'click' thiol-acrylate Michael addition reaction was used to form a stage 1 polymer matrix. The Michael addition reaction proceeds stoichiometrically under a wide range of conditions that allow numerous options with respect to monomer selection and reaction conditions such as the temperature and the presence or absence of solvents to yield crosslinked polymer systems.[6-8]. The Michael addition reactions also favor high conversions at ambient temperature and are used in applications that vary from industrial coatings to crosslinked hydrogels. [9-12] A stoichiometery of 1:1 thiol-acrylate ratio is required to form optimized networks. In our previous work, we exploited the ability to incorporate excess acrylate functional groups to enable greater versatility of these systems. In this way, residual acrylate groups are pervasive throughout the polymer network even after stage 1 curing. At a later stage,

the remaining acrylate functional groups were photopolymerized to form highly crosslinked stage 2 polymer networks. We demonstrated that by varying monomer type and the thiol to acrylate stoichiometric ratio, we could tailor the polymer formulation to yield a wide range of properties suitable for a number of different applications including shape memory polymers, impression materials, and optical materials.

We hypothesize that the use of composites materials in a two-stage reactive polymer system will favorably impact the stage 1 properties of the two-stage reactive polymer system. Here, we reinforce two-stage reactive polymer matrices with differing ratios of PET and Kevlar meshes to form composite laminates. In addition, we also formulate and characterize two-stage reactive polymer systems with methacrylated micron size filler particles. The systems were thermomechanically characterized to determine the stage 1 and stage 2 moduli and glass transition temperatures, along with tensile modulus and strain capacity at ambient conditions.

6.2 Experimental

Materials

Pentaerythritol tetra(3-mercaptopropionate) (PETMP) was donated by Bruno Bock, tricyclodecane dimethanol diacrylate (TCDDA) was donated by Sartomer, and Ebecryls 1290, and 8402 were donated by Cytec. The photoinitiator Irgacure 651 (2,2-dimethoxy-2-phenylacetophenone, I651) was donated by Ciba Specialty Chemicals. The chemical structure of the monomers and the photoinitiator are given in Figure 4. The inhibitor aluminum N-nitrosophenylhydroxylamine (N-PAL) was donated by Albemarle. Triethyl amine (TEA) was purchased from Sigma-Aldrich. All samples contained 0.05 wt% inhibitor, 0.8 wt% triethyl amine as a catalyst for the first stage reaction and 0.5 wt% I651 to initiate the second stage

photocuring reaction. For the second stage photopolymerization, samples were irradiated at 8 mW/cm^2 using a UV lamp (Black-Ray Model B100AP).

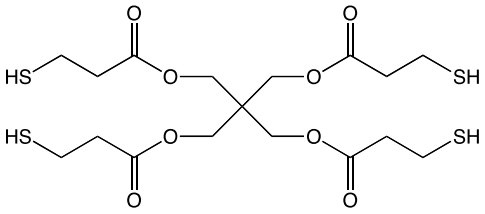

PETMP

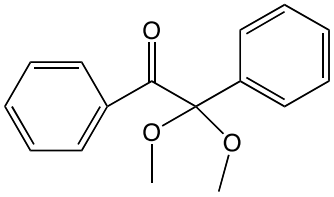

DMPA

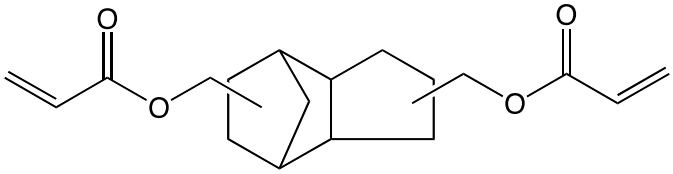

TCDDA

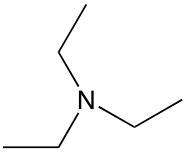

TEA

Figure 1. Chemical structures of the monomers used in this study.

Polymer Composites

The PET fibers were purchased from Surgical Meshes Inc and set in the polymer matrix in the cross-machine direction. The Kevlar veil was obtained from Fiber Glass Inc and the silica particles were donated by Esstech. A FlakTech speed mixer (DAC 150 FVZ) was used to disperse the silica particles within the polymer composite at a speed of 2500 RPM for 20seconds.

Dynamic Mechanical Analysis (DMA) was performed using a TA Instruments Q800 DMA.

Glass transition temperature (T_g) was determined from polymer samples with dimensions of 10 x 3.5 x 1 mm. Temperature was ramped at 3 ^oC/min from -50 to 300 ^oC with a frequency of 1 Hz and a strain of 0.01 % in tension. The T_g was assigned as the temperature at the tan δ

curve maximum. The rubbery modulus values were determined at a temperature 35° C above the T_g for the stage 1 and 65 °C above the T_g for the stage 2 polymers.

Materials Testing System (MTS)

Tensile test measurements were conducted on an Instron Universal Testing Machine (Insight 2.0) to ascertain the Peak stress, strain at break and toughness measures of the system at the end of stage 1 and stage 2. Dog bone shaped samples of dimensions 40 × 6.5 × 1 mm were used. The initial separation of the system was set at 22 mm and a crosshead speed of 5 mm/min was applied. All data was collected at ambient temperature.

Scanning Electron Microscope (SEM) images of stage 1 particle composites taken in a low vacuum chamber

6.3 Results and Discussion

Two, two-stage reactive thiol-acrylate systems were chosen as matrices for the polymer composite systems based on a desire to determine the effects of the stage 1 glass transition temperature. The thiol-acrylate system consisted of off stoichiometeric ratios of a tetrathiol (PETMP), a diacrylate (TCDDA) and a urethane hexaacrylate (Ebecryl 1290). Ebecryl 1290 has a molecular weight of 1000. The second polymer system consisted of PETMP/TCDDA and a long chain, diacrylate Ebecryl 8402 with a molecular weight of 900. The systems will be referred to as S1 and S2 respectively. The S1 system contained thiol and acrylate functional groups in the ratio 1:2 whereas the S2 system contained a thiol to acrylate functional group ratio of 1:3. In a previous study, thermomechanical analysis of both the S1 and S2 two-stage reactive systems showed that the S1 system had stage 1 and stage 2 glass transition temperatures (T_g) that were

higher than ambient temperature (22 ° C) at 30 ± 3 ºC and 82 ± 4 ºC, respectively. The S2 system exhibited stage 1 and stage 2 T_gs lower than or near ambient temperature at -2 ± 4 and 18 ± 5 ºC, respectively. The stage 1 polymer network was formed via a triethylamine catalyzed thiol-acrylate click Michael addition reaction. All formulations also contained a UV initiator IR 651 to initiate the acrylic homopolymerization to form the stage 2 network. The S1 formulation had a stage 1 modulus of 20 ± 2 MPa and a stage 2 modulus of 77 ± 20 MPa. The S2 formulation had a stage 1 modulus of 6 ± 2 MPa and a stage 2 modulus of 14 ± 5 MPa

The PET mesh and Kevlar veil that were chosen to reinforce the two-stage reactive polymers were mechanically characterized with the results shown in Table 1. The tensile data shows that the Kevlar veil forms a high modulus, rigid material with a very low strain at break of less than 0.1 mm/mm. The PET mesh forms a less rigid, high strain material with a modulus of 24 MPa and strain at break of 0.6 mm/mm

Table 1. The tensile modulus and strain at break were measured on dog-bone shaped Kevlar veil and PET mesh material at ambient conditions. The initial separation of the system was set at 22 mm and a crosshead speed of 5 mm/min was applied. All data was collected at ambient temperature

Reinforcement Material	**Modulus (MPa)**	**Strain at Break (mm/mm)**
Kevlar Veil	70 ± 20	0.05 ± .04
PET Mesh	24 ± 2	0.6 ± .02

Composite systems with differing filler content from the silica particles, the PET mesh and the Kevlar veil were formulated for both the S1 and S2 two-stage reactive polymer systems as shown in Table 2 and Table 3, respectively. For the remainder of the paper, the formulation will be referred to as shown in Tables 1 and 2.

Table 2. The details of the composite system for the S1 formulation along with the filler type and content.

Composite System	Polymer Matrix	Composite Filler	Volume per cent
S1-10P	S1	Silica Particles	10
S2-20P	S1	Silica Particles	20
S1-30K	S1	Kevlar Veil	30
S2-60K	S1	Kevlar Veil	60
S1-30PET	S1	PET mesh	30
S2-60PET	S1	PET mesh	60

Table 3. The details of the composite system for the S2 formulation along with the filler type and content

Composite System	Polymer Matrix	Composite Filler	Volume per cent
S2-10P	S2	Silica Particles	10
S2-20P	S2	Silica Particles	20
S2-30K	S2	Kevlar Veil	30
S2-60K	S2	Kevlar Veil	60
S2-30PET	S2	PET mesh	30
S2-60PET	S2	PET mesh	60

The silica particles were dispersed within the polymer matrix either at a 10% or 20% level on a volume basis. SEM images shown in Figure 1 present the silica particles within the S1 matrix at stage 1, and Figure 2 shows the stage 1 images of the silica composites for the S2 system.

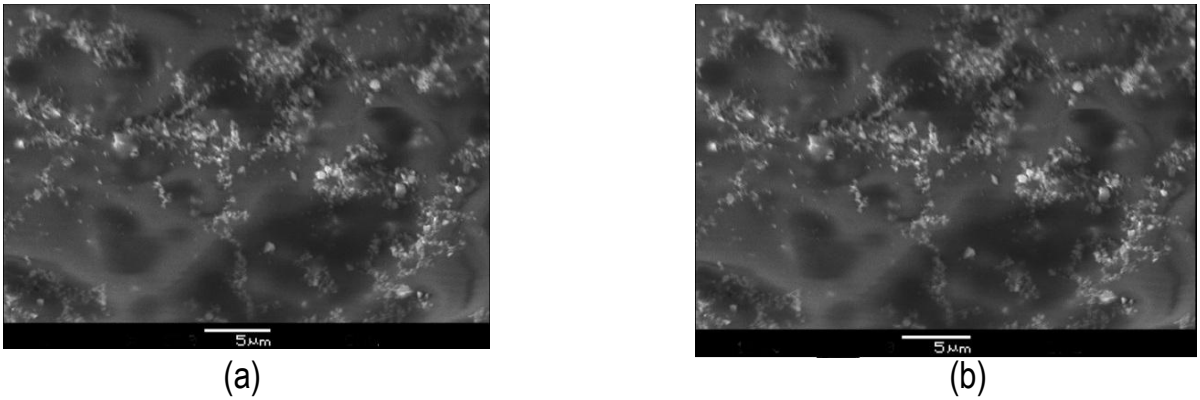

Figure 2. Scanning Electron Microscope (SEM) images of stage 1 particle S1 composites taken in a low vacuum chamber showing silica particle dispersion at 10%(a) and 20% (b).

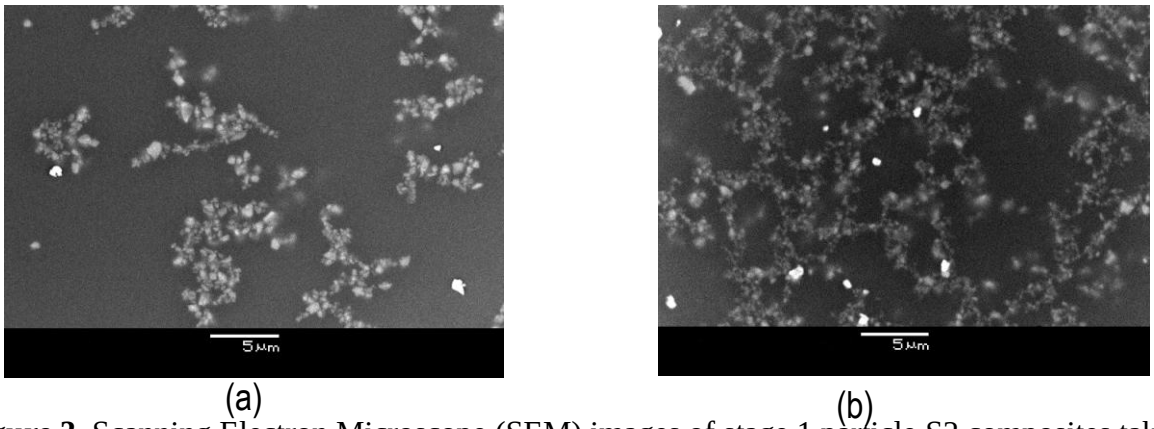

Figure 3. Scanning Electron Microscope (SEM) images of stage 1 particle S2 composites taken in a low vacuum chamber showing silica particle dispersion at 10%(a) and 20% (b).

In Figure 3, the stage 1 thermomechanical data of the S1 and S2 based composites are shown. The composite systems for both formulations did not show significant variations in the stage 1 T_g when compared with the T_g of the neat matrix where the S1 formulation had a T_g of 30 ± 3 ºC and the S2 formulation had a T_g of -2 ± 4º C. The lack of significant changes in T_g at stage 1 and stage 2 of both the composite systems is usually considered a criterion of compatibility between the neat matrix and the filler material in a polymer composite. [12] The presence of a single tan delta peak on the curve also indicates the formation of a relatively homogenous polymer composite.

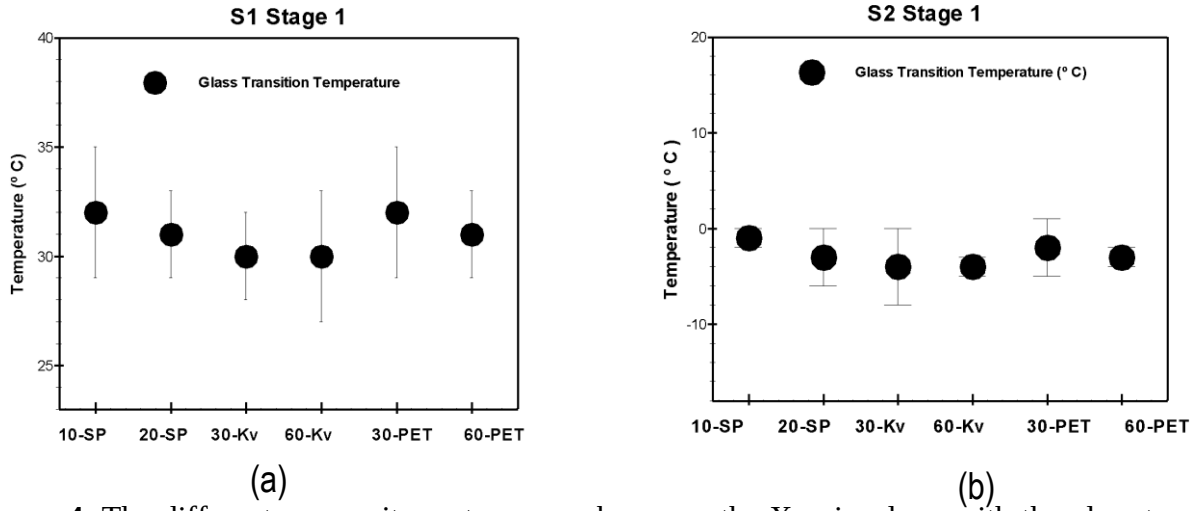

Figure 4. The different composite systems are shown on the X-axis, along with the glass transition temperatures on the Y-axis. The stage 1 T_g of S1 composites systems show no significant variation relative to that of the neat polymer matrix which has a T_g of 30 ± 3º C. (a). The S2 composites also did not significantly alter the T_g of the neat polymer matrix at -2 ±4º C (b). The peak of the tan delta curve was designated as the T_g

As hoped for and in contrast to the glass transition temperature, the modulus at stage 1 for the systems, however, was significantly altered by the presence of the fillers. The S1 composite

systems achieved an increase in the rubbery modulus in comparison with the neat polymer matrix as shown in Figure 4 where the S1 polymer matrix had a modulus of 20 MPa. The most dramatic change in modulus was observed for the S1-60K and S1-60PET composites, which achieved 275% and 350% increases in modulus, respectively. The increase in modulus observed for the PET and Kevlar S2 polymer composites followed a similar trend as the S1 composites, achieving up to a 200 % increase in modulus in the S2-60PET system when compared to the neat polymer system. However, overall the increase in modulus seen at stage 1 for the S2 systems was less dramatic in comparison with the S1 composites, with the silica particles failing to impact the rubbery modulus of the S2-silica composites to any significant extent. A possible reason for this result could be that the 1 to 3 thiol to acrylate off-stoichiometeric S2 system has 66% of the original acrylates remaining unreacted within the system at stage 1. The unreacted acrylate functional groups essentially function as network plasticizers, lending significant chain mobility within the polymer network. Also, as Ebecryl 8402 is a high molecular weight, long chain, difunctional molecule which allows considerable mobility of chains between the tethering crosslinks within the network, the untethered silica particles fail to add significantly to the modulus of the network in stage 1. Therefore, the S2-10P and S2-20P composites with 10% and 20% silica particles as reinforcements present within such a network would fail to add significant reinforcement to the composite at stage 1.

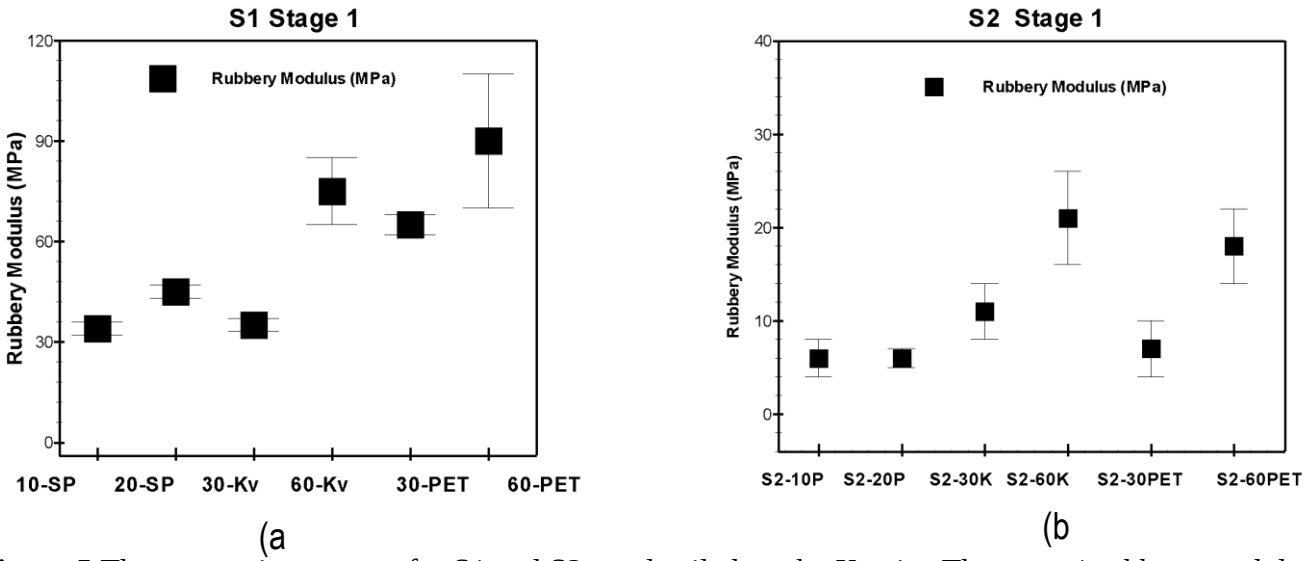

Figure 5.The composite systems for S1 and S2 are detailed on the X axis. The stage 1 rubbery modulus of S1 composite systems achieved an increase in modulus when compared to the neat polymer matrix. (a). A similar increase in modulus was observed for all S2 composites except the S2 silica particle composite (b). The neat polymer matrix modulus for S1 and S2 was 20 ± 2 MPa and 6 ± 2 MPa, respectively. The rubbery modulus was measured at a temperature of T_g + 35 ºC.

The stage 2 glass transition temperature of both the S1 and S2 composites are shown in Figure 5. There was no significant change in the stage 2 T_g when compared with the stage 2 T_g of the neat polymer matrix at 82º C. The slight drop in T_g seen in the S1 silica composites S1-20P and S1-10P at 10% and 6% was within error and any reduction could possibly be attributed to undercuring of the systems due to light scattering associated with the composite. Similarly, the S2 composites also demonstrated no significant change in the stage 2 T_g of the composite system when compared with the T_g of the neat matrix at 18º C. The T_g of the composite systems at stage 2 remained consistent with that of the neat polymer matrices.

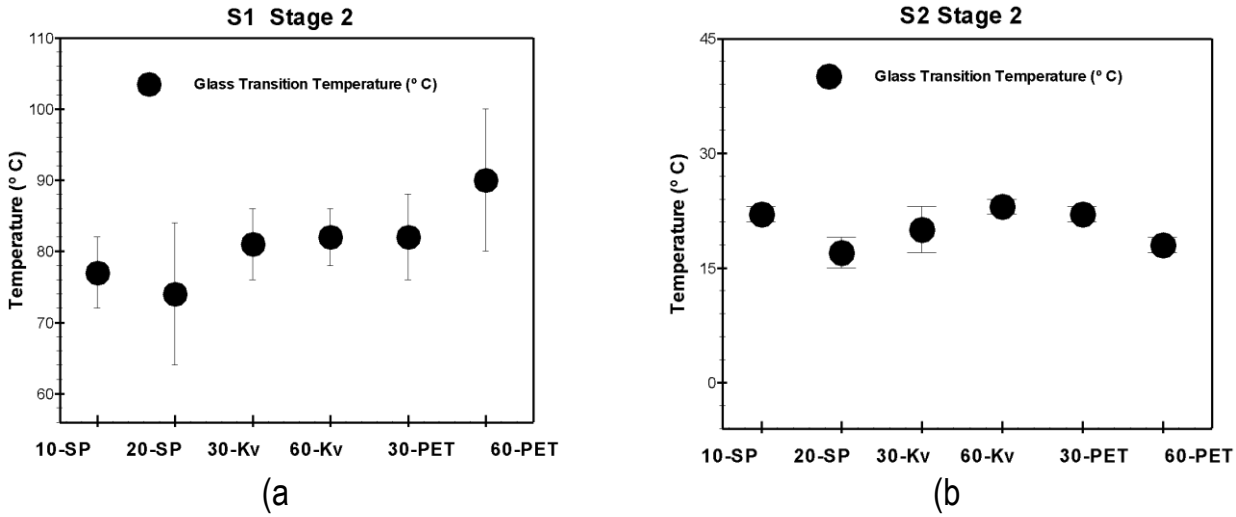

Figure 6. The composite formulations are shown on the X-axis in both (a) and (b). The stage 2 T_g of S1 composites systems also shows no significant variation relative to that of the neat polymer matrix which has a T_g of 82 ± 4 ºC. (a). The S2 composites also did not significantly alter the T_g of the neat polymer matrix at 18 ± 5 ºC (b).

The modulus at stage 2 for the S1 composites achieved significant increase when compared to that of the neat polymer matrix as seen in Figure 6. The PET composites considerably enhanced the stage 2 modulus of the S1 systems with the S1-60PET mesh composite system achieving an 80% increase in modulus. The S1-30PET composite, along with the Kevlar S1-30K composites and the S1-10P composite, achieved a modest increase in the average modulus between stage 1 and stage 2 of up to 30%. However, the S1-20P composite achieved over a two-fold increase in modulus at 155 MPa. This dramatic increase in modulus could be attributed to the methacrylated silica particles crosslinking with the polymer matrix at stage 2. [13] The S1-60K Kevlar composite also exhibited a significant 2-fold increase in stage 2 modulus. The results show that for the S1 composites system, the volume and type of filler played a significant part in determining the ultimate modulus of the material after all curing stages. The S2 composites, the S2-60K Kevlar composite and the S2-60PET composite show an increase in modulus of 250% and 200%,

respectively, when compared to the stage 1 modulus. In stage 2, the S2-60K and S2-30K Kevlar and PET mesh composites increase the modulus by similar values, with the Kevlar veil composites exhibiting a 140% increase in modulus and the PET composite achieving a 120% increase in modulus. The methacrylated silica particles that crosslink into the polymer matrix in stage 2 significantly increase the modulus by up to 100% as shown by the S2-60P silica composite.

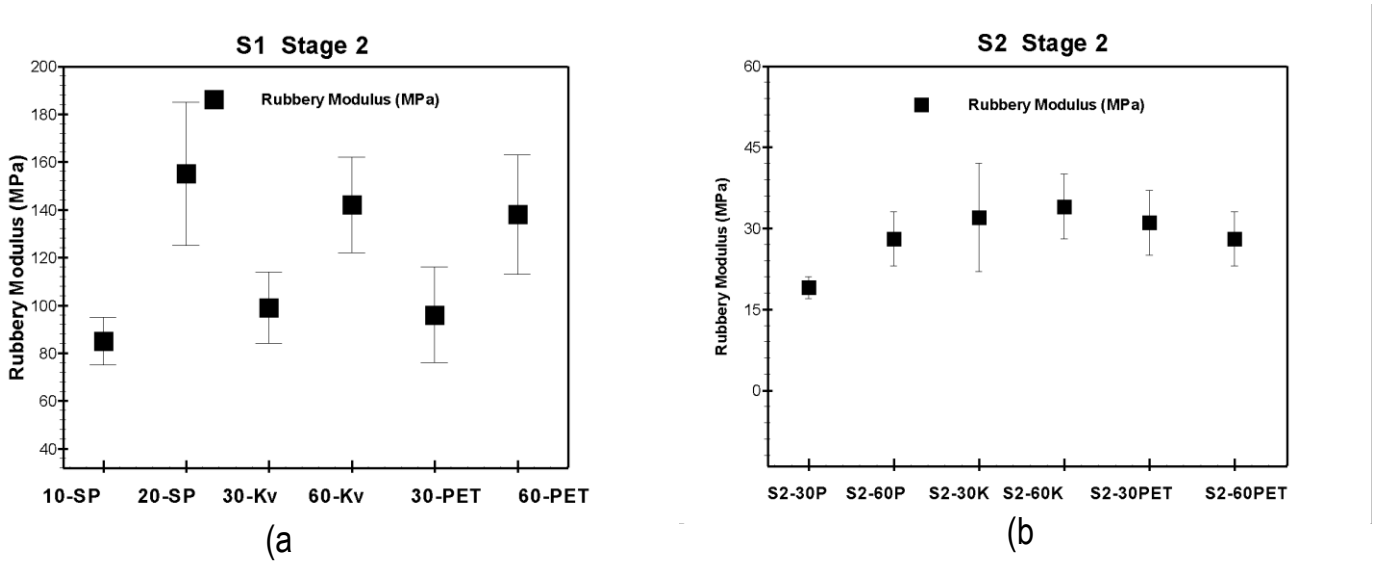

Figure 7. The rubbery moduli for the S1 composites at stage 2 (a) and the S2 composites at stage 2(b) were measured at a temperature of T_g + 65°C. The neat polymer matrix moduli at stage 2 for S1 and S2 polymers were 77 ± 10MPa and 14 ± 5 MPa, respectively.

Overall, for both the S1 and S2 systems the filler does not significantly impact the T_g at either stage 1 or stage 2. The modulus, however, at stage 1 was dominated by the filler type and content for both the S1 and S2 composites. For the S1 composites, the stage 2 modulus was markedly impacted by the filler concentration. There was an increase in modulus by the filler only if the filler was present in significant quantities, as seen in the S1-20P, S1-60K composite and the S1-

60PET composites. Otherwise, the matrix dominated the stage 2 modulus measure for this system. For the S2 system, however, the modulus at stage 2 continued to be dominated by both the filler type and concentration.

The tensile strength, strain at break and toughness of the polymer networks were characterized, and the data are presented in Tables 4-7. Based on the peak stress and the strain at break of these systems, the toughness of the network at the end of each stage was calculated. Table 4 details the tensile modulus data and the strain at break for the S1 composite systems and the data for the neat polymer matrix. The stage 1 silica composite systems of both S1-20P and S1-10P show a slight decrease in tensile strength, consistent with what is seen in particle filled composites in which the particles are not tethered to the network. [14] The Kevlar veil composites show an average 49 % increase in tensile strength, whereas the PET mesh composites show an average 270% increase. The tensile moduli for stage 2 of the composites systems were largely dominated by the tensile properties of the polymer matrix and did not show a significant variation when compared with the neat matrix. The strain at break of silica composite systems and the PET mesh composite systems at stage 1 increased by 50% and 80% respectively when compared to the neat polymer matrix. The Kevlar composites showed no appreciable increase in strain at break after stage 1 when compared with the neat matrix.

In comparing the composites between stage 1 and stage 2, all composites showed a reduction in strain at break along with an increase in the tensile modulus as expected due to the significant crosslinking at stage 2. However, on average, the increase in tensile modulus of the composites when compared to the neat matrix is less in stage 2 as compared to stage 1. While the composite filler type and quantity control the tensile modulus in stage 1, the stage 2 modulus is largely

controlled by the polymer matrix properties at ambient and therefore the filler type and content have less impact on the stage 2 composites.

Table 4. The stage 1 and the stage 2 tensile modulus and strain at break of the S2 composite system measured at ambient temperature (22ºC).

Polymer System	Stage 1 Tensile Modulus (MPa)	Stage 1 Strain at Break (mm/mm)	Stage 1 Tensile Modulus (GPa)	Stage 2 Strain at Break (mm/mm)
S1	43 ± 5	0.13 ± 0.01	1.6 ± 0.2	0.03 ± 0.001
S1-10P	38 ± 4	0.2 ± 0.01	1.7 ± 0.1	0.02 ± 0.004
S1-20P	31 ± 2	0.2 ± 0.05	1.8 ± 0.1	0.02 ± 0.01
S1-30K	75 ± 20	0.1 ± 0.04	1.5 ± 0.2	0.03 ± 0.01
S1-60K	53 ± 10	0.12 ± 0.02	1.5 ± 0.2	0.02 ± 0.003
S1-30PET	140 ± 30	0.23 ± 0.05	1.2 ± 0.2	0.05 ± 0.02
S1-60PET	180 ± 30	0.27 ± 0.02	1.7 ± 0.6	0.03 ± 0.01

Table 5 details the modulus and strain at break values for the S2 polymer system. The strain at break of the composites followed the same trend as the S1 systems, with the Kevlar composites alone showing no significant increase in strain at break after stage 1 curing. However, the tensile modulus increases significantly across all composites in stage 1 with the S2-60K Kevlar composite and S2-60PET mesh composite showing a 12 fold increase and 4 fold increase in modulus, respectively. In stage 2, all composite systems showed an increase in modulus when compared with the neat polymer matrix with the S2-20P composite showing a 3.7 fold increase

in tensile modulus. The S2-60K composite and the S2-60PET mesh composite showed a 3.5 fold increase and a 2.7 fold increase in tensile modulus values. Unlike the S1 system in which the stage 2 tensile modulus was largely controlled by the matrix properties, the differences in the stage 2 moduli of the S2 composite systems can be attributed to filler properties within the polymer matrix. As the S2 system has a T_g of 18º C at stage 2, S2 composites will retain sufficient mobility at ambient conditions compared to the S1, and therefore, the composite filler type is able to have a greater impact the properties at stage 2.

Table 5. The stage 1 and the stage 2 tensile modulus and strain at break of the S2 system measured at ambient temperature (22ºC).

Polymer System	Stage 1 Tensile Modulus (MPa)	Stage 1 Strain at Break (mm/mm)	Stage 2 Tensile Modulus (MPa)	Stage 2 Strain at Break (mm/mm)
S2	5 ± 2	0.16 ± 0.05	13 ± 8	0.13 ± 0.1
S2-10P	7 ± 0.3	0.2 ± 0.05	21 ± 1	0.10 ± .01
S2-20P	4 ± 1	0.3 ± 0.05	48 ± 5	0.13 ± 0.02
S2-30K	23 ± 6	0.1 ± 0.03	45 ± 10	0.05 ± 0.02
S2-60K	63 ± 8	0.1 ± 0.01	60 ± 20	0.1 ± 0.06
S2-30PET	7.4 ± 1	0.4 ± 0.2	17 ± 5	0.2 ± 0.01
S2-60PET	19 ± 10	0.3 ± 0.08	35 ± 10	0.2 ± 0.1

The toughness values for the S1 composite system at stage 1 and stage 2 are shown in Table 6. The toughness of the composite system depends on both the peak stress values a polymer can attain and the strain at which point the system breaks. There is a 130% increase in toughness seen as the system goes from stage 1 to stage 2 for the neat polymer matrix, implying that the reduced strain at break is offset by the increase in peak stresses that the system can endure. However, the silica particle and PET mesh composite systems tend to show a slight reduction in toughness as the systems go from stage 1 to stage 2. This reduction too is dominated by reduced strain at break values at stage 2 and implies that the stage 2 polymer composites are also relatively brittle compared to stage 1 materials. The Kevlar composites show an increase in toughness of greater than 100% as they go from stage 1 to stage 2, showing that the peak stresses that can be attained by the Kevlar composites in stage 2 are considerably higher than stage 1, even though there is slight reduction in strain that is observed.

Table 6. The stage 1 and the stage 2 calculated toughness values from the peak stress and strain at break measures of the S1 system at ambient conditions.

Polymer System	**Stage 1 Toughness (J/mm^3)**	**Stage 2 Toughness (J/mm^3)**
S1	0.3 ± 0.1	0.7 ± 0.1
S1-10P	0.4 ± 0.1	0.4 ±0.08
S1-20P	0.32 ± 0.2	0.24 ± 0.1
S1-30K	0.27 ± 0.02	0.5 ± 0.2
S1-60K	0.24 ± 0.1	0.5 ± 0.1
S1-30PET	1.4 ± 0.3	0.5 ± 0.1
S1-60PET	0.6 ±0.2	0.4 ± 0.2

The trend observed for S2 toughness measures between stage 1 and stage 2 showed that there was an increase in toughness as the material went from stage 1 to stage 2. The higher chain mobility of the stage 2 polymer in this system along with its T_g being close to ambient at stage 2 ensures that the composite systems are less brittle when compared with the stage 1 polymer systems, while enabling them to attain higher peak stresses at the end of both stage 1 and stage 2. The increase in toughness for the S2-60 PET mesh system was 9 fold higher when compared with the neat matrix.

Although the S1 composites, with a T_g at 30 ºC, are dominated by the filler type and quantity in stage 1 under ambient conditions, the matrix properties dominate the stage 2 properties for this system which is glassy at ambient with a stage 2 Tg of 82º C. For the S2 system with both stage 1 and stage 2 T_g s below ambient at -2 and 18 ºC, respectively, the filler type and content continue to influence both the stage 1 and stage 2 properties of the composites throughout all stages of the material's implementation.

Table 7. The stage 1 and the stage 2 calculated toughness values from the peak stress and strain at break measures of the S2 system at ambient conditions.

Polymer System	**Stage 1 Toughness (J/mm^3)**	**Stage 2 Toughness (J/mm^3)**
S2	0.1 ± 0 .07	0.3 ± 0.1
S2-10P	0.1 ± .02	0.1 ± .01
S2-20P	0.12 ±0.02	0.4 ±0.07
S2-30K	0.08 ±0.01	0.1 ± 0.01
S2-60K	0.04 ±.01	0.3 ± 0.1
S2-30PET	0.6 ± 0.4	0.6 ± 0.4
S2-60PET	0.5 ± 0.1	2.8 ± 1

6.4 Conclusions

Thermomechanical analysis of two-stage reactive polymer composite systems clearly shows the ability to control both the stage 1 and stage 2 behavior and properties of the S1 and S2 polymer composite systems through alterations in the filler type and content. For the S1 composite systems, a considerable increase in modulus at stage 1 and stage 2 was achieved by varying the filler type and content with moduli varying from 85 MPa to 155 MPa, although the polymer matrix dominated the mechanical properties at stage 2. For a low T_g, low modulus, system such as S2, the filler type and content dominated the mechanical properties of the system after both the initial and final curing stages. The S2-20P composite demonstrated the ability to have a stage 1 system which achieves no alteration in modulus in comparison with the neat polymer matrix, but can achieve a 360% increase in modulus at stage 2. Based on these results, the two-stage reactive composite platform can be formulated and tailored to meet a range of material processing and application specific mechanical requirements.

6.5 Acknowledgements

The authors would like to acknowledge National Science Foundation CBET 0626023, National Institute of Health T32HL072738 and the University of Colorado Technology Transfer Office CU2615B-01 for providing funding for this research.

6.6 References

[1] . O. Breuer ,U. Sundararaj, *Poly.Comp.*2004,**24**,630

[2] . R Vajtai, B Q Wei, Z J Zhang, Y Jung, G Ramanath,P M Ajayan, *Smart Mat. Struct.*,2002,**11**,691

[3] . R.F.J. McCarthy , G.H. Haines, R.A. Newley,*Comp.Man.*,1994,**5**,83

[4] . G.C. Jacob, J.F. Fellers, S.Simunovic, J.M. Starbuck, *J.Comp. Mat.*,2002,**36**,813

[5] . D.P.Nair, N.B. Cramer, J.C.Gaipa, M.M.McBride, E.M. Matherly, R.M. McLeod, R. Shandas, C.N. Bowman, *Adv. Func. Mat.*, 2011

[6] . B.D. Mather, K. Viswanathan, K.M. Miller, T.E. Long, *Prog. Poly.Sci.* 2006, **31**, 487

[7] . C.E. Hoyle, C.N. Bowman, *Angew. Chem. Int. Ed.* 2010, **49**, 1540

[8] . J. W. Chan, H Wei, H. Zhou, C.E. Hoyle, *Euro. Poly. J.* 2009, **45**, 2717

[9] . D.L Elbert , A.B. Pratt , M.P. Lutolf, S. Halstenberg J.A. Hubbell, *J. Control. Rel.* 2004, **76**,11.

[10] . A. M. Kloxin, M. Tibbitt, A.M. Kasko, J.A. Fairbairn, K.S. Anseth, *Adv. Mater.* 2010, **22**, 61.

[11] . A. E. Rydholm, C. N. Bowman, K. S. Anseth, *Biomaterials*, 2005, **26**, 4495

[12] . J**.** Cañavate1, P. Pagés, J. Saurina, X. Colom1, F. Carrasco, *Poly. Bulletin*, 2000, **44**, 293

[13] . M. S. Sreekala, C. Eger, *Poly.Comp*.2005,**1**,91

Chapter 7

Two-Stage Reactive Polymer Networks as Suture Anchor Systems

Two-stage reactive polymeric devices as orthopedic suture anchors for arthroscopic surgery are formulated and mechanically characterized in this study. Arthroscopic procedures have become more and more pronounced as they result in improved patient outcomes, faster recoveries, and less cost. Within arthroscopy, the suture anchor works as a staple or straight pin by holding the healing tissues or the soft tissue and bone together to enable reattachment. Studies over the past decade have shown that the primary contributor to device pull-out and migration is the modulus mismatch between the anchor and the surrounding bone. [1-3] In this work we utilize novel thiol-acrylate systems to design and formulate two-stage reactive shape memory polymer (SMP) systems which can be delivered arthroscopically. A thiol-acrylate SMP network formed by a 'click' Michael addition reaction with a stoichiometeric excess of acrylate groups relative to thiol groups, forms an initial, stage 1 polymer network. [4] After arthroscopic device placement, the residual acrylate functional groups can be photopolymerized in a second polymerization reaction to form a highly crosslinked final, stage 2 polymer that is designed to match the local bone modulus, thereby minimizing device failures. A series of two-stage reactive polymer systems with similar stage 1 glass transition temperatures of 30º C and modulus of 90 MPa were formulated to achieve varying stage 2 modulus up to 2.3 GPa. Additionally, anchor device pull-out tests achieved a pull-out strength of 138 N for the devices.

7.1 Introduction

Within arthroscopic procedures, the suture anchor, which consists of placing an implant into the surrounding bone or soft tissue, works as a staple or straight pin by holding the healing tissues or

the soft tissue and bone together to enable reattachment.[1-4] Over 4 million arthroscopies were performed in the U.S. in 2010 alone, dominated by knee and shoulder procedures. [5] Out of these, 75,000 repairs were designed to treat torn and/or damaged rotator-cuff injuries. [3] There are currently more than 30 different types of suture anchors available. Despite optimized surgical efforts, technical difficulties with the devices and complications related to the surgical procedure and/or related to the type of device inserted continue to occur. The major complications seen are 1) incorrect device placement 2) migration after placement 4) loosening and 4) device breakage.[6] Although the anchor design and placement play a considerable role in minimizing subsequent device failure, studies have shown that the most common issue that contributes to device pull-out and migration is the modulus mismatch between the anchor material and the surrounding bone. This large difference in modulus between the implant material and the bone also gives rise to the phenomenon of stress shielding, in which the mechanical load is unevenly shared between the bone and the implant. [7] Under these conditions, the bone is now subject to reduced stresses as a result of the high modulus implant in its immediate environment and in accordance with Wolfs Law, the reduction in stresses on the bone results in bone mass loss over time. The bone loss as result of the large difference in elastic modulus between bone and implant materials, can also lead to eventual implant failure.

The local quality of the bone into which the device is anchored can vary markedly, given that bone modulus and quality depend on factors such as the age, sex and disease as shown in Figure 1.[8] Although there have been studies that have looked into predicting the pull-out strength of various suture anchors and suture anchor devices such as the suture anchor bearing

area, suture anchor design and different anchor device placement techniques, the essential problem remains the difference in modulus between the implant and its local environment. [2,3,5]

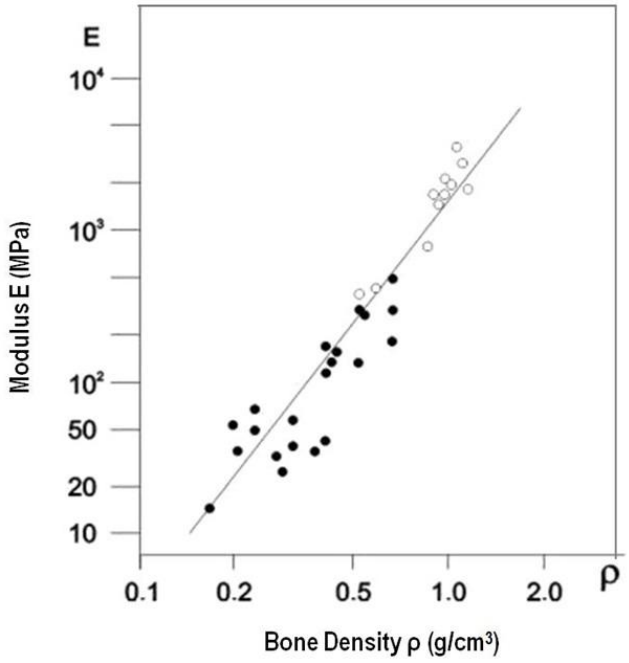

***Imagesource-http://www.feppd.org/ICB-dent/campus/biomechanics_in_dentistry/ldv_data/mech/basic*_bone.htm**

Figure 1. The graph plots the Young's modulus of trabecular bone as a function of density of bone. Bone density varies with age, sex and disease and directly correlates to bone strength. *Image taken from* http://www.feppd.org/ICB-dent/campus/biomechanics_in_dentistry/ldv_data/mech/basic_bone.htm

In this study, we propose a revolutionary new two-stage reactive shape memory polymer system that, through simple formulation manipulations, enables a range of previously unachievable properties that are ideal for use in orthopedic implants. Here, a thiol-acrylate

network formed by a click Michael addition reaction from an initial monomer mixture, with a stoichiometeric excess of acrylate groups relative to thiol groups, forms an initial polymer network with residual acrylate functional groups. The two-stage reactive polymer system first forms an initial matrix, after the stage 1 curing, that serves as a functional polymer device capable of being utilized as a shape memory polymer suture anchor which can be delivered arthroscopically. Shape memory polymers (SMPs) are characterized by their ability to store a temporary shape and recover their original shape once exposed to an appropriate stimulus such as a set temperature range.[9] Shape memory materials, as a whole, have enabled a range of potential biomedical applications including enabling a plethora of minimally invasive surgical (MIS) options in which an implant device constrained in its temporary shape within a catheter or cannula can be delivered to a targeted location within the body. [10] Once exposed to physiological temperatures, the device transforms into its permanent shape. In the two-stage reactive system described here, the residual acrylate functional groups within the device are photopolymerized in a second polymerization reaction that is orthogonal to the initial polymerization, to form a final polymer that matches the local bone modulus, thereby minimizing device failures. The key to the technique and to the application of the two-stage reactive concept is that this approach uniquely enables the polymer material to have two distinct and largely independent sets of material properties – one set of properties as required for device delivery and a second set of properties that aids the optimum function of the device as a suture anchor.

7.2 Experimental Section

Materials

Pentaerythritol tetra(3-mercaptopropionate)(PETMP) was donated by Bruno Bock, tricyclodecane dimethanol diacrylate (TCDDA) was donated by Sartomer, and Ebecryls 1290 and 8402 were donated by Cytec. The photoinitiator Irgacure 651 (2,2-dimethoxy-2-phenylacetophenone) was donated by Ciba Specialty Chemicals. The inhibitor, aluminum N-nitrosophenylhydroxylamine (N-PAL), was donated by Albemarle. All samples contained 0.05 wt% inhibitor, 0.8 wt% triethyl amine as a catalyst for the first stage reaction and 0.5 wt% Irgacure 651 to initiate the second reaction. For the photopolymerization during the second stage of the reaction, samples were cured at 8 mW/cm^2 using a UV lamp (Black-Ray Model B100AP).

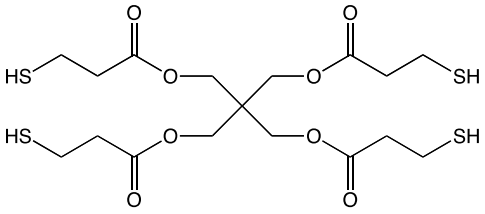

PETMP
pentaerythritol tetra(3-mercaptopropionate)

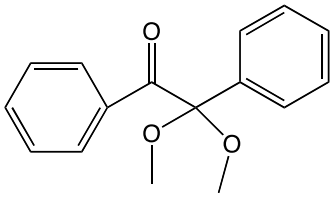

DMPA
2,2-Dimethoxy-2-phenylacetophenone

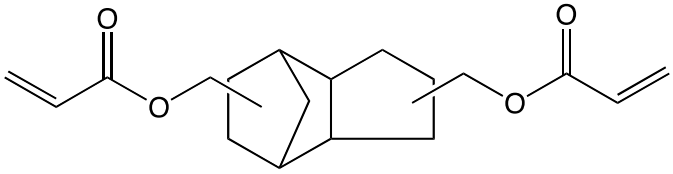

TCDDA

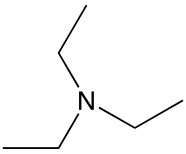

TEA
Triethylamine

Figure 2. Chemical structures of the monomers used in this study.

Polymer Composites

The PET fibers were obtained from Surgical Meshes Inc and set in the polymer matrix in the cross-machine direction. The Kevlar veil and Kevlar Mesh were obtained from Fiber Glass Inc, and the silica particles were donated by Esstech. A FlakTech speed mixer (DAC 150 FVZ) at 2500 rpm for 60 seconds was used to disperse the silica particles within the polymer composite.

Dynamic Mechanical Analysis (DMA)

DMA experiments were performed using a TA Instruments Q800 DMA.

Glass transition temperature (T_g) was determined from polymer samples with dimensions of 10 x 3.5 x 1 mm. Sample temperature was ramped at 3 ^oC/min from -50 to 300^oC with a frequency of 1 Hz and a strain of 0.01 % in tension. The T_g was assigned as the temperature at the tan δ curve maximum. The rubbery modulus values were determined at a temperature 35^oC above the T_g for the stage 1 and 65^oC above the T_g for the stage 2 polymers.

Materials Testing System (MTS)

Tensile test measurements were conducted on an Instron Universal Testing Machine (Insight 2.0) to ascertain the tensile modulus and strain at break for the suture anchor systems. For the suture anchor test, the bottom clamp was replaced by machined devise to hold the dog bone in place. Dog bone shaped samples of dimensions 40 × 6.5 × 1 mm were used. The initial separation of the system was set at 22 mm and a crosshead speed of 5 mm/min was applied. The stage 2 polymerization of the suture anchor device was done *in situ*, within the metal block at 8 mW/cm^2 using a UV lamp (Black-Ray Model B100AP).

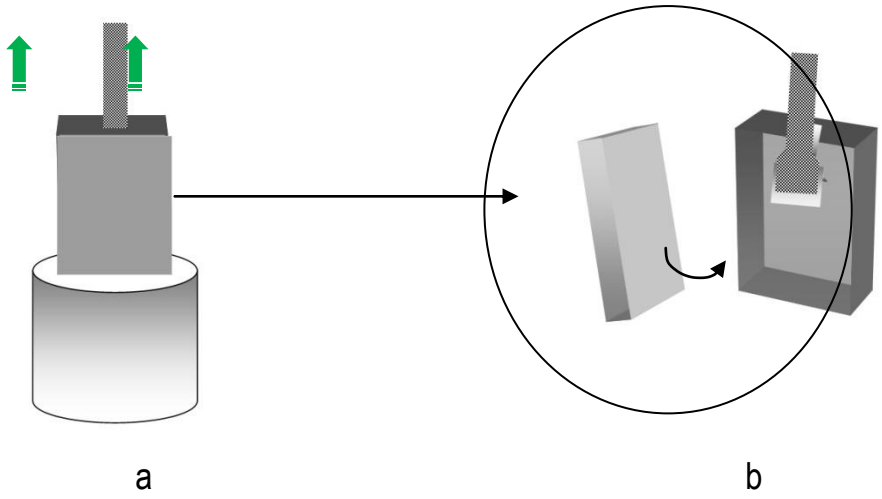

Figure 3. A dog-bone shape grip was machine to attach to the lower cylinder of the tensile test machine (a). Once the dog-bone was inserted in the cavity (b), the cover placed on the grip and held in place. The dog-bone was cured *in situ* within the grip at 8mW/cm$^{2.}$

7.3 Results and Discussion

The two-stage reactive polymer systems formulated and characterized in the study were aimed at enabling arthroscopic delivery of the anchor devices as implants, while maintaining the ability of the systems to tune in a higher, more appropriate modulus at a later stage to match the local bone environment.

Of all the variables that are measured to asses suture anchor failure, the yield strength of the bone has also been proposed as a marker for suture anchor pull-out, as loading the bone above this limit would create irreversible bone deformations and eventually lead to device failure.[11] The yield strength of the bone is dependent on many factors such as Bone Mineral Density (BMD), age and sex. In humans, the relationship between the strength of bone and its density has been well characterized, demonstrating increasing strength with increased BMD. BMD also plays an important role in anchor stability especially in elderly patients. [1,12]

In the two-stage reactive polymer system formulated here, the initial polymer, stage 1 devices that are to be delivered arthroscopically are soft and flexible with glass transition temperatures (T_g) in the range of 30 ºC and a modulus at 25 MPa at body temperature (38º C) as shown in Table 1. Thermomechanical analysis was performed on the two-stage reactive polymer composite systems containing different reinforcing materials -PET mesh, Kevlar veil, Kevlar mesh and micron size silica particles. The neat polymer matrix in all systems was an off stoichiometeric tetrathiol/diacrylate/ urethane hexaacrylate system with PETMP, TCDDA and Ebecryl 1290. This formulation had a thiol to acrylate ratio of 1 to 3. The composites are referred to as F-60-PET (60 volume% PET mesh), F-60-KV (60 volume% Kevlar Veil), F-20P (20 volume% silica particles) and F-60-KM (60 volume% Kevlar Mesh). The composites shown here are representative of the range of fillers that can be varied to achieve different moduli in the final, stage 2 polymer at 38º C while keeping the matrix the same. The initial polymer network has an advantage over metal suture anchor devices in which an inherent lack of flexibility of the metals restricts easy repositioning or realigning of the device during delivery and insertion.[13] Also, once a metal suture anchor has been inserted, the difference in modulus can create large defects which can eventually lead to device migration.[13] Alternatively, plastic suture anchors are subject to brittle fracture. Bioabsorbable plastic suture anchors perform as well as non-bioabsorbable plastics in terms of strength, but it is disputed as to whether the anchors remain in place and retain holding strength enough to facilitate complete healing. Recently, a new SMP suture anchor made from polyether ether ketone (PEEK) has obtained FDA approval.[15] While the use of a SMP improves the design over existing suture anchors, PEEK exhibits the same drawbacks as other SMPs with high modulus. PEEK has a glass transition temperature of 143

°C and therefore is glassy at body temperature and exhibits recoverable strains of less than 10%, leading to limited device designs and shape memory properties.

Table 1. The initial and final T_g and moduli at 38°C of the two-stage reactive composites show the distinct measures of each achieved at the end of each stage. The T_g was measured at the peak of the tan delta curve.

Polymer System	**St 1 -DMA Tg (ºC)**	**Modulus (GPa) @ 38º C**	**St 2 -DMA Tg (ºC)**	**Modulus (GPa) @ 38º C**
F-60-PET	32 ± 3	**0.09 ± 0.03**	82 ± 6	**2 ± 0.3**
F-60-KV	30 ± 3	**0.09 ± 0.01**	82 ± 4	**1.2 ± 0.5**
F-20-SP	31 ± 2	**0.07 ± 0.02**	64 ± 10	**2.3 ± 0.7**
F-60-KM	28 ± 2	**0.09 ± 0.02**	53 ± 5	**1.3 ± 0.3**

The ultimate, stage 2 properties of the two-stage reactive systems are achieved by the polymer once the device has been placed optimally. The second stage reaction, which can be initiated *in-situ*, on-command, can tailor the modulus of the polymer to match the local bone strength. Table 1 is representative of the maximum modulus that can be achieved within a particular two-stage reactive polymer system in which the stage 1 properties of the network are kept similar whereas a range of stage 2 moduli can be achieved based on a judicious selection of fillers. The polymer network in Table 1 is representative of the properties that can achieved by changing the filler type and concentration. By a judicious choice of monomers and stoichiometeries, a wide variety of polymer properties can be achieved at both stage 1 and stage 2.

Studies have also shown a correlation between pullout strength and Bone Mineral Density (BMD), suggesting that the pullout strength also increases with bone density.[18] The force required to pull the suture anchor device from the bone is termed the pullout strength and is

often used as a measure to compare the performance of different suture anchors. The pull-out strength of suture anchors from human trabecular bone is seen to be between 100 to 200 N.[16] In a modified suture anchor pull-out test, a dog-bone shaped for the F-60-PET dual-networking forming polymer system was tested in a specialized test-set up following both the initial and final reaction stages.

The polymer system following the initial reaction having a peak load of 16 N, is a low modulus, high strain, flexible system with a strain at break of 0.3, making it suitable to be delivered as a shape memory polymer in a minimally invasive manner. The polymer properties of this system following the second curing stage, however, had a peak load of 140 N. These values compare favorably to the peak load measures shown by suture anchor systems in the market today, while bearing in mind that the suture anchor pull-out tests for these are typically done in a test up which includes a suture anchor device embedded within bone at one end and tensile grip on the suture at the other end. As the yield strength of bone and steel differ by orders of magnitude, it is favorable to note that although the steel casing used in the pull-out test in this study could have precipitated early device failure, the material still failed at 140 N.

Table 2. Suture device pull-out test data after the initial and final curing stages for tensile modulus, strain at break and peak load for the F-60-PET two-stage reactive system which was recorded at ambient temperature.

	Stage 1		**Stage 2**	
Polymer System	**Strain at Break (mm/mm)**	**Peak Load (N)**	**Strain at Break (mm/mm)**	**Peak Load (N)**
F-60-PET	0.3 ± .01	16 ± 2	0.06 ± 0.01	140 ± 20

7.4 Conclusion

The study has shown a range of properties that are optimal for two-stage reactive suture anchor devices in which distinct initial and final moduli are achievable. Polymer implant systems with similar stage 1 properties along with the ability to vary the stage 2 properties to match the orthopedic moduli in the environment were shown with stage 1 moduli of 90 MPa at body temperature and stage 2 moduli of up to 2.3 GPa. Additionally, the pull-out strength of the F-60-PET system was tested and yielded a measure of 140 N, which compared favorably with current high-strength suture anchor systems.

In keeping the polymer network constant and varying the composite filler type, this study is representative of the range of properties that can be achieved in a two-stage reactive polymer system for an orthopedic suture anchor. However, it is by no means exhaustive in terms of the wide range of properties that can be achieved via the two-stage reactive composite polymer platform.

7.5 Acknowledgements

The authors would like to acknowledge National Science Foundation CBET 0626023, National Institute of Health T32HL072738 and the University of Colorado Technology Transfer Office CU2615B-01 for providing funding for this research.

7.6 References

[1] . M.J. Tingart, M. Apreleva, D. ZurakowskI, J.P.P Warner, *J. Bone.Joint.Surg*.2003,**85A**, 2190

[2] . E. S. Strauss, D. Frank, E. Kubiak, F. Kummer, A. Rokito, *J.Arthro.Surg.* ,2009,**25**,597

[3] . C.M.Yakacki, J. Griffis, M. Poukalova, K. Gall, *J. Ortho.Res*., 2009, **27**,1058

[4] . D.P.Nair, N.B. Cramer, J.C.Gaipa, M.M.McBride, E.M. Matherly, R.M. McLeod, R. Shandas, C.N. Bowman, *Adv. Func. Mat.*, 2011

[5] . *American Orthopaedic Society for Sports Medicine 2011 report*

[6] . H.B.Park, E. Keyurapan, H.S. Gill, H. S. Selhi, E. G. McFarland, *Am.J Sports. Med.*.2006,**34**,136

[7] . H.W.J. Huiskes, H. Weinans, B. van Rietbergen, *Clin. Orthop.*,1992,**274**,192

[8] . M. Poukalova ,C. M. Yakacki , R. E. Guldberg, A. Lin, M. Saing, S.D Gillogly, K. Gall, *J. Biomech.*,2010,**43**,1138

[9] . D.P.Nair, N.B. Cramer, T.F. Scott, C.N. Bowman,R. Shandas, *Polymer*, 2010 ,**51**,4383

[10] . C.M. Yakacki, R. Shandas, D. Safranski, A.M. Ortega, K .Sassaman, K. Gall, *Adv. Funct. Mater.* 2008 , **v**,2428

[11] . G. M. Gualtieri, S. Siegler, E. L. Hume, S. R. Kalidindi, *J.Ortho. Res.*, 2000,**18**,494

[12] . S.W Chung, J.H. Oh,H. S. Gong,J. Y. Kim, S. H. Kim, *Am.J Sports. Med.*.,2011,**39**,2099

[13] . J Parisien, "Current Techniques in Arthroscopy" 1998, Thieme Medical Publishers NY, USA.

[14] . P.W. Grutter, E.G.McFarland, B.A. Zikria, Z. Dai,S. A. Petersen. *Am.J Sports. Med,* 2010,**38**,1706

[15] . www.medshape.com/morphix.html

[16] . R. Mimar, D.Limb, R. M. Hall, *Brit. Elb.Shol. Soc*, 2009,**1**,31

Chapter 8

Conclusions and Recommendations for Future Work

This thesis was focused on investigating thiol-ene and thiol-acrylate systems as shape memory polymers and as a novel two-stage reactive polymer platform for potential applications that range from biomaterials to optical devices. Towards this goal, the relationships between monomer formulations and material properties of the thiol-ene and thiol-acrylate systems were studied using kinetic, thermomechanical and mechanical analysis. In Chapter 3, thiol-ene photopolymer systems were formulated and evaluated as shape memory polymer systems. The thermally activated shape memory formulations were designed to have glass transition temperatures close to body temperature and were thermomechanically and mechanically characterized and evaluated against a common acrylic shape memory system. The shape memory behavior of the thiol-ene systems exhibited free strain recoveries of greater than 96% and constrained stress recoveries of 100%. The thiol-ene polymers exhibited excellent shape fixity and rapid and distinct shape memory actuation responses. Relative to the acrylic systems, the thiol-ene SMPs exhibit a more rapid and distinct shape memory response as well as improved shape retention upon thermal stimulation.

In Chapter 4, two--stage reactive polymer systems were developed via an initial thiol-acrylate 'click' Michael addition reaction and subsequent photoinduced radical polymerization. The two-stage reactive thiol-acrylate network systems were formulated with differing off-stoichiometeric ratios as proof-of-concept for a new polymer technology platform. Two systems were characterized in detail for kinetic and material properties for each stage of the network. Further, the wide ranging applicability of the two-stage reactive polymer system was demonstrated by using the same monomers and varying the stoichiometery of the formulation to

achieve properties suitable for three dramatically different applications; a shape memory polymer, an impression material and an optical storage device. The dual cure systems showed a range of glass transition temperatures between the stage 1 and stage 2 networks that differed by as much as 210 ^{0}C. Further, a modulus increase of nearly 200 times was achieved following the final reaction.

In Chapter 5, by changing one monomer along with the stoichiometeric thiol-acrylate ratios in the dual cure polymer systems, enhanced dual network systems were formulated to demonstrate the tunability of the two-stage reactive polymer platform. Polymer networks were thermomechanicaly and mechanically characterized and demonstrated to exhibit stage 1 glass transition temperatures ranging from -10 to 30 °C, stage 2 glass transition temperatures ranging from 12 to 90 °C, stage 1 moduli ranging from 1 to 20 MPa, and stage 2 moduli ranging from 5 to 125 MPa.

In Chapter 6, two-stage reactive polymer composite systems were examined. Three different composite materials (silica particles, Kevlar veil, and PET meshes) with varying compositions were formulated and characterized. The composite systems demonstrated that improvements in material properties such as modulus and strength can be achieved at the end of the stage 1 cure, and in some cases at the end of the stage 2 cure, without significantly compromising the strain at break or glass transition temperatures of the polymer systems.

Chapter 7 was devoted to demonstrating a dual-network polymer device as an orthopedic suture anchor. Two-stage reactive polymer devices were formulated and tested as suture anchor systems within a custom test apparatus designed to mimic the environment within which the device is expected to function. In addition to achieving modulus that could match the modulus of a range of trabecular bone, the results demonstrated suture anchor pull-out strengths of up to

nearly 140 N, compared to the range of 100 to 200 N as a representative other type of suture anchor.

Recommendations for future work include evaluating a broader range of monomers towards developing the two-stage reactive polymer systems as shape memory polymer-based platform. A prototype of a suture anchor device has been tested in an *in vitro* set up in which the ability of the device to exhibit distinct stage 2 properties such as a higher modulus was characterized. Thus far, the work has concentrated on formulating the material properties of a two-stage reactive suture anchor. Future work in this area will include designing and testing a SMP based suture anchor device that can be delivered via minimally invasive procedures. Once this device has been delivered and actuated into its permanent shape, the *in vitro* curing capability and stage 2 properties will be evaluated. We expect that a working prototype device will exhibit the properties necessary for an orthopedic suture anchor and dramatically exceed the properties of any other similar device. Additionally, the potential of a two-stage reactive polymer network for other minimally invasively delivered biomedical devices such as cardiovascular stents can also be examined.

More work in the arena of two-stage reactive composite systems with different fillers designed to enhance the material properties of the polymer matrix is also recommended to develop additional properties and applications. The nature of the interaction between each of the composite fillers and the matrix and the interface of the two components can also be characterized in detail to understand and exploit the development of stage 1 and stage 2 capabilities of the polymer. In addition, using alternate methods to induce the stage 2 reaction,

such as a thermally induced free radical polymerization should be explored in detail for the application of two-stage reactive systems in devices where photoinduced stage 2 polymerization is not an option.

Bibliography

[1] . A. R. Kannurpatti, K. J. Anderson, J. W. Anseth, C. N. Bowman, *J. Polym. Sci. Part B*, 1997, **35**, 2297

[2] . P.T. Mather, X Luo, I.A. Rousseau, *Ann. Rev. Mater. Research*. 2009, **39**, 445

[3] . C. Liu, H. Qin, P.T Mather, *J. Mater. Chem.* 2007**, 17**, 1543

[4] . F. Chen, W. D. Cook, *Euro. Poly. J*, 2008, **44**, 1796

[5] . J. J. Singh , R. H. Pater, A. Eftekhari, 1998 ,**134**, 113

[6] . G. David, M. Pinteala, B. C. Simionescu, *Dig. J. Nano. Bio.*,2006, **1**, 129

[7] . J.G. Woods, **I***n Radiation Curable Adhesives in Radiation Curing: Science and Technology;* Pappas, S. P., *Ed.; Plenum:* New York, 1992*; pp* 333–398.

[8] . C.E. Hoyle, C.N. Bowman, *Angew. Chem. Int. Ed.* 2010, **49**, 1540

[9] . C. E. Hoyle, T. Y. Lee, T. Roper, *J. Polym. Sci. Part A* 2004, **42**, 5301.

[10] . B.D. Mather, K. Viswanathan, K.M. Miller, T.E. Long, *Prog. Poly.Sci.* 2006, **31**, 487

[11] . D.L Elbert, A.B. Pratt , M.P. Lutolf, S. Halstenberg J.A. Hubbell, *J. Control. Rel.* 2004, **76**,11.

[12] . A. M. Kloxin, M. Tibbitt, A.M. Kasko, J.A. Fairbairn, K.S. Anseth, *Adv. Mater.* 2010, **22**, 61.

[13] . A. E. Rydholm, C. N. Bowman, K. S. Anseth, *Biomaterials*, 2005, **26**, 4495

[14] . A. F. Jacobine, *In Radiation Curing in Polymer Science and Technology III: Polymerization Mechanisms;* J. D. Fouassier, J. F. Rabek, *Elsevier:* London, 1993

[15] . N. B. Cramer, C. N. Bowman, *J. Poly. Sci. Part A* 2001, **39,** *3311.*

[16] . J. W. Chan, H Wei, H. Zhou, C.E. Hoyle, *Euro. Poly. J.* 2009, **45**, 2717

[17] . N.B. Cramer, J.P. Scott, C.N. Bowman, *Macromolecules*, 2002, **35**, 5361

[18] . M. Cole, M. Bachemin, C.K. Nguyen, Viswanathan, C.E Hoyle, *RadTech Japan*, 2000, 211

[19] . S.K. Reddy, N.B. Cramer, A.K. O'Brien, T. Cross, R. Raj ,C.N. Bowman. *Macromolecular Symposia*, 2004, **206**, 361

[20] . C.M. Yakacki, R. Shandas, C. Lanning, B. Rech, A. Eckstein, K. Gall, *Biomaterials*, 2007, **28**, 2255

[21] . K. Otsuka, C.M. Wayman in *Shape Memory Materials* . (Eds: University Press, Cambridge, UK , 1998)

[22] . T.W. Duerig, D. Stoeckel, A. Pelton, *Mater. Sci. Eng.* 1999, **273**, 149

[23] . A. Lendlein, S. Kelch , *Angew. Chem.* Int. Ed. 2002, **114**, 2138

[24] . D.P.Nair, N.B. Cramer, T.F. Scott, C.N. Bowman,R. Shandas, *Polymer*, 2010 ,**51**,4383

[25] . I.A. Rousseau, *Poly. Eng. Sci.* 2008,**48**, 2075

[26] . D. Ratna, J. Karger-kocsis. *J. Mater. Sci.* 2008, **8**, 254

[27] . V.S. Khire, Y. Youngwoo, N.A. Clark , *Adv. Mater.* 2007, **20**, 3308

[28] . H.D. Rowland, W.P. King, *Appl. Phys.A: Mater. Sci. Process.* 2005 **, 81**,1331

[29] . T.C Bailey, S.C. Johnson, S.V. Sreenivasan, J.G. Ekerdt, C.G. Willson, D.J. Resnick, . J. *Photopolymer Sci. Technol*. **15**, 481

[30] . J. P. Rolland, E. C. Hagberg, G. M. Denison, K. R. Carter, J. M. DeSimone, *Angew. Chem. Int. Ed*. 2004, **43**, 5796.

[31] . R. R. A. Syms in *Practical Volume Holography* (Oxford University Press, Oxford, 1990).

[32] . V. W. Krongauz, A. D. Trifunac in *Processes In Photoreactive Photopolymers* (Chapman & Hall, New York, 1994).

[33] . B. J. Chang, C. D. Leonard, Appl. Opt. 1979, **48**, 2407

[34] . D. H. Close, A. D. Jacobson, R. C. Magerum, R. G. Brault, F. J. McClung, Appl. Phys. Lett. 1969, **14**, 159-160 (1969).

[35] . S.A . Madbouly , A. Lendlein, *Adv Polym Sci* ,2010, **226,** 41

[36] . W. D. Callister. Composites, chapter 16, page 527. Material Science and Engineering an Introduction. John Wiley and Sons, Inc., sixth edition, 2003.

[37] . S. Ramakrishna, J. Mayer, E. Wintermantel, K. M. Leong. *Comp. Sci. Tech*, 2001, **61**,1189

[38] . J Parisien "Current Techniques in Arthroscopy" 1998, Thieme Medical Publishers NY, USA.

[39] . P.W. Grutter, E.G. McFarland, B.A. Zikria, Z. Dai, S.A Petersen , *Amer. J. Sports Med.* 2010,**38**,1706

[40] . C.M. Yakacki, R. Shandas, D. Safranski, A.M. Ortega, K .Sassaman, K. Gall, *Adv. Funct. Mater.* 2008 , **v**,2428

[41] . W.J. van Rooija , M. Sluzewskia, Am. J. Neuro. Radio.2007, **28**,368

[42] . Lendlein, R. Langer, *Science*, 2002, **296**,1673

[43] . S. Ramakrishna, J. Mayer, E. Wintermantel, K. M. Leong. *Comp. Sci. Tech*, 2001, **61**,1189

[44] . C. N. Bowman, C. J. Kloxin, *AIChE Journal*, 2008, **54**, 2775

[45] . L. Qin, D.A. Wicks, C.E. Hoyle, *J. Poly. Sci. A* 2007, **45**, 5103

[46] . J. W. Chan, C.E. Hoyle, A.B. Lowe, *J.A.C.S* 2009,**131**,16

[47] . J. W. Chan, C.E. Hoyle, A.B. Lowe, M. Bowman, *Macromolecules* 2010,**43**, 15

[48] . A.B. Lowe, *Poly.Chem.* 2010,**1**,17

[49] . C. Liu, H. Qin, P.T Mather, *J. Mater. Chem.* 2007**, 17**, 1543

[50] . M.Y. Razzaq , L. Frormann , *Poly.Comp.* 2007 , **28**, 287

[51] . Q.H. Meng, J.F. Hu ,*Composites*, 2008, **39**,314

[52] . J.W. Xu , W.F. Shi, W.M. Pang. *Polymer*, 2006 **47**,457

[53] . K.Gall, M.L. Dunn, Y. Liu *Microscope,* 2002, **50**,5115

[54] . T. Xie, I.A. Rousseau , *Polymers,* 2009, **50**,1852

[55] . Y. Xia, G. M. Whitesides, *Angew. Chem. Int. Ed*. 1998, **37**, 550

[56] . V.S. Khire, Y. Youngwoo, N.A. Clark , *Adv. Mater.* 2007, **20**, 3308

[57] . R. R. A. Syms in *Practical Volume Holography* (Oxford University Press, Oxford, 1990).

[58] . V. W. Krongauz, A. D. Trifunac in *Processes In Photoreactive Photopolymers* (Chapman & Hall, New York, 1994).

[59] . D. H. Close, A. D. Jacobson, R. C. Magerum, R. G. Brault, F. J. McClung, Appl. Phys. Lett. 1969, **14**, 159-160 (1969).

[60] . W. S. Colburn , K. A. Haines, , *Appl. Opt.* 1971,**10**, 1636

[61] . L. Dhar, A. Hale, H. E. Katz, M. L. Schilling, M. G. Schnoes, F. C. Schilling, *Opti. Lett.* 1999, **24**, 487

[62] . K. Curtis, L. Dhar, A. Hill, W. Wilson, M. Ayres, in *Holographic Data Storage: From Theory to Practical Systems*. (Wiley, New York, 2010).

[63] . A. Sato, M. Scepanovic, and R. K. Kostuk, Appl. Opt. 2003, **42**, 778

[64] . C. Ye, R. R. McLeod, *Opt. Lett.* 2008, **33**, 2575

[65] . A. C. Sullivan, M. W. Grabowski, R. R. McLeod, *App. Opt.* 2007**, 46,** 295

[66] . H. Matsushima, J. Shin, C. N. Bowman, C. E. Hoyle, J. Poly. Sci. , 2010,48,3255

[67] . Lowe, C. E. Hoyle, C. N. Bowman, *J. Mater. Chem.*, 2010, **20**, 4745

[68] . L. M. Campos, K.L. Killops, R. Sakai, J.M. J. Paulusse, D. Damiron, E. Drockenmuller, B. W. Messmore , C. J. Hawker, *Macromolecules*, 2008, **41**, 7063

[69] . G. Andrei, D. Dima, L. Andrei, *J. Optoelectronics Adv. Mat*., 2006, **8**, 726

[70] . K. P. Matabola ,A. R. De Vries , F. S. Moolman , A. S. Luyt, *J. Mater Sci.* 2009, **44**,6213

[71] . Decker, *Poly.Int.*,1998,**45**,133

[72] . J.G. Kloosterboer, *Adv.Poly.Sci.*,1988,**84**,1

[73] . D.P.Nair, N.B. Cramer, J.C.Gaipa, M.M.McBride, E.M. Matherly, R.M. McLeod, R. Shandas, C.N. Bowman, *Adv. Func. Mat.*, 2011

[74] . F.Chiellini, *J. Bioactive Compatible Poly.* 2006,**21**,157

[75] . H. H. Winter**,** *Korea-Australia Rheology J*,1999,**11**,275

[76] . J. Park, Q. Ye, E. M. Topp, C. H. Lee, E.L. Kostoryz, A.Misra, P. Spencer, *J Biomed Mater Res B Appl Biomater,* 2009,**91**,61

[77] . B.S. Graham,D.W. Jones, E.J. Sutow, *J. Dent Res.*,1991,**70**,870

[78] . Y. Wang, G. A. Ameer, B.J. Sheppard, R. Langer,*nature biotechnology*,2002,**20**,602

[79] . V. W. Krongauz, A. D. Trifunac in *Processes In Photoreactive Photopolymers* (Chapman & Hall, New York, 1994).

[80] . S.Ye, N. B. Cramer, C. N. Bowman, Macromolecules, 2011,**44**,490

[81] . A.F. Senyurt, H. Wei, C. E Hoyle, S. G Piland, T. E Gould, Macromolecules,2007,**40**,4901

[82] . O. Breuer ,U. Sundararaj, *Poly.Comp.* ,2004,24,630

[83] . R Vajtai, B Q Wei, Z J Zhang, Y Jung, G Ramanath,P M Ajayan, *Smart Mat. Struct.*,2002,**11**,691

[84] . R.F.J. McCarthy , G.H. Haines, R.A. Newley,*Comp.Man.*,1994,**5**,83

[85] . G.C. Jacob, J.F. Fellers, S.Simunovic, J.M. Starbuck, *J.Comp. Mat.*,2002,**36**,813

[86] . J**.** Cañavate1, P. Pagés, J. Saurina, X. Colom1, F. Carrasco, *Poly. Bulletin*, 2000, **44**, 293

[87] . M. S. Sreekala, C. Eger, *Poly.Comp*.2005,**1**,91

[88] . M.J. Tingart, M. Apreleva, D. ZurakowskI, J.P.P Warner, *J. Bone.Joint.Surg*.2003,**85A**, 2190

[89] . E. S. Strauss, D. Frank, E. Kubiak, F. Kummer, A. Rokito, *J.Arthro.Surg.* ,2009,**25**,597

[90] . C.M.Yakacki, J. Griffis, M. Poukalova, K. Gall, *J. Ortho.Res*., 2009, **27**,1058

[91] . *American Orthopaedic Society for Sports Medicine 2011 report*

[92] . H.B.Park, E. Keyurapan, H.S. Gill, H. S. Selhi, E. G. McFarland, *Am.J Sports. Med.*.2006,**34**,136

[93] . H.W.J. Huiskes, H. Weinans, B. van Rietbergen, *Clin. Orthop.*,1992,**274**,192

[94] . M. Poukalova ,C. M. Yakacki , R. E. Guldberg, A. Lin, M. Saing, S.D Gillogly, K. Gall, *J. Biomech.*,2010,**43**,1138

[95] . G. M. Gualtieri, S. Siegler, E. L. Hume, S. R. Kalidindi, *J.Ortho. Res.*, 2000,**18**,494

[96] . S.W Chung, J.H. Oh,H. S. Gong,J. Y. Kim, S. H. Kim, *Am.J Sports. Med.*.,2011,**39**,2099

[97] . www.medshape.com/morphix.html

[98] . R. Mimar, D.Limb, R. M. Hall, *Brit. Elb.Shol. Soc*, 2009,**1**,31